

國立中央大學  
National Central University

土木工程學系  
碩士論文

Department of Civil Engineering  
Master Thesis

氯離子入侵混凝土之擴散係數時間效應與飛灰之影響

The Effect of Fly Ash and Time Dependent Chloride  
Diffusion Coefficient on the Chloride Ingress in Concrete

研究生：Isach W.Z. Karmiadjj

指導教授：Prof. Huang Wei Hsing

中華民國 99 年 6 月



## 國立中央大學圖書館 碩博士論文電子檔授權書

(98年4月最新修正版)

本授權書所授權之論文全文電子檔(不包含紙本、詳備註1說明)，為本人於國立中央大學，撰寫之碩/博士學位論文。(以下請擇一勾選)

- 同意** (立即開放)
- 同意** (一年後開放)，原因是：\_\_\_\_\_
- 同意** (二年後開放)，原因是：\_\_\_\_\_
- 同意** (三年後開放)，原因是：\_\_\_\_\_
- 不同意**，原因是：\_\_\_\_\_

以非專屬、無償授權國立中央大學圖書館與國家圖書館，基於推動「資源共享、互惠合作」之理念，於回饋社會與學術研究之目的，得不限地域、時間與次數，以紙本、微縮、光碟及其它各種方法將上列論文收錄、重製、公開陳列、與發行，或再授權他人以各種方法重製與利用，並得將數位化之上列論文與論文電子檔以上載網路方式，提供讀者基於個人非營利性質之線上檢索、閱覽、下載或列印。

研究生簽名： 陳仕豪 學號： 973202601

論文名稱： 氣離子入侵混凝土之擴散係數時間效應與飛灰之影響

指導教授姓名： 黃偉慶 博士

系所： 土木工程 所  博士班  碩士班

日期：民國 99 年 7 月 13 日

備註：

1. 本授權書之授權範圍僅限電子檔，紙本論文部分依著作權法第15條第3款之規定，採推定原則即預設同意圖書館得公開上架閱覽，如您有申請專利或投稿等考量，不同意紙本上架陳列，須另行加填聲明書，詳細說明與紙本聲明書請至 <http://thesis.lib.ncu.edu.tw/> 下載。
2. 本授權書請填寫並親筆簽名後，裝訂於各紙本論文封面後之次頁（全文電子檔內之授權書簽名，可用電腦打字代替）。
3. 請加印一份單張之授權書，填寫並親筆簽名後，於辦理離校時交圖書館（以統一代轉寄給國家圖書館）。
4. 讀者基於個人非營利性質之線上檢索、閱覽、下載或列印上列論文，應依著作權法相關規定辦理。

國立中央大學碩士班研究生

論文指導教授推薦書

土木工程 學系 陳仕豪 研究生

所提之論文

氯離子入侵混凝土之擴散係數時間效應與飛灰  
之影響

係由本人指導撰述，同意提付審查。

指導教授 黃偉慶 (簽章)

99年 7月 3日

國立中央大學碩士班研究生  
論文口試委員審定書

土木工程 學系 陳仕豪 研究生所提之  
論文

氯離子入侵混凝土之擴散係數時間效應與飛灰之  
影響

經本委員會審議，認定符合碩士資格標準。

學位考試委員會召集人

委

員

楊仲榮

黃偉慶

李國

李明月

中華民國 99 年 7 月 7 日

## 摘要

關鍵詞：氯離子、擴散、浸泡試驗、飛灰

低放射性最終處置設施之主體為混凝土，但不同於一般混凝土結構物之用途，低放射性最終處置設施的服務年限可能長達數百年之久。另外由於台灣環境氣候潮溼，四面環海，場址的選擇可能位於臨海區域且採用地表處置或隧道處置，此環境利於腐蝕反應之發生，使得最終處置設施長期在此環境下可能產生劣化，進而影響混凝土長期耐久性。

本研究乃針對添加不同含量飛灰之混凝土進行氯離子浸泡試驗(ponding test)，以實驗室模擬混凝土工程障壁受海水入侵作用下，不同飛灰使用量之混凝土對改善混凝土抵抗氯離子入侵的成效。實驗證實添加不同含量之飛灰對混凝土抵抗氯離子入侵有顯著的效果，且使擴散係數隨時間而降低；並利用試驗結果依據費克第二定律(Fick's second law)評估氯離子擴散係數與時間的效應及飛灰添加量之影響，同時以迴歸方法求取擴散係數隨時間變化之影響參數。另外，運用Life-365及4SIGHT等二個程式，預測氯離子入侵剖面與實驗所得氯離子入侵剖面的關連性，期未來可進一步發展，應用於低放射性廢棄物最終處置場混凝土障壁服務年限之推估。

## **Abstract**

Salt ponding test was conducted on mature concrete specimens dry-stored in laboratory condition and on concretes immediately exposed to chloride after 28 days of moist curing. Analysis on the various properties of concretes with fly ash addition and their implication to chloride ingress were done. Experimental result indicates that fly ash addition increases the maximum surface chloride value of concrete while reducing the chloride diffusivity with time. These concrete properties proved to have an important effect to the prediction of chloride ingress using error function solution to Fick's second law. The prolonged dry-storage does not seem to have a significant impact on the change in chloride diffusion properties of the concrete specimens. General agreement between experimental data with Life-365 & 4SIGHT predicted values of concrete properties indicate the applicability of both concrete performance prediction software in considering the influence of fly ash addition and the reduction of diffusion coefficient with time.

**Keywords:** Chloride; Diffusion; Life-365; 4SIGHT; Ponding; Fly ash; Prediction

## Acknowledgement

بِسْمِ اللَّهِ الرَّحْمَنِ الرَّحِيمِ

Alhamdulillah...

I would like to sincerely thank Professor Huang Wei Hsing for his outstanding support and guidance throughout this endeavor. My highest appreciation is also directed to my senior, Cheng Yu Kuan, for his quality input and humorous discussion. I would also like to mention my juniors, Lo Hsin Hui & Chiu Yao Hui, who have tirelessly helped me in preparing my many samples for this research.

My nights at the lab would be dull without the company of my good friend Shaw Ting Chun. He has always been there to assist and supported me from buying me a cold drink after a tiring day grinding my specimens to powder, to assisting me in proofreading my thesis before submission. Keep on fighting my friend.

My deepest thanks for my father, Professor Djoko W. Karmiadji, and mother, Tatiek R. Karmiadji SPd, for their help, assistance, support, and love throughout my research and throughout my life. I wish to thank also my most darling sister, Ziarini Zaki Karmiadji, for being there for me always. To my parent-in-law, H. Amiruddin Harun and Hj. Cut Murni, and for my brothers-in-law, Iponsyah Putra & Muhammad Aulia, I thank them for their continuous prayers and support.

Most importantly, I thank my wife, Iva Puspita, and my son Alfatih Muhammad Akhtar Karmiadji. Both of you have given me a meaning to life and the spirit to strive.

# TABLE OF CONTENT

CHAPTER ONE INTRODUCTION .....	1
1.1 Background .....	1
1.2 Objectives .....	2
1.3 Thesis Organization .....	3
CHAPTER TWO LITERATURE REVIEW .....	5
2.1 Reinforced Concrete Degradation.....	5
2.2 Chloride Penetration Mechanism.....	6
2.2.1 Sorptivity or Surface Absorption .....	6
2.2.2 Diffusion .....	7
2.2.3 Chloride Binding.....	7
2.2.4 Wicking Action .....	8
2.2.5 Dispersion .....	9
2.2.6 Permeation .....	9
2.3 Chloride Diffusion .....	9
2.3.1 Diffusion Reduction Coefficient.....	13
2.4 Factors Influencing Chloride Diffusion.....	16
2.4.1 w/cm Ratio .....	16
2.4.2 Cement Type .....	17
2.4.3 Type of Coarse Aggregate.....	17
2.4.4 Chemical Admixtures.....	18
2.4.5 Supplementary Cementing Materials (SCM).....	18
2.4.6 Curing Regimes .....	19
2.4.7 Age and Moisture Condition of Concrete .....	19

2.4.8 Others .....	20
2.5 Influence of Fly Ash.....	20
2.6 Chloride Penetration Resistance Test.....	24
2.6.1 NordTest NTBuild 443 Bulk Diffusion Test .....	25
2.6.2 AASHTO T259 Standard Method of Test for Resistance of Concrete to Chloride Ion Penetration (Salt Ponding Test) .....	26
2.7 Service Life Models .....	28
2.7.1 Life-365.....	28
2.7.2 4SIGHT .....	31
CHAPTER THREE EXPERIMENTAL METHODOLOGY .....	34
3.1 Overview .....	34
3.2 Materials .....	37
3.3 Specimen Mix Design.....	41
3.4 Salt Ponding .....	41
3.5 Specimen Cutting.....	43
3.6 Determination of Chloride Content .....	45
3.6.1. Bound (Total) Chloride Determination .....	46
3.7 Chloride Penetration Profile .....	48
3.8 Diffusion Properties Analysis and Comparison with Existing Models .....	48
3.8.1 Surface Chloride Concentration & Apparent Diffusion Determination .....	48
3.8.2 Diffusion Reduction Coefficient Calculation .....	49
3.8.3 Empirical Relationship Equation Determination .....	49
3.8.4 Comparison with Existing Lifetime Prediction Models .....	50
3.8.5 Validation of Empirical Relationship Equation .....	51

CHAPTER FOUR RESULTS AND DISCUSSION.....	52
4.1 Experimental Data .....	52
4.1.1 Series 1 Experimental Data.....	52
4.1.2 Series 2 Experimental Data.....	57
4.2 Determination of Concrete Properties .....	60
4.2.1 $D_{app}$ , $C_s$ , and $C_{max}$ Determination .....	60
4.2.2 Determination of $m$ and $D_{28}$ Values.....	65
4.3 Comparison between Experimental & Predicted Result.....	68
4.3.1 4SIGHT Approximation and Input Values .....	68
4.3.2 Life-365 Approximation and Input Values.....	71
4.3.3 Chloride Profile Comparison .....	72
4.3.4 Comparison of Experimental $m$ and $D_{28}$ Values with 4SIGHT and Life-365.....	80
4.4 Determination of Empirical Relationships.....	83
4.4.1 Empirical Relationship Equation .....	83
4.4.2 Relationship Equation Validation .....	85
CHAPTER FIVE CONCLUSIONS & SUGGESTIONS FOR FURTHER RESEARCH.....	95
5.1 Conclusions.....	95
5.2 Suggestions .....	97
REFERENCES .....	98
APPENDIX.....	104
1. Series 1 Data .....	104
1.1 30 Days Exposure .....	104
1.2 60 Days Exposure .....	105
1.3 90 Days Exposure .....	106

2. Series 2 Data .....	107
2.1 90 Days Exposure .....	107
2.2 180 Days Exposure .....	108
2.3 365 Days Exposure .....	109

## LIST OF FIGURES

Figure 2.1 Proportional and non-linear relationship between total and free chloride .	13
Figure 2.2 Different time basis used in the determination of $m$ value.....	14
Figure 2.3 Influence of different $m$ value to the calculated diffusion coefficient.....	16
Figure 2.4 Effect of water-to-cementitious material ratio on diffusion coefficient .....	17
Figure 2.5 Effect of SCM on chloride diffusivity .....	19
Figure 2.6 Influence of fly ash replacement on the depth of penetration of critical chloride threshold.....	22
Figure 2.7 Typical curve fitting to obtain diffusion coefficient & surface chloride concentration from bulk diffusion data.....	24
Figure 2.8 NordTest bulk diffusion test set up.....	26
Figure 2.9 AASHTO T259 Salt Ponding Test set up .....	27
Figure 3.1 Experiment Program Work Flow Diagram.....	36
Figure 3.2 Particle size distribution curves of fine aggregate.....	40
Figure 3.3 Specimen salt ponding test set up.....	42
Figure 3.4 Specimen storage condition during salt ponding test.....	43
Figure 3.5 Struers Minitom used for specimen cutting.....	44
Figure 3.6 Sliced specimen for the profiling of chloride concentration at various depths .....	44
Figure 3.7 Storage of powdered samples in Ziploc bags. ....	45
Figure 3.8 Titrino 877 automatic titration machine for chloride content determination .....	46
Figure 3.9 The menu of LAB Fit curve fitting software .....	50
Figure 4.1 Chloride profiles at different exposure times .....	54

Figure 4.2 The influence of fly ash addition to chloride ingress in concrete.....	56
Figure 4.3 Comparison between 90 days result of Series 1 and Series 2 .....	59
Figure 4.4 COPC Curve Fitting .....	62
Figure 4.5 CF10 Curve Fitting.....	62
Figure 4.6 CF20 Curve Fitting.....	62
Figure 4.7 C5% Curve Fitting.....	63
Figure 4.8 C10% Curve Fitting.....	63
Figure 4.9 Reduction of diffusion coefficient with time-total time basis .....	67
Figure 4.10 Reduction of diffusion coefficient with time-average time basis.....	67
Figure 4.11 Reduction of diffusion coefficient with time-effective time basis .....	67
Figure 4.12 Screenshot of 4SIGHT input options .....	69
Figure 4.13 COPC Profile Comparisons.....	74
Figure 4.14 CF10 Profile Comparisons .....	75
Figure 4.15 CF20 Profile Comparisons .....	76
Figure 4.16 C5% Profile Comparison.....	77
Figure 4.17 C10% Profile Comparison.....	78
Figure 4.18 Salt crystal formations on concrete surface.....	79
Figure 4.19 COPC with modified Life-365 calculation.....	88
Figure 4.20 CF10 with modified Life-365 calculation .....	89
Figure 4.21 CF20 with modified Life-365 calculation .....	90
Figure 4.22 C5% with modified Life-365 calculation.....	91
Figure 4.23 C10% with modified Life-365 calculation.....	92
Figure 4.24 Validation of empirical relation equations.....	94

## LIST OF TABLES

Table 2.1 Examples of $m$ values and $D_{28}$ values obtained from bulk diffusion test.....	25
Table 3.1 The chemical composition of experimental materials .....	38
Table 3.2 Coarse and fine aggregates physical properties .....	39
Table 3.3 Grain size distribution of fine aggregate .....	39
Table 3.4 Uses and sources of chemicals used .....	40
Table 3.5 Proportion of Concrete ( $\text{kg/m}^3$ ).....	41
Table 4.1 $C_{\text{max}}$ Values.....	58
Table 4.2 The values of $C_s$ and $D_{\text{app}}$ Obtained from Curve Fitting .....	64
Table 4.3 Experimental $D_{28}$ and $m$ Values .....	66
Table 4.4 Input Parameters for 4SIGHT Calculation.....	71
Table 4.5 Input Parameters for Life-365 Calculation .....	72
Table 4.6 $m$ and $D_{28}$ Values Comparison .....	81
Table 4.7 Empirical Relation Equations .....	84
Table 4.8 Input Values for Modified Life-365 Calculations .....	86

# CHAPTER ONE INTRODUCTION

## 1.1 Background

Corrosion of steel reinforcement is one of the biggest problems to the durability of reinforced concrete. From the 2007 NACE International estimate for the United States, the annual direct cost from corrosion for maintenance and capital cost for concrete bridge deck reaches \$2 billion with an additional \$2 billion for their concrete substructures [1]. These damages are due to the “depassivation” of the oxide film due to the presence of sufficient amount of chloride ions at the reinforcing bar surface. In addition to a tolerable level of chloride found as trace elements in aggregates or admixtures, unacceptably high level of chloride may diffuse through the concrete and build up on the reinforcement surface during the service life of the concrete structure [2]. The time required for surface chloride to diffuse and build up to the corrosion threshold concentration level (0.40% of binder content or 0.05% of concrete content) is taken as the initiation period of corrosion. This period is dependent on various factors such as surface chloride concentration, diffusion coefficient and crack width [3, 4]. Studies have shown that fly ash addition has successfully increased the predicted service life and durability of concrete. Although the utilization of fly ash only have little impact on the reduction of chloride diffusion coefficient in the early ages of concrete, after years of exposure the reduction in chloride diffusion coefficient reaches an order of magnitude. This indicates the time dependent nature of the chloride diffusion coefficient in concretes containing fly ash [5, 6].

Despite having a simplified assumption, the error function solution based of Fick’s second law, are still commonly used by engineers due to their practical expression [7].

Previous researches have concluded that the empirically determined reduction of chloride diffusion coefficient must be included if reliable predictions using error function solution of Fick's second law are to be made [5]. One of the most widely used service life calculation software "Life-365", developed as the first step towards creating a consensus corrosion service life model by a consortium formed within American Concrete Institute's (ACI) Strategic Development Council (SDC), incorporated this empirical constant in their Fick's law based calculation [4].

Due to the increasing utilization of fly ash to improve the durability of concrete, a research program was established by the National Central University to evaluate the impact of fly ash addition and replacement on concrete to chloride ion diffusion. The time dependent diffusion coefficient determined from the research program is expected to improve the reliability of service life calculation of reinforced concretes which utilizes fly ash addition.

## **1.2 Objectives**

This research project was intended to examine the influence of fly ash and time dependent diffusion coefficient on the service life of concrete. The research objective focuses on the following aspects:

1. Produce chloride ingress profile and determine diffusion coefficient of concrete with varying fly ash and water-to-cementitious material ratio (w/cm) content from salt ponding test result.
2. Compare between salt ponding test result with chloride profile prediction obtained from Life-365 and 4SIGHT computer program.

3. Determine the reduction coefficient ( $m$ ) using concrete maturity ( $m_{\text{total}}$ ), average age during the exposure period ( $m_{\text{avg}}$ ), and effective time ( $m_{\text{eff}}$ ) as the time basis for calculation.
4. Produce an experimental relationship equation between w/cm and diffusivity ( $D_{28}$  or diffusion at 28 days), in addition to relationship between fly ash replacement and w/cm to the reduction coefficient of fly ash concrete ( $m_{\text{total}}$ ,  $m_{\text{avg}}$ ,  $m_{\text{eff}}$ ).
5. Analyze the service life implication of fly ash and w/cm content and time basis assumption of reduction coefficient using available service lifetime prediction software based on Fick's second law solution (Life-365).

Thus it is expected that after the course of the research, an empirical relationship to determine  $C_{\text{max}}$ ,  $m_{\text{total}}$ ,  $m_{\text{avg}}$ ,  $m_{\text{eff}}$  and their respective  $D_{28}$  and chloride build up time value for use in the service life calculation of concrete with varying fly ash and w/cm ratio can be established.

### **1.3 Thesis Organization**

In order to effectively present the content of the research, the thesis is divided into five parts. CHAPTER ONE presents the background information, objective and thesis organization on this research. CHAPTER TWO contains theories and previous researches from literature review that have become the underlying basics of this study. This chapter discusses chloride diffusion into concrete, influences of fly ash and water-to-cementitious (w/cm) ratio on the property of concrete, methods in

determining chloride diffusion coefficient and reduction coefficient ( $m$ ), and review of existing service lifetime prediction model. CHAPTER THREE discusses the various materials and methodology used during this research. Sample production and chloride diffusion test procedure used in this research are explained. Method to determine total chloride through titration test is also discussed. CHAPTER FOUR presents the results of the chloride diffusion test. Chloride profile and diffusion coefficient calculation are given. Influence of fly ash and w/cm ratio are analyzed. Determination of concrete diffusion properties is presented. Determination and validation of the empirical relationship equations for  $m$ ,  $D_{28}$ , chloride build up time, and  $C_{\max}$  are also shown. CHAPTER FIVE lists the conclusion of this research and suggestions for further study.

## **CHAPTER TWO LITERATURE REVIEW**

### **2.1 Reinforced Concrete Degradation**

Reinforced concretes are used as a structural material due to its combination of the good compressive strength and economical price of concrete with the ability of its steel reinforcement to resist both compressive and tensile stresses. Since the 1920's reinforced concrete has been used to produce both economical and enduring structures. Nevertheless, many reinforced concrete structures have lasted below its designed lifetime. The corrosion of its embedded steel is usually the cause of this untimely deterioration [8].

Embedded reinforcing steel are normally protected from the environment and corrosion by their concrete matrix. The high alkalinity ( $\text{pH} > 13$ ) which exists in the pore solution of concrete allows for the covering of the embedded steel by a passive, protective oxide films, preventing the initiation of corrosion. This protective film can be depassivated, hence corrosion initiated, through the penetration of chloride ions from the environment (sea water, ground water, deicing salt, etc) into the concrete cover [9]. Corrosion of embedded steel accounts for expensive multi-million dollar repairs and maintenance.

Not all ions penetrating the concrete cover are detrimental to corrosion. Some chlorides will be chemically bounded by reacting with the hydration compounds of cement, particularly tri-calcium aluminates ( $\text{C}_3\text{A}$ ), to form Friedel's salt or calcium monochloroaluminate [10]. In addition, some chloride ions will be physically bounded or attracted to the pore surfaces by weak Van der Waal's forces in a

chemisorbed state. Damage to the passive protective films are due to the unbound chloride ions that remain dissolved in the liquid phase of concrete, which at this state could react and possibly destroy the protective film in the steel surface. The penetration of free chlorides lowers the pH or alkalinity of the pore solution of concrete, hence reducing the ability of the dissociated hydroxyl ions to create a passive film of iron oxide to protect the steel reinforcement. Corrosion is initiated when the ratio of free chloride ions to hydroxyl ions exceed a threshold value, depending on the type of cement, supplementary cementing materials, and other factors [11].

## **2.2 Chloride Penetration Mechanism**

Chloride penetration is influenced by the ingress or movement of chloride ions which are dissolved in water into the concrete. There are basically six different mechanisms which governs the ingress of chloride into the concrete [12]. These different transport mechanisms may occur simultaneously within the concrete and complement one another to influence the ingress of chloride ions.

### **2.2.1 Sorptivity or Surface Absorption**

Near the concrete's surface sorptivity is the predominant transport process. It is highly dependent on the moisture condition of the concrete. In an unsaturated concrete, capillary action may even be the dominant transport mechanism of chloride ions. Capillary tension can cause chloride ions to penetrate from 5 to 15 mm deep within the concrete in hours or days of exposure until the surface layer becomes saturated. In addition, initial sorption will significantly affect the long term diffusion coefficient calculated, if it is not accounted for [13].

Due to capillary action, structures exposed to daily or seasonal wetting and drying cycles such as bridges, marine structures, etc., are found to have a greater ingress of chloride ions than is caused by ionic diffusion alone. It was also observed that the sorptivity of high performance concretes with w/cm ratio of 0.30 containing silica fume to be high. Chloride ions are transported to a depth of influence, where a relative constant chloride concentration is maintained for that depth, by continuous capillary suction. Absorption values, described by its rate of absorption or sorptivity, are also known to be related to the permeability and moisture content of the concrete [12].

### **2.2.2 Diffusion**

In the case of saturated concretes which are exposed to a chloride solution at normal pressure, pure ion diffusion will be the predominant driving mechanism. Diffusion is the simplest transport mechanism to be modeled by using Fick's second law and has been studied by numerous researchers. In a saturated concrete with at least one surface exposed to chloride solution, diffusion will occur to maintain equilibrium of the solutions. Therefore chloride ions will move from high concentration to low concentration within the concrete. Differences in concentration of chloride ions create a chloride concentration gradient between the surfaces and pore solutions which becomes the driving force of the diffusion process. In addition, the diffusion process is affected by the bonding of chloride ions [14].

### **2.2.3 Chloride Binding**

Chlorides exist in three states, freely in the pore solution, chemically bound to hydration products, and physically held to the surface of hydration products. This means that some chloride ions will react and bind with the hydrated phases of cement paste during its ingress into the concrete, regardless of the transport mechanism.

Chloride binding reduces the chloride ingress on concrete by immobilizing chlorides so that they do not diffuse or actively cause corrosion. Chloride binding was also found to be influenced by the  $C_3A$  content. Chloride binding were found to increase with increasing curing temperature. The alkalinity of the pore solution was also found to influence chloride binding. It was discovered that the lower the alkalinity of the pore solutions, the higher the degree of chloride binding. The cation, associated with the penetrating chloride ions, plays a role in affecting the alkalinity of the pore solution hence also the degree of chloride binding. This can be seen by the higher chloride binding level when a solution of calcium chloride or magnesium chloride, which lowers the alkalinity of pore solution, was used in place of sodium chloride, which increases the alkalinity of pore solution. The methods of chloride binding are formation of calcium chloro-aluminate (Friedel's salt:  $Ca_2Al(OH)_6(Cl, OH) \cdot 2H_2O$ ), formation of calcium chloro-ferrite ( $3CaO \cdot Fe_2O_3 \cdot CaCl_2 \cdot 10H_2O$ ) and by physical binding of the C-S-H sheets. It is thought that most of the bound chlorides are physically bound to ion exchange sites of the calcium silicate hydrate C-S-H gel, which implies a significant degree of reversibility. Therefore reduction of chloride concentration in the pore solution will cause bound chlorides to become free [11, 12].

#### **2.2.4 Wicking Action**

When a concrete surface away from the chloride source is exposed to air with a relative humidity of less than 100%, wicking can occur. Chloride in the pore water from the wet surface in contact with the chloride solution will be drawn inward to the drier surface by moisture gradient and evaporation. Evaporation of the water will empty the pores, pre-crystallize the chlorides and increase the chloride concentration in the concrete. Wicking action increases the ingress of chloride ion in addition to other mechanism such as diffusion [15, 16].

### **2.2.5 Dispersion**

Dispersion of the chloride front occurs as it moves through the concrete cover. It is commonly observed in the flow of contaminant in groundwater through soil. It is related to the differences in the velocity of chloride ion ingress at the diffusion front. This will either cause the ions to move faster or slower than the average diffusion rate. Dispersion is not considered as a mechanism of ingress than it is as an issue which affects the ingress of chlorides.

### **2.2.6 Permeation**

Permeation describes the flux of water (or chloride solution) due to a hydraulic pressure gradient across the concrete. Darcy's Law describes the driving force of permeation, where there is a pressure gradient across the concrete. Permeation is usually observed in underground structures of deep offshore structures. Hydrostatic pressure forces chloride ions in the water surrounding these structures to penetrate inside. Permeation can complement diffusion and other mechanism to increase the rate of chloride ingress [12, 14].

## **2.3 Chloride Diffusion**

In underground concrete structures, although the initial penetration of chloride ions can occur due to hydraulic pressure gradients or capillary suction of ground water [17], but the process occurs primarily due to non-steady state diffusion. Diffusion is also the prevalent mechanism of chloride ingress when deicing salts are used in bridges and roads. Therefore, the time for corrosion initiation is highly dependent on the rate of diffusion of chloride through the concrete covers to the embedded reinforcing steel. This diffusion value is highly dependent on the concrete itself.

Alternative solutions to prevent corrosion have been done through the use of impermeable coatings for the concrete to prevent chloride ingress and the use of epoxy coating for steel to prevent rust. Yet, the most economical solution is to modify the properties of concrete to make the concrete itself more resistant to chloride ion penetration. Many approaches are taken to improve the resistance of concrete to chloride ions. These are done, among others through the use of low water-to-cementitious materials (w/cm), low total water content, supplementary cementitious materials, and thicker concrete cover [4]. Curing regimes, compaction and construction details are also considered. As previously described, diffusion is a complex process which are influenced by other transport mechanism and factors. Among these are the binding reactions between the diffusing chloride ions with the hydrated compounds of cement which reduce the rate of chloride penetration. The use of supplementary cementitious materials may also serves to reduce the diffusion rates by refining the pore structure of the concrete. Meanwhile, cracks which may be caused by shrinkage, freezing and thawing, alkali aggregate reactions or structural defects can shorten the distance chloride ions must travel to reach the reinforcing steel and reduces the time needed for corrosion initiation [12-14].

Diffusion in saturated concrete is due to the attempt to attain equilibrium throughout its pore solution and is theoretically explained through Fick's law of diffusion. Fick's first law states that the chloride ion flux is proportional to the concentration gradient [18].

$$J = -D_{\text{eff}} \frac{dC}{dx} \dots\dots\dots (2.1)$$

where:

$J$  = flux (mol/m<sup>2</sup> s)

$D_{\text{eff}}$  = diffusion coefficient (m<sup>2</sup>/s)

$C$  = concentration (mol/m<sup>3</sup>)

$x$  = depth from the surface of the concrete (m)

In applying Fick's first law, the following three assumptions are made:

1. The system is at steady state
2. The concentration is the only driving force
3. There is no interaction between the diffusing ions and the solution.

To calculate the rate of change of the species concentration, Fick's second law of diffusion is developed by considering mass conservation in a unit control volume.

$$\frac{\delta C}{\delta t} = D_{\text{eff}} \frac{\delta^2 C}{\delta x^2} \dots\dots\dots (2.2)$$

where:

$D_{\text{eff}}$  = diffusion coefficient (m<sup>2</sup>/s)

$C$  = concentration (mol/m<sup>3</sup>)

$x$  = depth from the surface of the concrete (m)

$t$  = time (s)

The solution to the differential equation of Fick's second law is obtained by using Cranks solution with the following three boundary conditions [18]:

1.  $C_{(x=0, t>0)} = C_0$  : the surface concentration is constant at  $C_0$
2.  $C_{(x>0, t=0)} = 0$  : the initial concentration in the concrete is 0
3.  $C_{(x=\infty, t>0)} = 0$  : far enough away from the surface, the concentration will always be 0

$$C(x, t) = C_0 \left( 1 - \operatorname{erf} \left( \frac{x}{2\sqrt{Dt}} \right) \right) \dots\dots\dots (2.3)$$

where:

$C_0$  = surface chloride concentration (mol/m<sup>3</sup>)

$C_{(x, t)}$  = chloride concentration at distance  $x$  and time  $t$  (mol/m<sup>3</sup>)

erf = error function (a numerical function available in mathematical tables)

Chloride profiles and diffusion coefficient derived using Fick's laws of diffusion and Crank's solution are considered helpful for estimating the time to corrosion of reinforced concrete structures. Yet, the assumptions used in the solution are considered overly simplistic [19, 20, 21]. This is especially true since the assumption of steady state is not present in normal concrete structures. Concrete as a hydraulic material, will continually hydrate if there is moisture available. Continued hydration will cause the refining of pore structure and subsequently will lower the diffusion coefficient with time. The steady state assumption is also annulled due to the effect of chloride binding on diffusion. Another significant factor that affects the diffusion coefficient is the fact that most concrete structures do not experience a consistently saturated moisture condition. As previously discussed, true diffusion occurs when concrete is saturated. Yet, reinforced concrete structures are subjected to a variety of moisture states where water and vapor flow in and out of the concrete by capillary suction through continuous pores. The relationship between bound and free chlorides is assumed to be linear by Crank's solution, an assumption that has been found to be

untrue in the field. The proportional and non-linear relationship between total and free (water-soluble) chloride can be seen in Figure 2.1 below. Counter diffusion of hydroxyl ions out of the samples is also a problem that negates the linear nature of binding assumed by Crank's solution [22]. Finally the diffusion coefficient calculated would not be an instantaneous diffusion value. Instead it would be a diffusion value averaged over the entire exposure time of the concrete. This is problematic especially in fly ash and other modified concretes where the diffusion value has been shown to dramatically decrease over time [5].

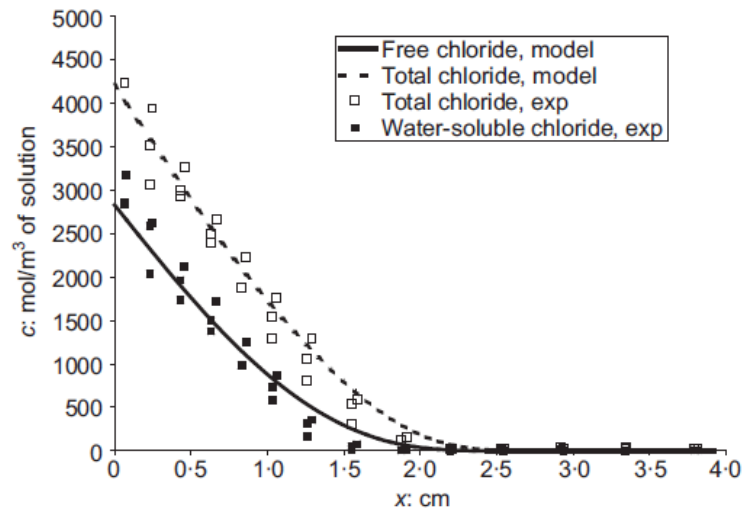


Figure 2.1 Proportional and non-linear relationship between total and free chloride [19].

### 2.3.1 Diffusion Reduction Coefficient

Along with an increase in its utilization, a considerable reduction in diffusivity with time is observed for concretes containing fly ash or slag [6]. This raises question on the usefulness of using the simple numerical solution of Fick's law to determine the service life of new concrete structures. A consideration must be made on the ability of the cementitious system of concretes with fly ash or slag to refine its pore structures as it matures. A coefficient that accounts for the decay in transport rate must be included for reliable lifetime predictions to be made [23, 24].

This reduction coefficient, designated as  $m$ , is determined empirically by using the following equation:

$$D(t) = D_{\text{ref}} \left( \frac{t_{\text{ref}}}{t} \right)^m \dots\dots\dots (2.4)$$

where

$D_{(t)}$  = diffusion coefficient at time  $t$

$D_{\text{ref}}$  = diffusion coefficient at some reference time  $t_{\text{ref}}$

$m$  = reduction coefficient (depending on mix proportions).

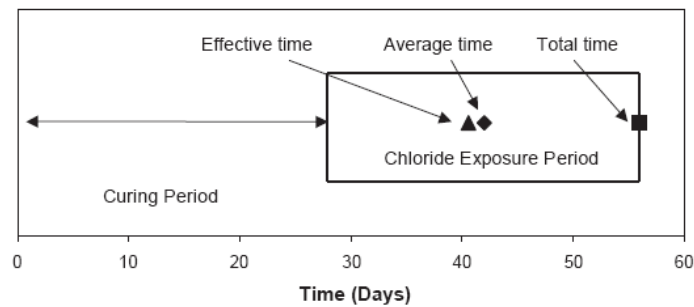


Figure 2.2 Different time basis used in the determination of  $m$  value [24].

The diffusion reduction coefficient,  $m$ , is determined by linear regression of diffusion values calculated using Cranks solution to Fick’s laws with time on a log-log scale. Various assumptions are used in determining the time basis to calculate  $m$  and therefore different  $m$  values are obtained as seen in Figure 2.2 above. The first method,  $m_{\text{total}}$ , uses the concrete maturity, as the time basis, versus the calculated apparent diffusion coefficient. Meanwhile, the second method,  $m_{\text{avg}}$ , considers the average age of the concrete during the exposure period versus the calculated apparent diffusion coefficient. The third method, known as  $m_{\text{eff}}$ , takes into account both maturity and exposure time. As an example, for a sample which has been cured for 28 days and exposed to chloride for 28 days, the time used to calculate  $m_{\text{total}}$  would be 56 days or

the total age the concrete has matured. For  $m_{avg}$ , the time used for calculation would be 42 days, or the age of the concrete at the average exposure period (between 28 days and 56 days or  $[1/2(t_1 + t_2)]$ ). Meanwhile,  $m_{eff}$  is determined from the following iterative procedures [23]:

1. Assume a value of  $m$ .
2. For each bulk diffusion test, using the following equation to calculate the effective age using the assumed value of  $m$  and the test parameters.

$$t_{eff} = \begin{cases} \left[ \frac{(1-m)(t_2-t_1)}{t_2^{1-m} - t_1^{1-m}} \right]^{1/m} & m \neq 0, 1 \\ \frac{t_2-t_1}{\ln\left(\frac{t_2}{t_1}\right)} & m = 1 \end{cases} \dots\dots\dots (2.5)$$

3. Determine the logarithms of the average diffusion coefficients ( $D_{avg}$ ) and the effective ages from Step 2 for each test.
4. Determine the value of  $m$  from the negative slope of the line of best fit using the logs of the average diffusion coefficients as the  $y$ -values and the logs of the effective ages as the  $x$ -values.
5. Repeat Steps 2 through 4 with the new value of  $m$ . When the  $m$ -value determined from Step 4 is equal to the  $m$ -value used in Step 2, the value of  $m$  is established for the concrete.
6. The intercept of the line of best fit will be the log of the 1-day diffusion coefficient (if age is given in days). Correct to the reference age using Eq. 2.4 and the value of  $m$  just determined.

The concept of effective time is of great interest since by the method above we could determine the time ( $t_{eff}$ ) when the apparent diffusion coefficient observed from the experimental chloride profile equals to the instantaneous diffusion coefficient.

When the three methods for the determination of  $m$  are compared, the total time method would yield the lowest  $m$  value, while the effective time approach yields the highest [24]. The influence of  $m$  to the calculated apparent diffusion coefficient is seen in Figure 2.3. The reduction coefficient determined by one method can be transformed to those from another method if the age at initial exposure and the exposure period of each specimen is known.

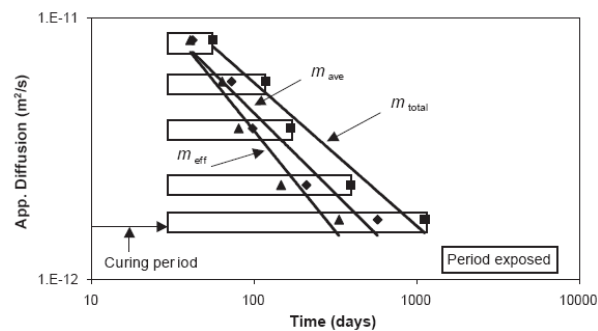


Figure 2.3 Influence of different  $m$  value to the calculated diffusion coefficient [24].

## 2.4 Factors Influencing Chloride Diffusion

### 2.4.1 w/cm Ratio

Water-to-cementitious material ratio influences the capillary pores and interfacial zones of concrete. Increasing w/cm ratio will also increase the volume of capillary pores content and creates a weaker interfacial zone between the coarse aggregate and the paste. This creates a path for the chloride ions and increases its penetration rate. Permeability is experimentally found to be directly related to the w/cm ratio. Concretes with w/cm ratio of less than 0.30 were described as virtually impermeable to water and chloride ions, especially when supplementary cementitious materials such as silica fume were added [12, 25]. The influence of w/cm on chloride diffusion is seen in Figure 2.4 below.

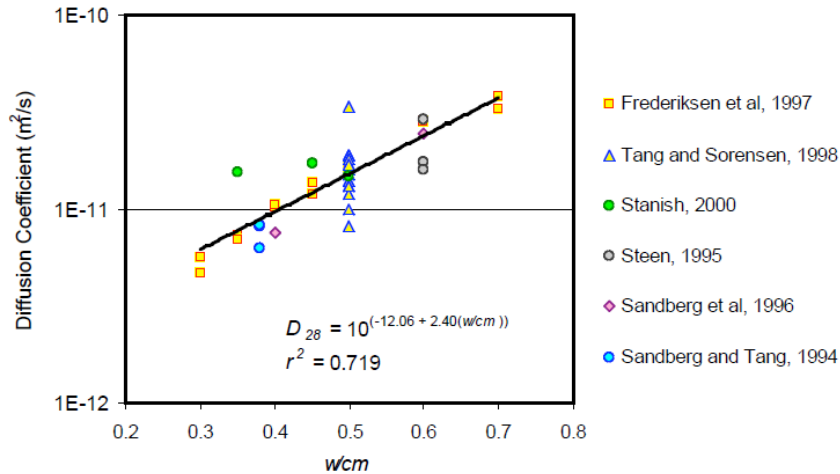


Figure 2.4 Effect of water-to-cementitious material ratio on diffusion coefficient [4].

### 2.4.2 Cement Type

There is a relatively minor effect of the cement type on chloride resistance. It was believed that these differences between cement types are due to the  $C_3A$  content which will increase the degree of chloride binding [26]. Yet it should be noted that the effect of  $C_3A$  content on chloride binding is not significant when the chlorides are derived from external sources.

### 2.4.3 Type of Coarse Aggregate

It has been discovered that the maximum aggregate size will affect chloride permeability. When two dense grade aggregates were used, it was found that concrete with a 12.5 mm (1/2 in) maximum size aggregate has a lower chloride permeability than the one with 19.0 mm (3/4 in) maximum size aggregate due to its higher surface area to volume ratio. Gap-graded aggregates were also found to give a higher permeability while a well-graded aggregate gives the lowest permeability. In addition it has been concluded that a high quality and dense mortar is more essential than the aggregate porosity in producing a watertight concrete [27].

#### **2.4.4 Chemical Admixtures**

Although the effects of different kinds of chemical admixture on chloride resistance have not been studied extensively, it has been found that the permeability of concrete increases as the entrained air content increases. Chloride resistance could be improved as well through the use of water reducing agents which makes low w/cm ratio concrete mixes possible [28, 29]. Superplasticizer also reduces chloride penetration by allowing the use of lower w/cm ratio concretes.

#### **2.4.5 Supplementary Cementing Materials (SCM)**

Supplementary cementing materials are added to concrete to improve the durability of concrete by enhancing its various properties, such as strength, porosity, and chloride resistance. Physically, this is achieved by filling the very fine pores of concretes with supplementary cementing materials (SCM). Meanwhile, chemically, SCM will react with the calcium hydroxide by product of cement hydration to produce a denser cement matrix with a better interfacial zone. Concrete mixes with SCM will produce a lower permeability if it is properly designed and cured. In the long term, the use of SCM will improve the durability of concrete by continuously reacting to further refining the pore structure of the concrete. It has been shown that the chloride resistance of concrete mixes with fly ash and slag increases continuously and significantly from 6 months onwards. Meanwhile ordinary Portland cement, OPC, would only exhibit a modest increase in chloride resistance within the same time period [30-32]. The effect of SCM on the reduction of the diffusion coefficient is seen in Figure 2.5 below.

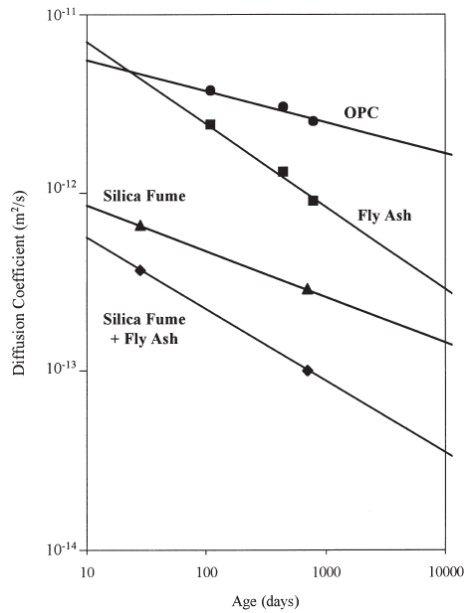


Figure 2.5 Effect of SCM on chloride diffusivity [30].

#### 2.4.6 Curing Regimes

Longer moist curing period will result in higher chloride resistance of concrete. It is believed that the continued hydration during moist curing will cause a decrease in porosity and pore size. Air dried cover concrete, meanwhile, would be extremely heterogeneous with small shrinkage cracks, interconnected voids, and open capillaries. This would allow chloride ion to penetrate faster into the concrete below [33, 34]. High curing temperatures in precast plants have also shown to reduce the resistance of plain Portland cement concrete to chloride ingress.

#### 2.4.7 Age and Moisture Condition of Concrete

The continuing hydration process of concrete improves its chloride resistance. This is especially true for concretes which are moist cured continuously. Meanwhile hydration of air dried concrete may stop near the surface soon after moisture is removed. The dry surface will assist in drawing chloride ions into the concrete through capillary action [33].

## **2.4.8 Others**

### ***Temperature***

Diffusion rate and ion exchange increases with increasing temperature. This will allow the chloride ion to penetrate to a greater depth. It has been shown that the effective diffusion coefficient is temperature dependent. An increase of 10 °C in temperature would double the effective diffusion coefficient value and reduces concrete resistance to chloride ingress [35].

### ***Type of Chloride Solution***

Due to the different binding capacity of different cations, it was discovered that the chloride diffusion is also affected by the type of chloride solution that the concrete structure is exposed to [36, 37].

### ***Construction Defects***

Construction defect in the form of cracks will shorten the distance needed for chloride ion to reach the embedded steel. Therefore the quality of construction is paramount in producing a chloride resistant concrete since no matter the quality of the mix, a defective construction would not protect the reinforcement from corrosion [38].

## **2.5 Influence of Fly Ash**

Fly ash is a supplementary cementitious material (SCM) for concrete which is obtained from industrial by-products. Fly ash is obtained from the flue gas of coal-fired thermal generating plants by using mechanical and electrostatic precipitator. It is considered as an inexpensive replacement for cement and produces a more economical concrete. The particles of fly ash are generally 1 to 150 micrometer in

diameter and are fine, glassy and spherical. These particles are made up of aluminosilicate glasses which contain various proportions of calcium, iron, magnesium and alkali metals. ASTM C 618 classifies fly ash into two different categories.

#### *Class C*

- ASTM requirement;  $\text{SiO}_2 + \text{Al}_2\text{O}_3 + \text{Fe}_2\text{O}_3 > 50\%$
- usually produced from lignite or sub-bituminous coals
- high calcium contents, typically 8 to 30% CaO
- may possess some hydraulic properties in addition to pozzolanic properties

#### *Class F*

- ASTM requirement;  $\text{SiO}_2 + \text{Al}_2\text{O}_3 + \text{Fe}_2\text{O}_3 > 70\%$
- usually produced from bituminous or lignite coal
- low calcium content, typically less than 8% CaO
- possesses pozzolanic properties (needs source of lime or other activator to react)

Fly ash is known to improve workability, pumpability, ultimate strength and impermeability of concrete. Since diffusion occurs through the pore solution, strength and durability can be improved through reducing the porosity of the concrete by using fly ash. In addition, long term strength and durability, and likelihood of thermal cracking are reduced due to the slower hydrating reaction of fly ash compared with cement. In the precast industry where elevated curing temperatures were used, partial replacement of OPC in concrete with fly ash has shown to improve the strength and durability of the concrete [5, 6, 30-32].

With regards to chloride binding it has been discovered that the use of fly ash causes an increase in the chloride binding capacity due to the higher surface area and adsorptivity of fly ash cement. This would increase the formation of Friedel's salt after pozzolanic reactions have occurred [9, 39]. Although the use of fly ash would reduce the threshold levels for corrosion initiation, it was also discovered that this detrimental effect is outweighed by the ability of fly ash replacement to provide better protection to steel by its ability to lower the rate of diffusion [6].

The diffusivity of fly ash concrete is more sensitive to aging than plain Portland concrete. It has been shown that although at early ages, the diffusivity of concrete containing 25% to 30% fly ash may have a similar chloride ion diffusivity as an equivalent grade of Portland cement concrete, after approximately 2 years the diffusivity of fly ash concrete may be one order of magnitude lower than the Portland cement and would further decrease to two orders of magnitude after 100 years (see Fig. 2.6). This would significantly influence the long-term performance of concrete in chloride environment.

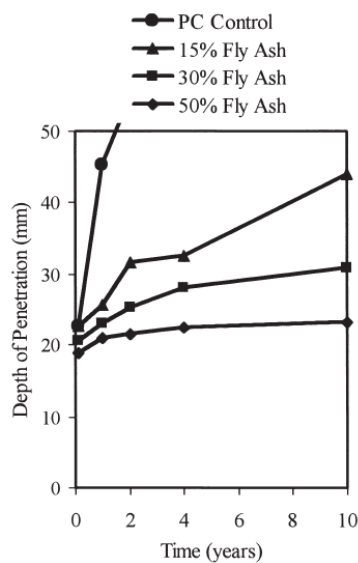


Figure 2.6 Influence of fly ash replacement on the depth of penetration of critical chloride threshold [5].

Since the property of fly ash vary greatly between suppliers and may vary over time, a careful monitoring related to its fineness, loss on ignition, and CaO must be done. The effects of these factors of fly ash are summarized on the October 2001 NFESC Technical Paper where [40]:

- New concretes are recommended to include a cement replacement of 25% to 40% Class F fly ash (or Class N pozzolan)
- Class F fly ash should have a maximum of 1.5% available alkali, a maximum of 6% loss on ignition (although 3% would be better), and a maximum of 8% CaO (up to 10% CaO if a minimum replacement of 30% is used)
- If the minimum replacement is not met, this would result in a lower quality and more expensive concrete
- In addition to mitigating ASR problem, the use recommended Class F fly ash replacement are expected to: (1) reduce concrete costs, (2) significantly enhance the durability of concrete, (3) increase fly ash recycling, (4) support the 1997 Kyoto protocol y significantly reducing CO<sub>2</sub> production. A 25% fly ash replacement of cement would give a total saving of the United States economy by more than \$1 billion a year.
- It has also been determined that: (1) even if Class F fly ash were used, the current practice of only using 15% fly ash cement replacement may worsen the ASR expansion, (2) Class C fly ash is not recommended for ASR mitigation, (3) lithium nitrate may be needed in addition to Class F fly ash for very reactive aggregates, (4) ASR mitigation by lithium nitrate, silica fume, or calcined concrete will increase the cost of concrete whereas using Class F fly ash would reduce the cost of concrete by 4% . .

## 2.6 Chloride Penetration Resistance Test

Two popular tests are created to determine the chloride penetration characteristic of concrete. These tests are the rapid chloride penetration test (RCPT) and the bulk diffusion test. Rapid chloride penetration test uses current that passes through two reservoirs, one simulating de-icer salts and the other pore chemistry, to determine the chloride penetration potential of concrete. In theory, since concrete is a highly resistive materials, most of the electrical charge should pass through the pore fluid. Therefore the connectivity of the pores, which are needed for chloride penetration, is related to the total charge passed, measured in coulombs. Yet, it is the bulk diffusion test that is considered more fundamental since it measures the actual ingress of chloride ion with time [18]. Apparent diffusion coefficient, or sometimes referred to as average diffusion coefficient, & surface chloride concentration ( $C_s$ ) can also be derived from curve fitting data of bulk diffusion tests to the error function solution of Fick's second law (see Fig. 2.7).

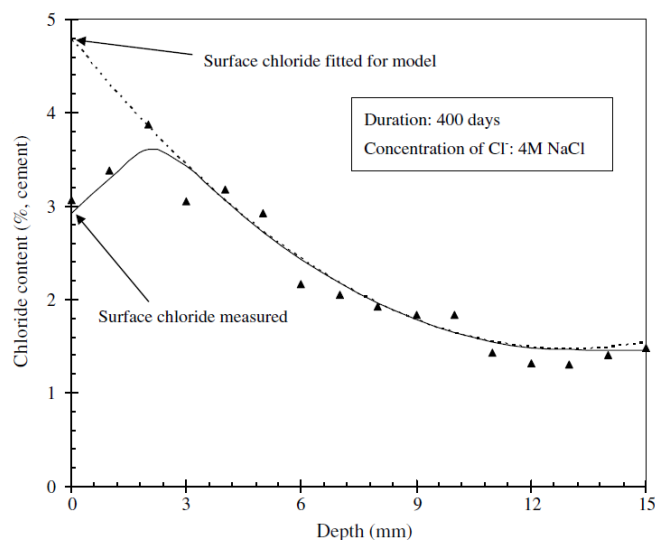


Figure 2.7 Typical curve fitting to obtain diffusion coefficient & surface chloride concentration from bulk diffusion data [29].

Two commonly used methods for bulk diffusion is the NordTest NTBuild 443 Bulk Diffusion Test and the AASHTO T259 Salt Ponding Test. In both of these tests concrete or mortar samples are normally saturated to ensure that diffusion is the main transport mechanism of chloride ions. The sides and bottom of the samples are also covered with an impermeable material to ensure a unidirectional diffusion and prevent edge effects. The specimens are then exposed to chloride by immersion in a chloride solution for a set period of time. At the end of the exposure period, the samples are analyzed to obtain its profile content. Fick's second law is used to determine the diffusion coefficient of the concrete material [35, 41]. An example of diffusion coefficient at 28 days and  $m$  values obtained from bulk diffusion test is seen in Table 2.1 below.

Table 2.1 Examples of  $m$  values and  $D_{28}$  values obtained from bulk diffusion test [30]

Cement type	$D_{28}$ (m <sup>2</sup> /s)	$m$
Control	$4.3 \times 10^{-12}$	0.23
25% fly ash	$4.4 \times 10^{-12}$	0.62
Type 10SF <sup>a</sup> (8% silica fume)	$6.6 \times 10^{-13}$	0.25
Type 10SF + 25% fly ash	$3.7 \times 10^{-13}$	0.40

### 2.6.1 NordTest NTBuild 443 Bulk Diffusion Test

To overcome some deficiencies of previous tests, NordTest modified various parameters of the commonly used salt ponding test. The  $D_{28}$  value used in the default of Life-365 were obtained through this testing method. To prevent initial sorption effect when chloride solution is introduced, limewater is used to saturate the sample for 28 days instead of being air dried. In addition only the face of the sample is left uncovered and exposed to a 2.8M NaCl solution (see Fig. 2.8). The sample was then left in the solution for a minimum of 35 days before evaluation. If high quality

concrete is tested, the sample is immersed in the solution for 90 days or longer. Evaluation is done by using a mill or lathe to grind the concrete to dust at depth increments on the order of 0.5 mm. The chloride content is determined by AASHTO T260. The error function of Fick's Second Law is then used to fit the curve and determine the diffusion value and surface chloride concentration of the specimen [4, 18, 41].

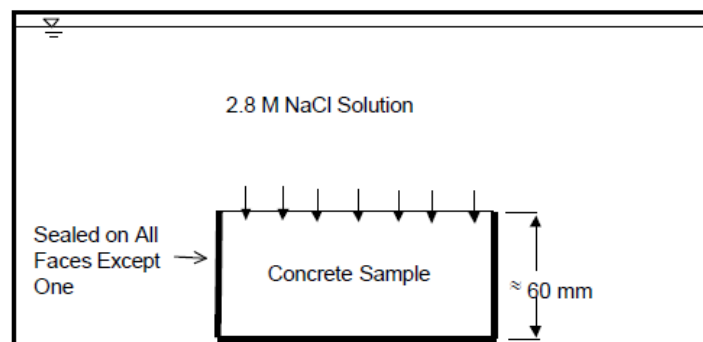


Figure 2.8 NordTest bulk diffusion test set up [18].

### **2.6.2 AASHTO T259 Standard Method of Test for Resistance of Concrete to Chloride Ion Penetration (Salt Ponding Test)**

The AASHTO T259 test uses three slabs or cores of at least 75 mm thick with a surface area of 300 mm square to measure the penetration of chloride ions into the concrete. Before exposure, the slabs are moist cure for 14 days and then stored in a drying room with 50% relative humidity for 28 days. After this conditioning period, the sample is then ponded in a 3% NaCl solution. Only the top face is exposed to the sodium chloride solution while the sides of the slabs are sealed. Meanwhile, the bottom face of the sample is left exposed to the drying environment (see Fig. 2.9). At the end of the exposure period, the samples are sliced at 0.5 inch interval, grounded and tested for chloride concentration [18, 41].

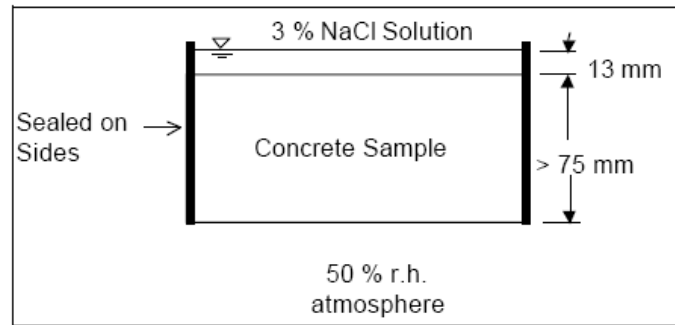


Figure 2.9 AASHTO T259 Salt Ponding Test set up [18].

A problem that arises during AASHTO Salt Ponding Testing is that due to the thick interval used, little information is gathered about the chloride profile. Chloride content value would be the average chloride concentration in each 0.5 inch slices, not the actual variation of chloride concentration over that 0.5 inch. In this case, two different concretes may have the same average chloride concentration, although one may have an approximately uniform chloride concentration while the other has a higher concentration near the surface and lower further in. Even though the first case would result in a faster chloride initiation period, AASHTO Salt Ponding Test could not detect this critical difference. In addition, since air drying is done for 28 days prior to exposure, initial sorptivity will occur when the concrete surface are in contact with the ponding solution. This would result in salt solution being drawn quickly from the salt solution to the pores of the concrete. Since the bottom face of the concrete is left exposed to a 50% relative humidity environment, transport mechanism in the form of wicking action occurs. Chloride ions in the water are transported from the wet front of the concrete to the drier atmosphere at the external face, which causes more chloride ions to penetrate [18, 41-43].

The transport mechanism that occurs during AASHTO Salt Ponding Test may be present in concrete structures, making this bulk diffusion test more realistic to the

condition experienced by concrete during its service life, but the relative importance of each transport mechanism is not reflected by the test's result. Since the relative amount of chloride which enters the chloride by capillary absorption to diffusion is greater when the test is done for 90 days and less than during the entire service life of concrete and also since the relative humidity gradient of a true concrete structure is less than that which occurs during the test, the importance of sorption and wicking will be overemphasized. Since insufficient chloride may penetrate the concrete in the 90 days for a meaningful chloride profile to develop, an extension of the test period is needed to assess the property of high quality concrete. Yet, despite the fact that the dominant transport mechanism is not pure diffusion, Fick's second law is still commonly used to determine the apparent diffusion coefficient [44, 45]. It should be remembered that the apparent diffusion coefficient obtained from Fick's second law does not correspond to the diffusion characteristic of the specimen at that time but is dependent on the entire exposure history of the concrete [18].

## **2.7 Service Life Models**

Numerical service life modeling has been used to predict the long term performance of a concrete mix design. Many ionic transport models have been developed in North America, Europe and Japan. The present state-of-the-art models include Life-365 and 4SIGHT.

### **2.7.1 Life-365**

Life-365 was created in the year 2000 by a consortium comprising of Grace Construction Product, Master Builders Technologies, and the Silica Fume Association. This model predicts the initiation period assuming diffusion to be the dominant

mechanism as governed by Fick's second law. The  $m$  factor is also considered to account for time-dependent changes in diffusion. The time required for the computer to perform this simulation is only a few seconds. A Windows interface is used in running the program. Meanwhile, a database is included in the model for the user to select some input parameters such as the chloride diffusion coefficient of the concrete mix [4]. This program is downloadable for free from the internet [46].

Life-365 is also able to estimate life-cycle costs based on the selected protection strategies and estimated construction, mitigation, and repair cost. In its analysis of life-cycle costs, the model calculates the estimated time for corrosion initiation of the concrete's steel reinforcement. In turn, it would then calculate estimates for the cost of initial construction, corrosion protection, and repairs during concrete's design service life.

In order to calculate life-cycle cost and predict the service life of concrete using Fickian diffusion modeling, Life-365 requires the user to input:

- Type and dimensions of concrete structural members
- Geographic location and exposure of the structure
- Depth of clear concrete cover to the reinforcing steel
- Details of concrete design method used (water-to-cementitious materials ratio, supplementary cementitious materials, corrosion inhibitors, barriers applied to the surface and type of reinforcing steel)
- Costs of the concrete constituent materials (mixture ingredients, reinforcement, corrosion protection strategies)
- Details and costs of the concrete repair strategy (frequency of repairs, average percent repaired, cost per unit area of repair, and inflation and discount rates).

With respect to the prediction of chloride ingress, only the exposure condition, reinforcement depth, and concrete design method is necessary for input. Default values from Life-365 can be used for input but it is strongly suggested that user update these values accordingly.

Despite being commonly used and considered the state-of-the-art computer modeling of concrete ingress, Life-365 has the following limitation:

- (1) Only the transport of a single ionic species is considered, which is the chloride ion
- (2) The numerical simulation can only be carried out when concrete is in a saturated condition, this means that advection is not considered as a transport mechanism for chloride ions.

In calculating the diffusion of chloride in concretes with fly ash addition, Life-365 considers the following assumptions [4]:

- (1) Fly ash are assumed to not affect the value of  $D_{28}$ , this is since results showing the effect of fly ash on the early age diffusion coefficient of concrete are inconclusive. Therefore the  $D_{28}$  of concretes with fly ash addition are calculated as that of OPC using the following empirical relationship which is based on its w/cm content:

$$D_{28} = 10^{(-12.06 + 2.40 (w/cm))} \dots\dots\dots (2.6)$$

- (2) Fly ash along with slag addition would significantly influence the time-dependent nature of the diffusion coefficient as reflected by the coefficient  $m$ . The value of  $m$  is determined through the following empirical relationship:

$$m = 0.2 + 0.4 (\%FA/50 + \%SG/70) \dots\dots\dots (2.7)$$

where

$\%FA$  = percentage of fly ash replacement in the concrete mix

$\%SG$  = percentage of slag replacement in the concrete mix

(3) For concrete structures in submerged condition,  $C_{\max}$  or maximum surface chloride concentration is calculated using the following relationship:

$$C_{\max} = (\text{chloride mass as fraction of solution}) \times (\text{density of solution}) \times (\text{concrete porosity as fraction of volume}) / (\text{density of concrete}) \times 100 \% \dots\dots\dots(2.8)$$

### 2.7.2 4SIGHT

4SIGHT is a free computer model from the National Institute of Standards and Technology in Gaithersburg, Maryland, which is available online through an html interface [47]. In contrast with Life-365, the computer model allows for the prediction of numerous ionic species simultaneously. However, the program considered that no electrical coupling occurs between the ionic species. 4SIGHT are also able to account for both diffusion and wetting and drying that represent the intertidal zone (advection). The influence of dissolution and precipitation of hydrated phases on the ionic transport properties are also considered when calculating the service life of concrete.

4SIGHT program was originally written to assess the performance of Low Level Waste (LLW) disposal facility by predicting the service life and hydraulic conductivity of the vault. The program incorporates multiple degradation mechanism by using a single transport equation for ions. Individual degradation mechanisms are generally controlled by a single ion species, such as chloride. However, as various ion species diffuse into the concrete, the transport properties change, which changes the rate of ion diffusion. The transport equation is converted into a finite difference equation for use in 4SIGHT. Therefore time would progress in discrete interval, whereby after every time interval, each computational element is put in chemical equilibrium using solubility products and a charge balance. Chemical equilibrium is achieved by satisfying the following conditions:

1. If a salt exists as solid, the constituent ion concentration product equals the solubility product.
2. The sum of the free charges from all available ions equals zero, insuring local charge neutrality.

As the pore solution pH changes, the available salts in the pore would either precipitate or go into solution. Any change in the quantity of solid salts in the pore space will change the porosity of the concrete which in turn would change the transport properties within the concrete. The synergism of the different degradation mechanism (chloride and sulfate attack) will be affected by the act of maintaining chemical equilibrium of these ionic species within the pore. By maintaining the system in chemical equilibrium, 4SIGHT allows for the interaction of degradation mechanisms within the concrete.

Despite the model's more comprehensive approach to chloride transport than Life-365, 4SIGHT is still limited in its ability to accurately assess the durability of concrete over time. One of its problems is the approach the model used for the chemical degradation of concrete during a sulfate attack. The degradation depth related to the penetration of sulfate ions and decalcification of the material is based on the Atkinson-Hearne model. This model is weak because the kinetics of degradation is not related to the real pores solution ionic concentration. This would lead to a numerical solution without any physical sense. Since 4SIGHT was initially develop to predict the long-term behavior of concrete containers used to store radioactive waste materials buried in soil, temperature and humidity conditions are considered constant. Therefore, the model does not allow for any variation of the boundary conditions through time, a feature that is readily available in Life-365 [34, 38].

4SIGHT allows for approximation and calculation for physical properties used as inputs in the program if no experimental data is available. These relationships are [34, 28]:

(1) Cement porosity ( $\emptyset$ ) can be approximated based on its degree of hydration ( $\alpha$ ) and w/cm ratio :

$$\emptyset = 1 - \frac{1+1.16\alpha}{1+3.2\frac{w}{c}} \dots\dots\dots (2.9)$$

where

$$\alpha = 0.65 + 0.1 \frac{(\frac{w}{c}-0.39)}{(0.45-0.39)} \dots\dots\dots (2.10)$$

(2) Permeability can be approximated for w/c in the range of 0.35 to 0.80 by:

$$k = 10^{5.0\frac{w}{c}} \times 10^{-21} \text{ m}^2 \dots\dots\dots (2.11)$$

(3) Formation factor is defined as the ratio of pore solution diffusivity ( $D_{\text{poresoln}}$ ) and the diffusivity of the bulk specimen ( $D_{\text{specimen}}$ ):

$$F = \frac{D_{\text{poresoln}}}{D_{\text{specimen}}} \dots\dots\dots (2.12)$$

where

$$\begin{aligned} \log_{10} \left( \frac{D_{\text{specimen}}}{D_{\text{poresoln}}} \right) = & \left( -5 - 0.82\frac{w}{c} + 32.55\left(\frac{w}{c}\right)^2 \right. \\ & + 8.374\text{CSF} + 15.36(\text{CSF})^2 \\ & + 23.15\left(\frac{w}{c}\right)\text{CSF} + 5.79\alpha - 21.1\left(\frac{w}{c}\right)\alpha \\ & \left. - 43.15(\text{CSF})\alpha - 1.705V_{\text{agg}} \right). \end{aligned} \dots (2.13)$$

where

CSF = fly ash addition rate multiplied by both its SiO<sub>2</sub> fractional content and an efficiency factor of 0.5.

V<sub>agg</sub> = volume fraction of aggregate

## CHAPTER THREE EXPERIMENTAL METHODOLOGY

### 3.1 Overview

An experiment program was set up to study the influence of fly ash content and time dependent diffusion coefficient on the service life of concrete. The flow diagram of the program can be seen in Figure 3.1. The program began with the obtaining of casted concrete specimens with varying w/cm and fly ash content. Series 1 utilizes already casted specimens, which has been stored in room condition for 285 and 650 days. Series 2 specimens were set for exposure immediately after 28 days in moist curing environment. Series 1 will be used to determine  $D_{28}$  and  $m$  parameters of concrete, while Series 2 will be used to determine  $C_{max}$  during exposure and to validate relationship models obtained from Series 1 result. These specimens were then exposed to chloride through ponding in 3% NaCl solution in accordance to a modified AASHTO T259 method to simulate one-dimensional chloride diffusion into concrete. After a determined exposure period of 30, 60, 90 days for Series 1 and 90, 180, 365 days for Series 2, the chloride exposure were terminated and specimen taken out for cutting and grinding. All specimens with 90 days or below exposure were cut at an interval of 2, 4, 6, 8, 10, 20, 30 mm, meanwhile those exposed to 180 days or above were cut at an interval of 5, 10, 20, 30 mm. This was done assuming that at chloride ingress were lower and shallower at early exposure periods, therefore smaller slices were needed. At later exposure period, it was assumed that the chloride ingress was deeper and its quantities more significant, therefore larger slices were sufficient in obtaining a meaningful chloride profile. The cut samples were then grounded to powder, passing the No. 50 mesh in accordance to the requirement of AASHTO T260/ASTM C114/ASTM C1152 [41, 48-49]. Automatic titration machine was used to determine acid soluble (total) chloride content according to the above AASHTO

and ASTM standards. Chloride profiles were then plotted and the diffusion coefficients are determined through curve-fitting method. These experimentally obtained profiles were then compared to profiles obtained from calculation using Life-365 and 4SIGHT. For Series 1, the reduction coefficient ( $m$ ) were then determined using concrete maturity ( $m_{total}$ ), average age during the exposure period ( $m_{avg}$ ), and effective time ( $m_{eff}$ ) as the time basis in addition to determination of their respective  $D_{28}$  values. The values of  $C_{max}$  were taken from Series 2 data. A relationship equation or models were then developed for the various fly ash content, w/cm ratio and exposure time. These relationships were then compared with similar relations obtained as default Life-365 relations and calculation from calculated profiles obtained by 4SIGHT lifetime prediction software. The predicted chloride profiles obtained from the relationship equations determined in this experiment were also compared with Life-365 and 4SIGHT for evaluation and validation. To verify the result of this experiment program, the obtained experimental relationship were used as input for Life-365 and the resulting predicted chloride profile will be compared with Series 1 and selected Series 2 experimental chloride profile.

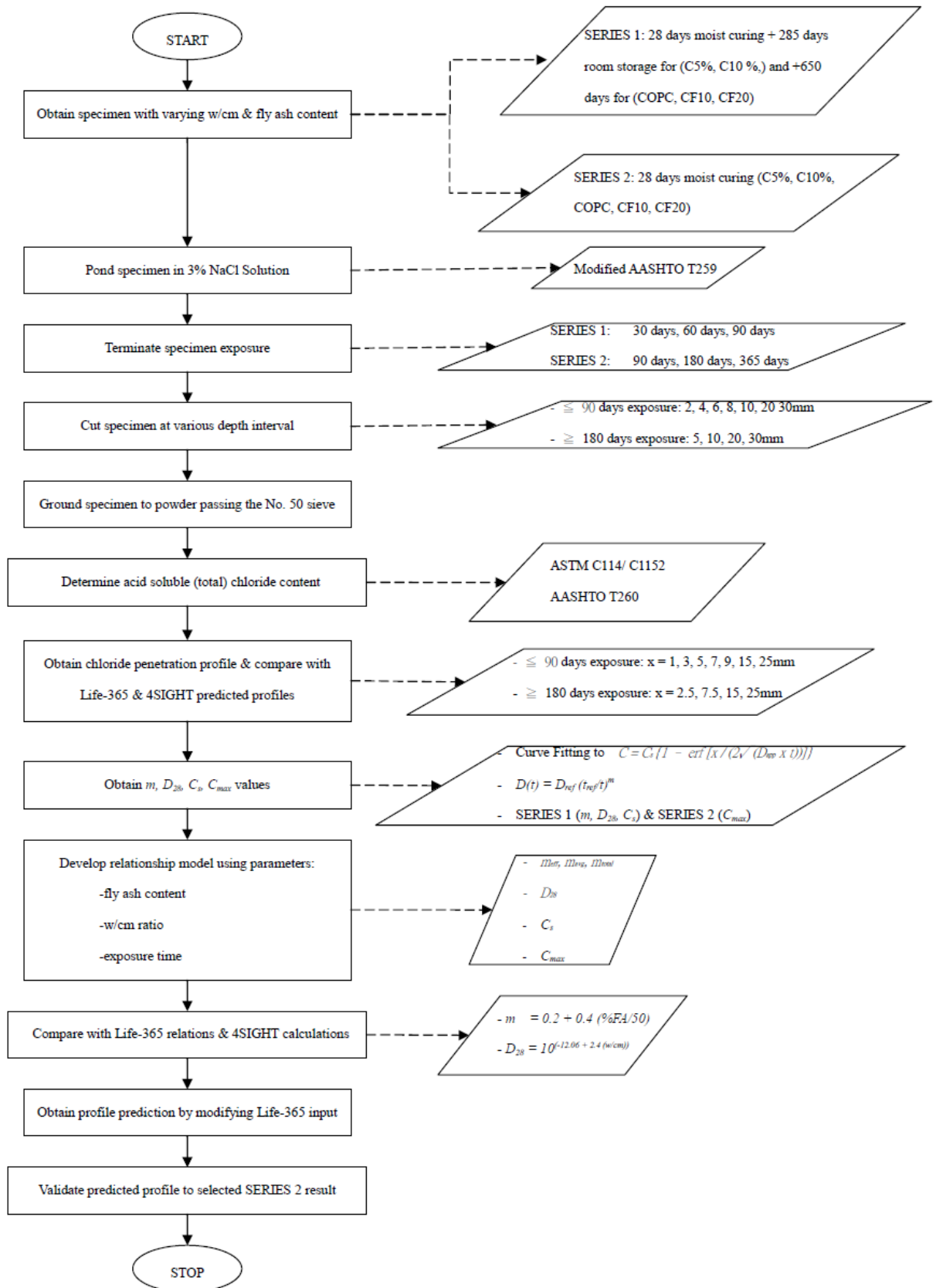


Figure 3.1 Experiment Program Work Flow Diagram

## 3.2 Materials

In order to obtain concrete specimens for the determination of chloride diffusion coefficient through ponding test and titration test, test specimens were casted by varying fly ash content of 0%, 10% replacement, 20% replacement, 5% addition, and 10% addition from the cement content. The materials used in the casting of the test specimens, ponding, and titrations were as follow:

1. The Portland cement used for the test specimens is Portland cement Type II which was produced by the Taiwan Cement Corporation. The Portland cement were purchased in bulk in sealed bag and placed in a dry storage room to avoid moisture affecting the properties and chemical composition of the cement. The chemical composition of the cement is shown in Table 3.1
2. Fly ash is a pozzolanic material which is obtained as a byproduct of coal-fired power plants. The fly ash used in the test specimens are Class F fly ash with main oxide components ( $\text{SiO}_2 + \text{Al}_2\text{O}_3 + \text{Fe}_2\text{O}_3$ ) of 91.07%, in accordance with the CNS 3036 minimum requirement of 70%. The source of the fly ash was the Taiwan Power Company's Taichung thermal power plant. The fly ash was sealed and stored to maintain the chemical composition of the material which is shown in Table 3.1.

Table 3.1 The chemical composition of experimental materials

Chemical Composition (%)	Main Test Materials	
	Portland cement type II	Fly ash
SiO <sub>2</sub>	24.42	54.09
Al <sub>2</sub> O <sub>3</sub>	4.45	28.94
Fe <sub>2</sub> O <sub>3</sub>	3.82	8.04
CaO	62.07	3.28
MgO	3.38	1.46
SO <sub>3</sub>	2.05	0.17
Na <sub>2</sub> O	0.15	0.57
K <sub>2</sub> O	0.60	1.54
C <sub>3</sub> S	46.00	-
C <sub>2</sub> S	27.00	-
C <sub>3</sub> A	5.30	-
C <sub>4</sub> AF	11.60	-
Loss on ignition	-	5
Fineness (m <sup>2</sup> /kg)	-	380

3. The coarse and fine aggregates used in this experiment were purchased from the domestic ready-mixed concrete companies with its plant in Chungli. The source of the coarse and fine aggregates is debris and natural stones from the Min River in Mainland China. The physical properties of the coarse and fine aggregates are seen in Table 3.2. The distribution of fine aggregates is seen in Table 3.3 while its particle size distribution curve is seen in Figure 3.2.

Table 3.2 Coarse and fine aggregates physical properties

Material Properties	Test Materials		Test Specification
	Coarse-grained materials	Fine aggregates	
BSG <sub>SSD</sub>	2.6	2.54	CNS 488
Water Absorption (%)	1.0	0.57	CNS 488
Unit weight (kg/m <sup>3</sup> )	1636	–	CNS 1163
Maximum size (mm)	12.5	–	CNS 486
Fineness modulus	-	2.60	CNS 486

Table 3.3 Grain size distribution of fine aggregate

Sieve Size No.	Amount Retained (wt. %)	Cumulative Amount Retained (%)	Cumulative Amount Passing (%)
#4	2	2	98
#8	9	11	89
#16	16	27	73
#30	25	52	48
#50	37	89	11
#100	10	99	1

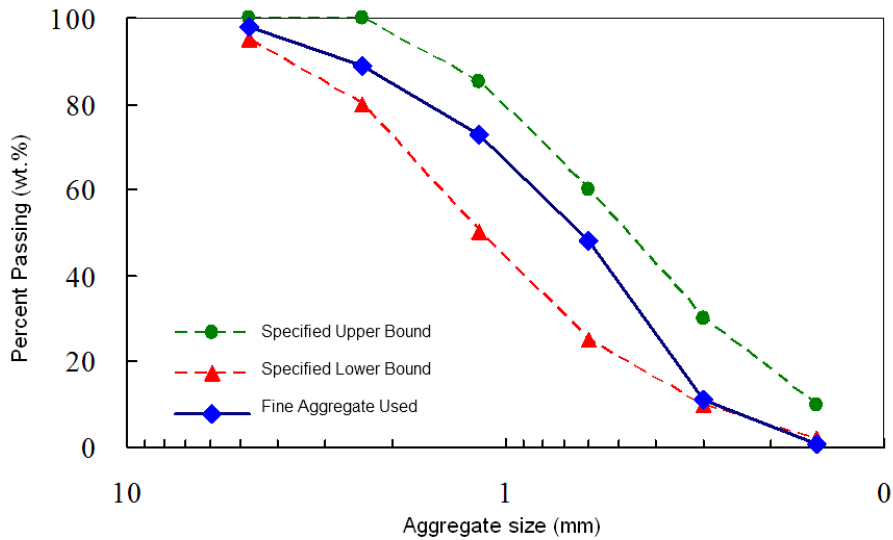


Figure 3.2 Particle size distribution curves of fine aggregate

4. Chemical agents used during the experiment include sodium chloride (NaCl), methyl orange ( $C_{14}H_{14}N_3NaO_3S$ ), ethyl alcohol ( $C_2H_5OH$ ), nitric acid ( $HNO_3$ ), and silver nitrate ( $AgNO_3$ ). The uses and origin of these agents are shown in Table 3.4.

Table 3.4 Uses and sources of chemicals used

Chemical Formula	Uses	Pharmacy Source
NaCl	Ponding Test	Japan Kojima, Inc. (reagent grade)
$C_{14}H_{14}N_3NaO_3S$	Chloride Determination	Koch-Light Lab. (reagent grade)
$C_2H_5OH$	Chloride Determination	Japan Kojima, Inc. (reagent grade)
$HNO_3$	Chloride Determination	63 Pure Chemicals (reagent grade)
$AgNO_3$	Chloride Determination	PANREAC (reagent grade)

5. The superplasticizer used in this experiment was the water reducing F-type superplasticizer produced by the Taiwan Sika Corporation with a water-reducing efficiency of 13%.

### 3.3 Specimen Mix Design

The ratio of water, admixture, and cementitious materials were proportioned to meet the nuclear safety requirements for concrete structures outlined in ACI 349-97 for a minimum compressive strength of 4000 psi and produced in accordance to ASTM C305-94. Concrete specimens were designated with ‘C’ in the specimen id. The suffix F10 indicates 10% fly ash replacement by weight of cement, F20 indicates 20% fly ash replacement, 5% indicates 5% fly ash addition, 10% indicates 10% fly ash addition, while OPC indicates only Portland cement without fly ash additions were used. The specimens were casted to a 5 × 5 cm cylindrical specimens, the form were removed after 28 days of moist curing in 100% humidity.

Table 3.5 Proportion of Concrete (kg/m<sup>3</sup>)

Mix ID	Cementitious material		Aggregates		Water	Water-reducing agent
	Type II cement	Fly ash	Coarse	Fine		
COPC	403.51	-	974.89	680.97	230	4.035
CF10	363.16	40.35	974.89	680.97	230	4.035
CF20	322.81	80.70	974.89	680.97	230	4.035
C5%	403.51	20.18	974.89	680.97	230	4.035
C10%	403.51	40.35	974.89	680.97	230	4.035

w / b: 0.57 for COPC, CF10 & CF20; 0.54 for C5%; 0.52 for C10%

### 3.4 Salt Ponding

Chloride exposure was achieved through ponding test based on a modified AASHTO

T259-02 (2002), “Standard Method of Test for Resistance of Concrete to Chloride Ion Penetration”. Prior to ponding, the specimens were saturated by being immersed in distilled water for 24 hours to ensure that diffusion would be the primary transport mechanism of chloride ingress. Ponding was done in a 3% (by weight) NaCl solution. Cut off 5 cm diameter PVC pipes were fitted on top of the cylinder test specimen and used to hold the NaCl solution used for exposure. This was done to achieve a unidirectional diffusion since only the top face was exposed to chloride solution. Silicone paste sealant was used on the edges between the PVC pipe and surface of the test specimen to prevent leaking of the solution and to hold the PVC pipe in place. This set up is seen in Figure 3.3. Plastic wraps were then used to cover the PVC pipes to prevent evaporation from the salt solution. The storage condition of the specimen during salt ponding test is seen below in Figure 3.4. The exposure periods were 30, 60, 90 days for Series 1 and 90, 180, and 365 days for Series 2. During exposure, the specimens were left in a laboratory environment. The NaCl solution was replaced once a decrease in the level of chloride solution was visually observed. After the exposure periods were reached, one specimen from each mix design of each series was removed, its surface dried and cleaned, and prepared for the next step in the experimental program.



Figure 3.3 Specimen salt ponding test set up



Figure 3.4 Specimen storage condition during salt ponding test

### 3.5 Specimen Cutting

After exposure, the cylindrical specimens were sampled by cutting. To facilitate precision sampling by the use of a circular diamond tip saw, the specimens were first cut half through its  $y$ -axis (top to bottom) using a carbide saw. Carbide saw cutting utilizes water as the coolant and lubrication while the specimens were held in place (jig) by hand. Specimens were dried after cutting to prevent contamination since transport mechanism of chlorides are facilitated by water. The halved specimens were then cut using a circular diamond tip saw (see Fig. 3.4). The specimens were held in place with a clamp and cutting depth was adjusted using a micrometer. Non-toxic chemical coolant and lubricant were used during the cutting. The specimens were then precision sampled at various depths. Specimens exposed to chloride for 90 days or less were cut at depth of 2, 4, 6, 8, 10, 20, and 30 mm to provide a more detailed chloride profile near the exposed surface while specimens exposed to chloride for at least 180 days were cut at 5, 10, 20, and 30 mm depths to reduce fluctuation of chloride content in addition to providing for more powdered samples for determination of chloride content.



Figure 3.5 Struers Minitom used for specimen cutting.

After cutting, each cut sample was cleaned and dried to prevent contamination, placed in a Ziploc bag and a permanent marker was used to indicate the depth, exposure period, and mix design of the sample. The remaining halved cylindrical specimens were also sealed in a Ziploc bag, marked, and stored. Sliced specimens during the experiment can be seen in Figure 3.5 below.



Figure 3.6 Sliced specimen for the profiling of chloride concentration at various depths

Samples from each depth interval were crushed to fine powder until all materials passes a 0.300 mm (No. 50) sieve by using a steel mortar and pestle. A steel hammer was first used to break the samples into smaller pieces. Grinding action was used to crush the samples. The steel mortar and pestle and the hammer were then cleaned by water and dried to prevent cross contamination. Each resulting grounded specimen powder was placed in a Ziploc bag and marked. Figure 3.6 shows the storage of powdered samples in Ziploc bags to prevent contamination.

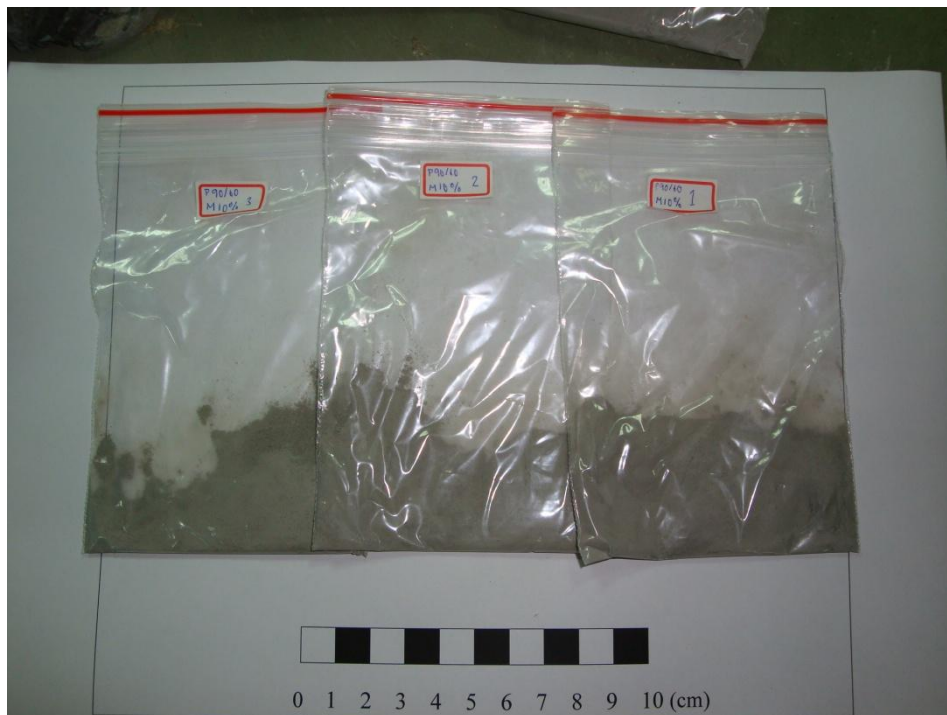


Figure 3.7 Storage of powdered samples in Ziploc bags.

### 3.6 Determination of Chloride Content

Powdered samples taken from various slices with different depth, mix design, and exposure periods are tested according to AASHTO T260 with a minimum sample requirement of 3 grams. Titration for total chloride determination were done using Titrimo automatic titration machine (see Fig. 3.5). The testing method is described below.



Figure 3.8 Titration 877 automatic titration machine for chloride content determination.

### 3.6.1. Bound (Total) Chloride Determination

AASHTO T-260 describes the procedure of determining chloride content obtained through acid digestion. The result of this test is the total chloride content in an obtained aqueous solution of the sample expressed as a percentage of weight of the dry sample. Total chlorides was attained since it was assumed that all chloride complexes (mainly chloroaluminates) present in the concrete sample will decompose by nitric acid and will enter the solution as chloride ions. The procedure of AASHTO T-260 followed in this experiment is described below.

1. Three grams of grounded samples were weighed to the nearest milligram.
2. The sample was then placed in a 250 ml beaker and 10 ml of distilled H<sub>2</sub>O were added, swirling to bring the powder into suspension.
3. Three milliliters of concentrated HNO<sub>3</sub> were added with continued swirling until the material is completely decomposed.
4. Forty milliliters of hot H<sub>2</sub>O were added while swirling to ensure complete sample digestion.
5. Since no sulfide bearing material were found in the sample, 3 ml of

hydrogen peroxide was added to decompose the chloride complexes in the sample. Five drops of orange methyl indicator (2 grams of methyl orange dissolved in 1 liter of ethanol) were added to the solution to confirm that the solution is sufficiently acidic, as indicated by the solution turning a persistent red color.

6. The beaker was then covered by aluminum foil and placed on top of a hot plate until boiling.
7. The beaker was removed from the hot plate and allows cooling until it was safe to handle.
8. The solution was filtered to a 250 ml Buchner flask through a coned, number 1, coarse-textured, filter paper (which was washed with distilled water before use) on a plastic filtration funnel. A vacuum pump was attached to the flask to assist filtration.
9. Sixty milliliters of hot distilled H<sub>2</sub>O were incrementally used to empty the slurry residue from the beaker into the filtration cone.
10. The filtrate was then returned from the flask into the empty beaker.
11. Forty milliliters of hot distilled H<sub>2</sub>O were used to wash the flask and the underside of the aluminum foil which was used to cover the beaker during boiling.
12. The washing were then collected and emptied into the original beaker along with the filtrate solution.
13. The approximately 150 ml final solution was divided into three equal portions for titration.
14. The solution was then titrated with 0.01M AgNO<sub>3</sub> solution with the endpoint of the titration being reached when the change in mV per volume of titrant added was at the maximum.

15. Percentage of chloride ion in the sample were calculated from the average determined from the three 50 ml titration portion using the formula:

$$Cl, \% = 3.5453 \times V \times N \dots\dots\dots (3.1)$$

where:

$V$  = volume of  $AgNO_3$  used for the sample titration

$N$  = normality of  $AgNO_3$  solution

### **3.7 Chloride Penetration Profile**

In order to plot the chloride concentration profile, average chloride concentration per slice against the midpoint of each depth interval was used. This would produce a plot of chloride values for depth of 1, 3, 5, 7, 9, 15, 25 mm for specimens exposed to salt solution for 90 days or less and 2.5, 7.5, 15, 25 mm for specimens exposed to salt solution for at least 180 days.

### **3.8 Diffusion Properties Analysis and Comparison with Existing Models**

#### **3.8.1 Surface Chloride Concentration & Apparent Diffusion Determination**

Chloride diffusion coefficient for each sample was then determined by fitting the data obtained in the chloride profile analysis to Fick's Diffusion Second law solution equation in Eq. 2.3. This was done through non-linear regression analysis in accordance with the method of least square fit. A trial version of a curve fitting computer program, DataFit Version 9.0, obtained freely through the internet [50] was used to assist this calculation.

Fick's second law error function solution was set as the curve for fitting with the time  $t$  set as the time of exposure in second. Chloride depth in meter was set as the  $x$ -value and measured chloride concentration in percent of concrete from the titration test is set as the  $y$ -value. The  $C_s$  and  $D_{app}$  value were then obtained from the curve fitting result calculated by the software. The goodness of fit of the curve was evaluated by the  $R^2$  (coefficient of multiple determination) value, which was also calculated by the software. A  $R^2$  value of 1 indicates a perfect fit whereby the best fit curve passes through all the data points while a value of 0 indicates a poor fit whereby the curve fits the data no better than a straight line going through the mean of all the  $y$ -values.

### **3.8.2 Diffusion Reduction Coefficient Calculation**

Diffusion reduction coefficients were calculated using the apparent diffusion coefficient determined using DataFit. The value of  $m_{total}$ ,  $m_{avg}$ , and  $m_{eff}$ , were determined by each different time basis for the calculation of  $m$  in accordance to the methods outlined in Section 2.3.1. Due to their simple determination of time basis,  $m_{total}$  and  $m_{avg}$  can be obtained using direct calculation of the diffusion reduction equation. Meanwhile  $m_{eff}$ , since iterative steps are taken for determination, are obtained by using Microsoft Excel.

### **3.8.3 Empirical Relationship Equation Determination**

In order to find an empirical relationship function between concrete properties,  $m_{total}$ ,  $m_{avg}$ ,  $m_{eff}$ , and  $D_{28}$  (diffusion coefficient at 28 days) with concrete design parameters of w/cm ratio and fly ash content, a free trial version of LAB Fit software [51] was used. Since these relationship functions are purely experimental, then no theoretical function was used to fit the data. Instead, LAB Fit was used to select the most appropriate functions in its function library for the data obtained. To do so, the "Find"

button was used. The numbers of parameters of the relationship functions are selected in the “Conditions” dialog box and “OK” is clicked. The computer program will then initiate the selection process to obtain the best fitting result including its  $R^2$  (coefficient of multiple determination) value. The menu of LAB Fit is seen in Figure 3.5 below.

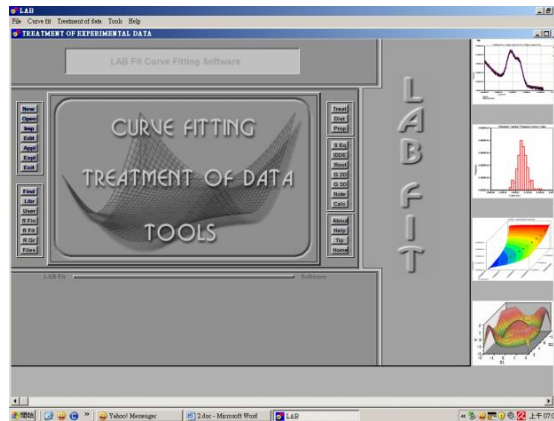


Figure 3.9 The menu of LAB Fit curve fitting software.

### 3.8.4 Comparison with Existing Lifetime Prediction Models

In order to compare the result of the relationship function obtained from the experimental data with existing lifetime prediction models, two comparison methods were selected. Only Series 1 experimentally obtained profile were used in the comparison. The first comparison method would compare the  $m_{total}$ ,  $m_{avg}$ ,  $m_{eff}$  along with their respective  $D_{28}$  value and the  $C_s$  buildup rate obtained from the experimental data with that of Life-365 and 4SIGHT. Comparison with Life-365 was done simply by comparing the mentioned values with the default value used in Life-365 for similar fly ash replacement and water to cementitious material ratio. Meanwhile comparison with 4SIGHT was done by using predicted chloride profile from 4SIGHT and using them similarly to that of the experimental data to calculate the mentioned values. The second comparison method would compare the chloride profile or penetration curve predicted by Life-365 and 4SIGHT with that of real experimental data.

In determining the input parameter necessary for Life-365 and 4SIGHT calculation, the approximation in Section 2.7.1 and 2.7.2 were used. In addition to the approximation in Chapter 2, for 4SIGHT, values of the internal chloride concentration were approximated by using an online pore solution calculator which was also provided by NIST [52], meanwhile concrete density value are calculated from NIST Virtual RCPT website [53]. While for  $C_{\max}$  calculation in Life-365, density of solution water was obtained from Mettler Toledo's online data table [54].

### **3.8.5 Validation of Empirical Relationship Equation**

To validate the relationship model for concrete with fly ash addition obtained from Series 1 data of this research, the empirical relationship equations for  $D_{28}$  and  $m$  values were used to replace the default Life-365 relations. The  $C_s$  build up time obtained from Series 1 will also be used to modify the exposure condition of Life-365. Meanwhile the  $C_{\max}$  value from Series 2 will be used as the  $C_{\max}$  value for Life-365 input. Due to the similarities between the transport mechanism and assumption concerning diffusion taken by Life-365 computer software with that of this research, Life-365 can be used as a platform to run and evaluate this research's empirical relationship result since Life-365 allows the user to change the  $D_{28}$ ,  $m$ ,  $C_s$  build up time, and  $C_{\max}$  from its default value to a user determined value.

Evaluation was done by comparing the chloride profile prediction obtained from the modification of Life-365 parameters using this research's empirical relations (with effective, average, and total time as basis of calculation) with that of selected Series 2 chloride profile obtained from Salt Pounding Test for 90, 180 and 365 days.

## CHAPTER FOUR RESULTS AND DISCUSSION

### 4.1 Experimental Data

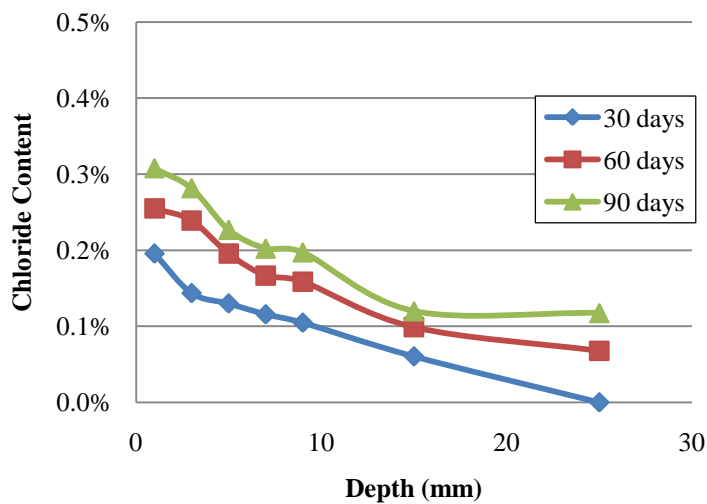
After specimens were exposed to chloride through a modified AASHTO T259 Salt Ponding Test, it was then cut, profiled, ground and its chloride content determined by titration through the methods outlined in Chapter 3. After subtracting the relatively small background chloride value (ranging from 0.006% to 0.008%, depending on chloride mix), the chloride contents (in percent of concrete weight) were set as the  $y$ -values and plotted against the average depth per profile section as the  $x$ -value.

The influence of fly ash towards the diffusivity of concrete was apparent from Series 1 experimental result. Series 1 specimens were mature concretes which have been stored for 285 or 650 days prior to exposure for 30, 60, and 90 days. Meanwhile, Series 2 indicated the maximum surface chloride ( $C_{max}$ ) reached during exposure to chloride through salt ponding. Series 2 were concrete specimens which were immediately exposed to chloride after 28 days of moist curing for a period of 90, 180, and 365 days.

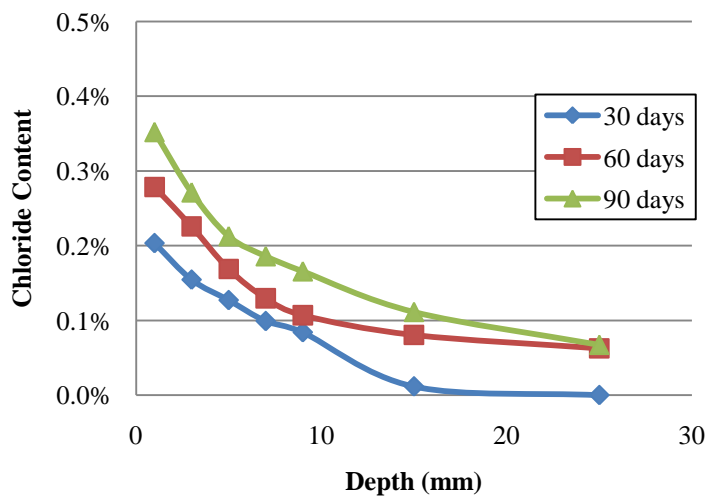
#### 4.1.1 Series 1 Experimental Data

Figure 4.1 shows the chloride penetration profile obtained from samples with various exposure times for the five concrete mixes in this study. As can be seen from Figure 4.1 below, for all concrete mixes, chloride continues to diffuse into concrete with time. This was clearly seen by the increase in chloride concentration inside the concrete (measured by percent of concrete's weight), which continues to increase with time. Meanwhile, the steepness of the curve indicates the rate of diffusion. A flat curve would be an indicator that chloride diffuses very quickly that the concentration of

chloride inside the concrete equals to the concentration on the concrete's surface. A steep curve on the other hand would indicate that the diffusion is slower; although the concentration on the surface is high, the concentration inside the concrete is low due to slow ingress of chloride from the surface to the concrete's interior. As indicated also from Figure 4.1, it was observed that the rate of diffusion or diffusivity of chloride into concrete reduces with time. This was seen from the apparent increase in the steepness of the curve with time.

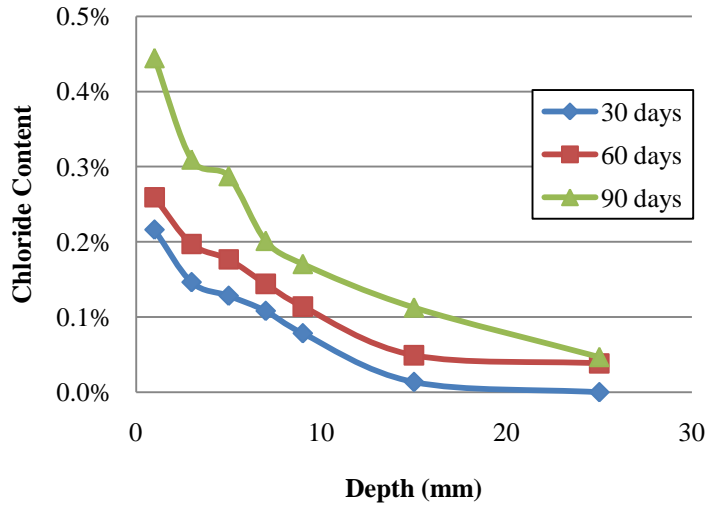


(a) COPC

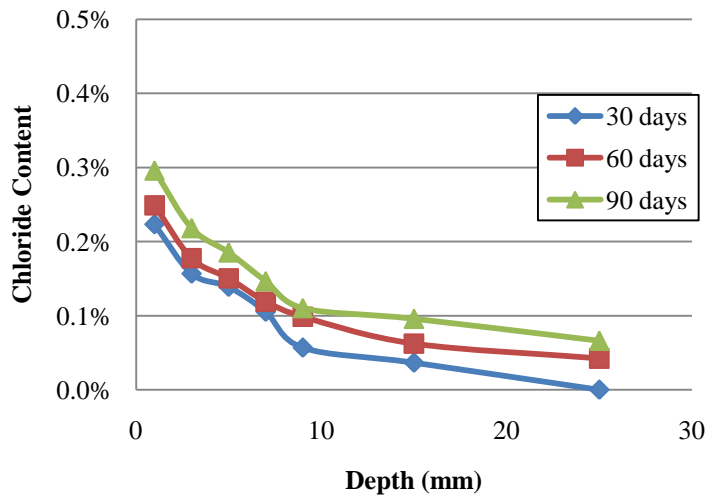


(b) CF10

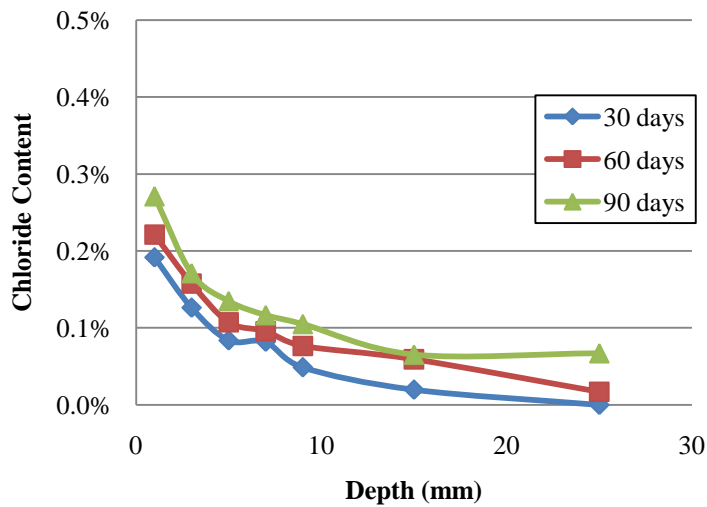
Fig. 4.1 to be continued



(c) CF20



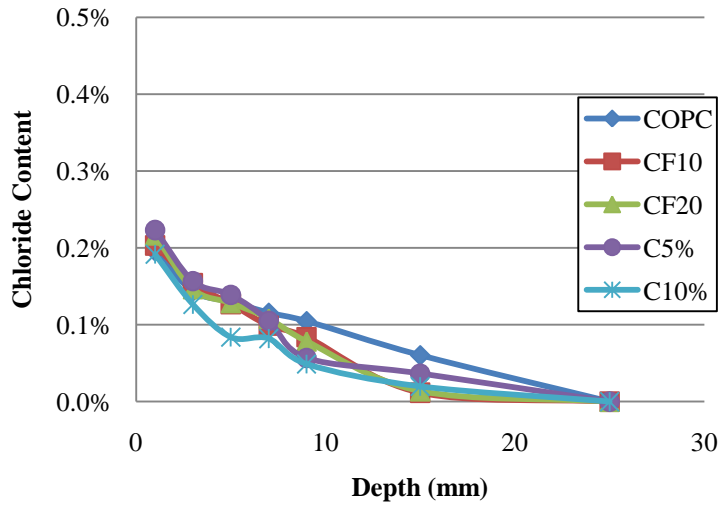
(d) C5%



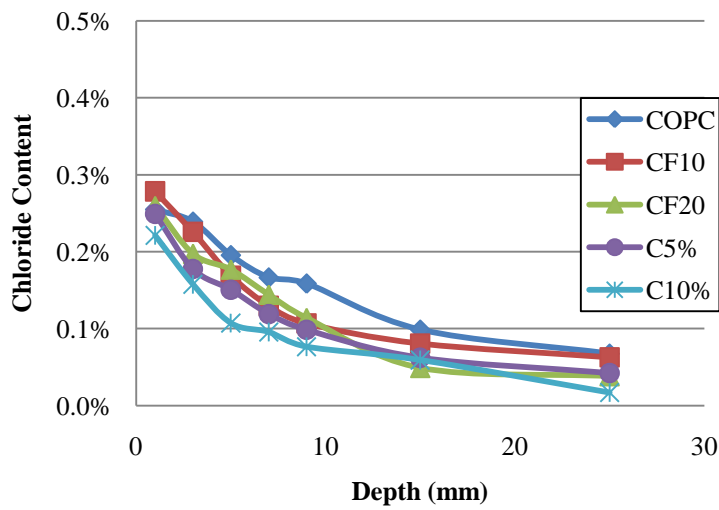
(e) C10%

Figure 4.1 Chloride profiles at different exposure times

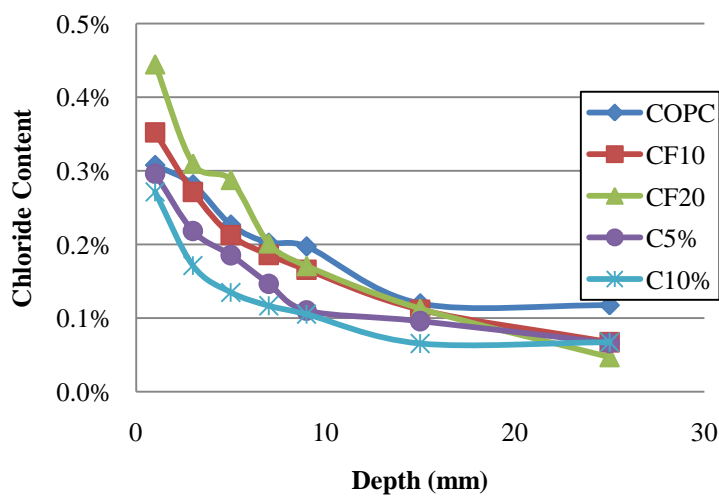
As indicated in Figure 4.2, the experimental result of Series 1 also shows that at early ages, the influence of fly ash on diffusivity was not starkly apparent. At later age, 90 days, it can be clearly observed that higher fly ash addition would reduce diffusivity. The steepness of the CF20 curve compared to the relative flat curve of COPC was an indicator of the influence of fly ash on reducing the rate of chloride ingress. The fact that C10%, which has the lowest w/cm ratio, continues to have the smallest value was an indicator of the importance of low w/cm ratio in reducing chloride diffusivity.



(a) 30 days



(b) 60 days



(c) 90 days

Figure 4.2 The influence of fly ash addition to chloride ingress in concrete

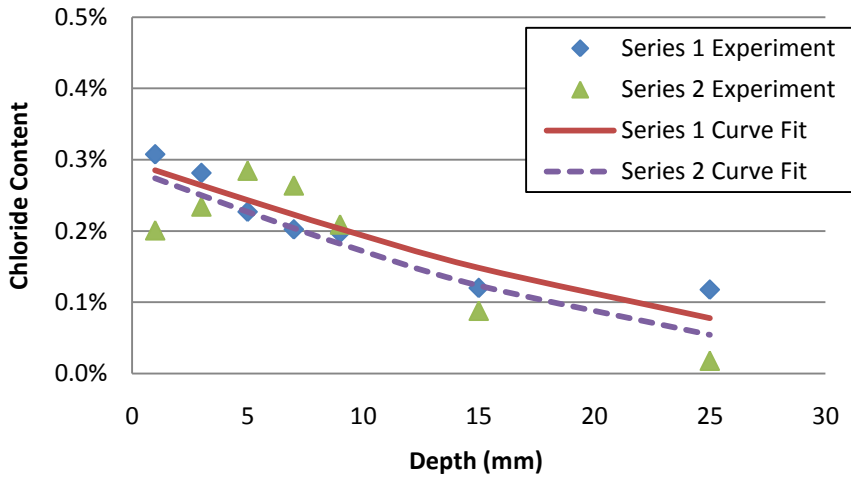
#### 4.1.2 Series 2 Experimental Data

In Series 2 specimens, experiment was done to determine the maximum surface concentration ( $C_{\max}$ ) that would be reached during exposure to chloride through ponding.  $C_{\max}$  is attained when there is a chemical equilibrium between the solution and the concrete surface, hence once the  $C_s$  reaches the  $C_{\max}$  value; it would continue to remain relatively unchanged despite increased exposure time. This was done by observing the surface chloride value ( $C_s$ ) at different exposure time. The maximum concentration reached would be designated as the  $C_{\max}$  value of the concrete mix. The value of  $C_{\max}$  can be seen in Table 4.1. Series 2 results indicate that by 180 or 365 days exposure,  $C_{\max}$  has been reached and its value stabilized when chemical equilibrium between the concrete and the ponding solution was achieved [29]. It was also worth noting that the general result of  $C_{\max}$  obtained in Series 2 (with the exception of COPC) confirms finding from previous research that there is a reduction of  $C_{\max}$  value with increasing w/cm ratio. This was since higher w/cm is more likely to have a thicker cement paste layer on the concrete surface which would enhance the dielectric activity between hydroxyl ions in the concrete surface and chloride ions in solution, and thus the increased repulsive force removes chloride ions from the surface of the concrete. For concrete containing fly ash with similar w/cm ratio, it was also confirmed that higher level of fly ash addition would increase the  $C_{\max}$  value. This was due to the influence of fly ash in increasing chloride binding capacity, which would increase the total chloride content near the surface of the concrete but decrease chloride concentration deeper in the concrete [29].

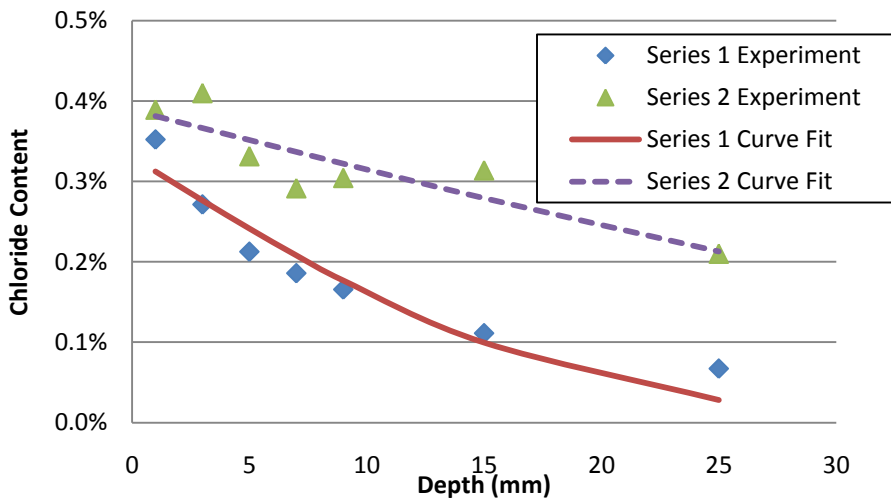
Table 4.1  $C_{\max}$  Values

Properties	Concrete Mix				
	COPC	CF10	CF20	C5%	C10%
$C_{\max}$ (% wt. concrete)	0.561	0.525	0.698	0.767	0.796
Observed Exposure Period (days)	180	180	365	180	180

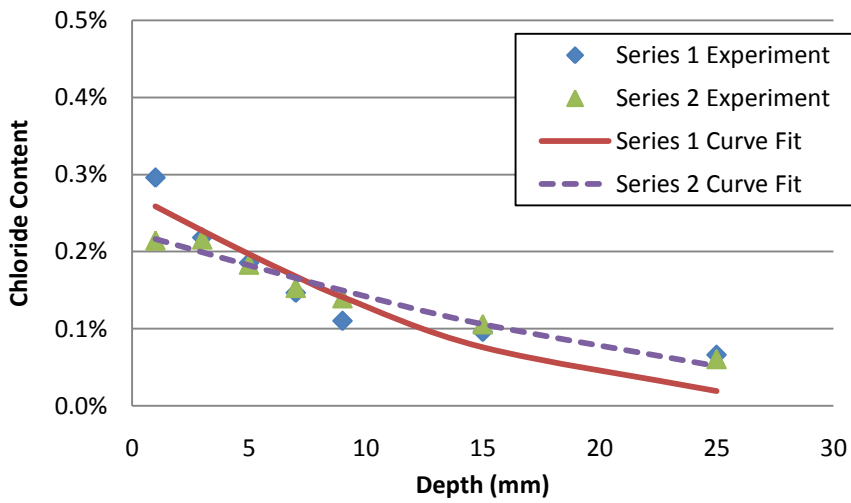
In Figure 4.3, comparison between the profile and curve fitting of COPC, CF10, and C5% specimens from Series 2 exposed to 90 days ponding with that of Series 1 with similar exposure time is shown. It is clear that despite the extended storage time of Series 1 specimens prior to exposure; no significant difference in their profile result and diffusion properties can be concluded. Profiles seem to indicate that the diffusion value of stored specimen were either similar or slightly lower than those immediately exposed to chloride after moist curing. It can thus be deducted that the process of hydration, which improves the chloride resistance of the material, seems to be hampered due to storage at dry condition.



(a) COPC



(b) CF10



(c) C5%

Figure 4.3 Comparison between 90 days result of Series 1 and Series 2

The majority of Series 2 result, especially for 180 days and 365 exposures, shows erratic trend, therefore producing curve fits with low  $R^2$  value. The reason for this erratic behavior may be the possible contamination of the sample during long storage. Leak in the silicone paste sealant was also probable since in some cases, the interior of the concrete has much larger chloride ion concentration than the surface. The high concentration in the internal of the concrete may also be explained by the fact that the side of Series 2 specimens was not covered in wax like that of Series 1. This would allow evaporation to occur in the middle of the specimen from the exposed side, evaporation would then cause salt crystallization hence producing high chloride concentration. Since such result does not conform to the existing diffusion theories, the determination of diffusion parameters such as  $D_{28}$  and  $m$  were not done using Series 2 data. A complete result of Series 2 data can be seen in the Appendix.

## **4.2 Determination of Concrete Properties**

### **4.2.1 $D_{app}$ , $C_s$ , and $C_{max}$ Determination**

To determine the properties of concrete, data from the two series were used. Series 1 data were used to determine the surface chloride concentration,  $C_s$ , and apparent diffusion coefficient,  $D_{app}$ , using DataFit curve fitting software as outlined in Section 3.8. The same method was used for Series 2 data to determine the maximum surface chloride,  $C_{max}$ , reached during exposure through salt ponding test. DataFit software also allows for the determination of  $R^2$  (coefficient of multiple determination), which would be an indicator as to how error function solution to Fick's second law could explain the chloride penetration result from the ponding test.

The curve fitting of the error function solution of Fick's second law for Series 1 can be seen in Figure 4.4 to 4.8. Meanwhile, the value of  $C_s$ ,  $D_{app}$ , and the fitting curve's  $R^2$  can be seen in Table 4.2. As discussed in Section 4.1.2, for the determination of  $C_{max}$ ,  $C_s$  value from the curve fitting of Series 2 was used.  $C_{max}$  was taken as the highest  $C_s$  value for each concrete mix determined during the test. The value of  $C_{max}$ , and the exposure period in which it was obtained can be seen in Table 4.1.

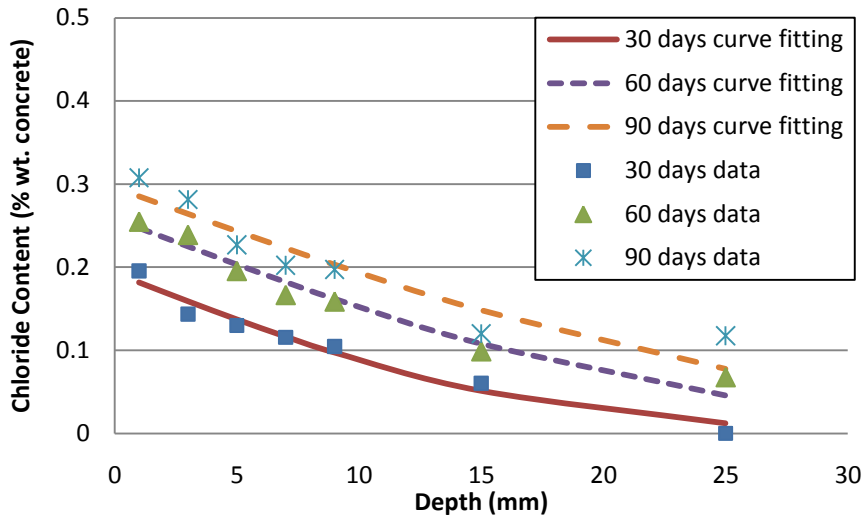


Figure 4.4 COPC Curve Fitting

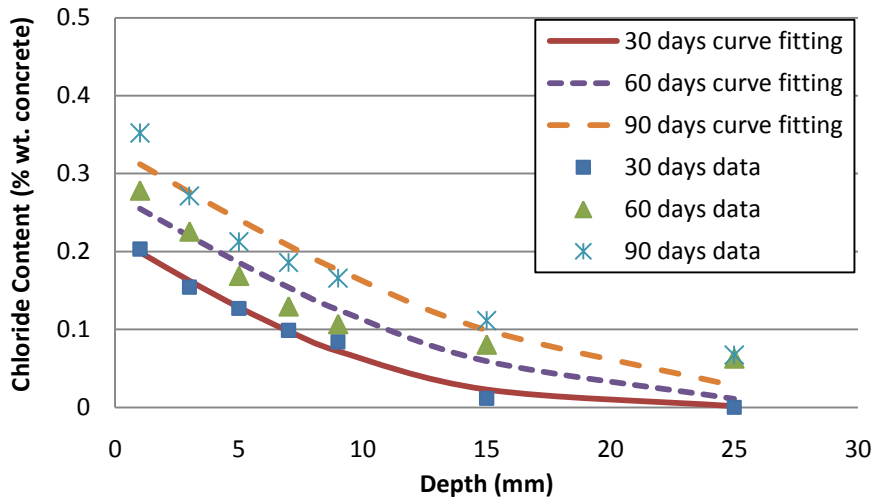


Figure 4.5 CF10 Curve Fitting

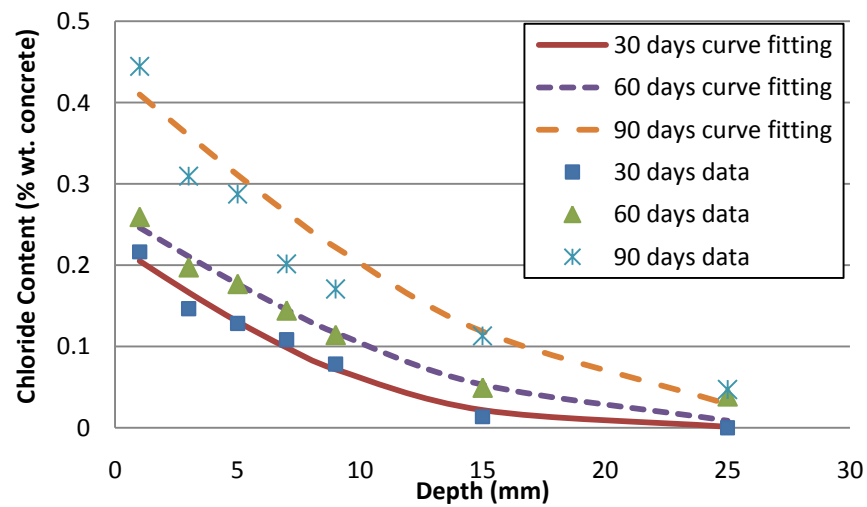


Figure 4.6 CF20 Curve Fitting

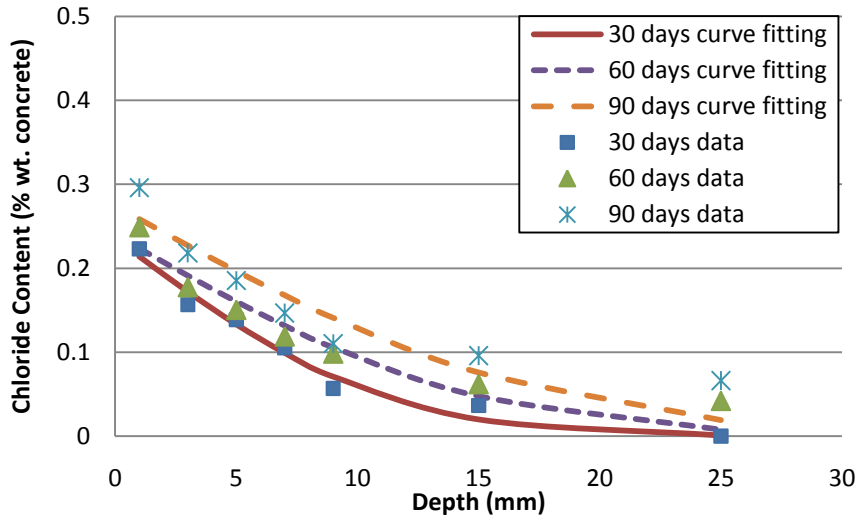


Figure 4.7 C5% Curve Fitting

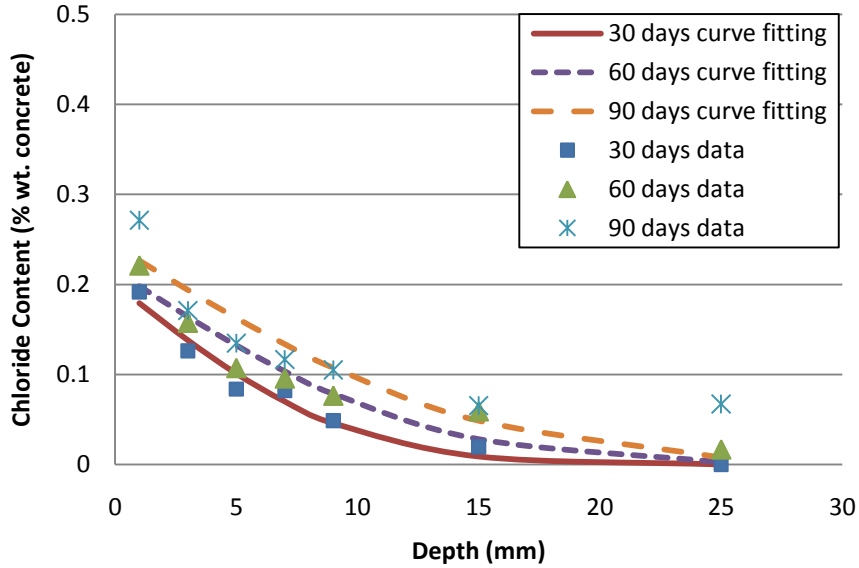


Figure 4.8 C10% Curve Fitting

Table 4.2 The values of  $C_s$  and  $D_{app}$  Obtained from Curve Fitting

Exposure	Properties	Concrete Mix				
		COPC	CF10	CF20	C5%	C10%
30 days	$C_s$ (% wt. concrete)	0.193	0.218	0.225	0.235	0.200
	$D_{app}$ ( $\times 10^{-11}$ m <sup>2</sup> /s)	3.51	1.65	1.58	1.46	1.08
	$R^2$	0.967	0.989	0.979	0.976	0.967
60 days	$C_s$ (% wt. concrete)	0.258	0.273	0.264	0.240	0.216
	$D_{app}$ ( $\times 10^{-11}$ m <sup>2</sup> /s)	3.31	1.42	1.33	1.32	0.95
	$R^2$	0.960	0.867	0.967	0.916	0.910
90 days	$C_s$ (% wt. concrete)	0.296	0.330	0.435	0.274	0.243
	$D_{app}$ ( $\times 10^{-11}$ m <sup>2</sup> /s)	3.2	1.35	1.2	1.22	0.88
	$R^2$	0.876	0.914	0.941	0.852	0.758

From the  $R^2$  value of Series 1, it was noticed that relatively high  $R^2$  value were obtained for all concrete mix during 30 day exposure (above 0.90). This value generally decreases with longer exposure period. Since  $R^2$  value indicates how good the curve of error function solution of Fick's second law explains the data points, it can thus be concluded that diffusion governed by Fick's second law was the dominant chloride ingress mechanism in the early exposure period. The immersion of the relatively small specimen in distilled water for 24 hours has allowed sufficient saturation to prevent significant wicking and sorption during early age exposure. Although still relatively high, the reduction in  $R^2$  value with longer time exposure shows that in addition to diffusion, other mechanism or factors influences the transport of chloride ions at longer exposure periods. This factor may be due to

wicking which occurs because of the drying of the exposed bottom side of the specimen with time [41], in addition to the crystallization of salt on the pores of concrete (which influences its transport properties) [4].

Series 1 data show that surface chloride concentration was observed to have increased with time. This indicates the time dependent nature of  $C_s$  as observed in previous researches [29]. The diffusion coefficient obtained from Series 1 indicates the influence of fly ash content and w/cm ratio on the diffusivity of concrete. It was generally observed that diffusivity values for all exposure period decreases with decreasing w/cm ratio. This was in agreement with generally accepted notion that a lower w/cm ratio would produce a denser concrete with smaller capillary pores, hence reducing chloride diffusivity. The influence of fly ash was also apparent for concretes with similar w/cm ratio. Higher fly ash content was shown to reduce the diffusivity. As previously discussed in Chapter 2, this reduction in diffusivity was achieved mainly by the densification of the matrix by refining the pore structure of the concrete and to a limited effect through the reduction of thickness of the interfacial zone.

#### **4.2.2 Determination of $m$ and $D_{28}$ Values**

The value of  $m_{total}$ ,  $m_{eff}$ , and  $m_{avg}$  of Series 1 were determined using methods outlined in Section 2.3.1. Storage period were not considered in the calculation of the time basis for  $m$  value determination. The time taken into account was the initial 28 days curing of the specimen during production with the exposure period during salt ponding test. The different time basis (average, effective, total) used in the calculation of  $m$  would also have an implication on the value of  $D_{28}$ . The value of  $D_{28}$  was calculated by using the regression equation of diffusivity versus time on log-log basis for the different time basis. Table 4.3 summarized the  $D_{28}$  and  $m$  values calculated

using the three different time basis. Figure 4.9 to Figure 4.11 shows the reduction of diffusion coefficient with time on a log-log basis (as indicated by the  $m$  value) for the different time basis.

Table 4.3 Experimental  $D_{28}$  and  $m$  Values

Properties	Concrete Mix				
	COPC	CF10	CF20	C5%	C10%
$D_{28, total}$ ( $\times 10^{-11}$ m <sup>2</sup> /s)	3.88	1.91	2.2	1.71	1.16
$D_{28, avg}$ ( $\times 10^{-11}$ m <sup>2</sup> /s)	3.88	1.93	1.97	1.59	1.4
$D_{28, eff}$ ( $\times 10^{-11}$ m <sup>2</sup> /s)	3.79	1.96	2.01	1.71	1.29
$m_{total}$	0.131	0.289	0.388	0.255	0.284
$m_{avg}$	0.177	0.387	0.522	0.343	0.382
$m_{eff}$	0.200	0.454	0.626	0.399	0.447

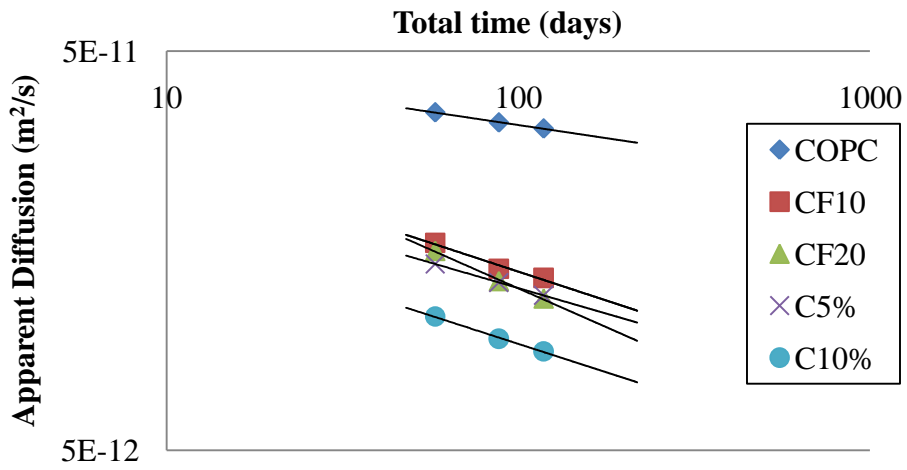


Figure 4.9 Reduction of diffusion coefficient with time-total time basis

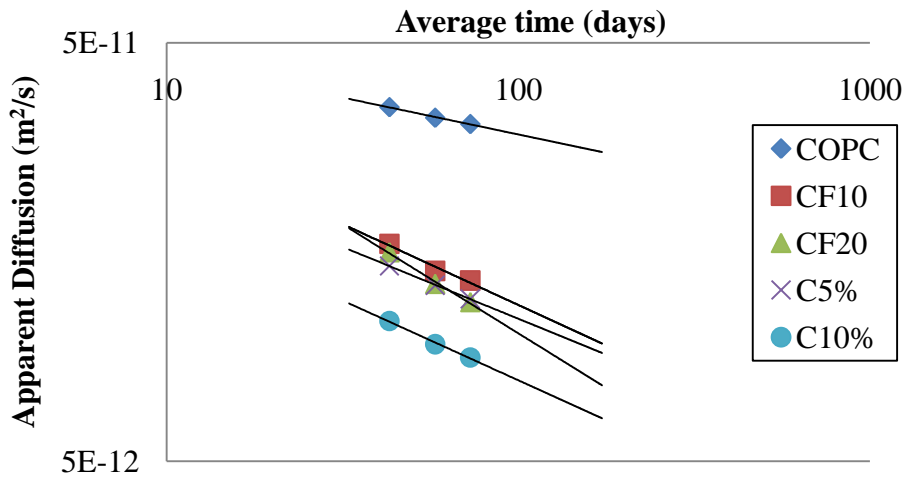


Figure 4.10 Reduction of diffusion coefficient with time-average time basis

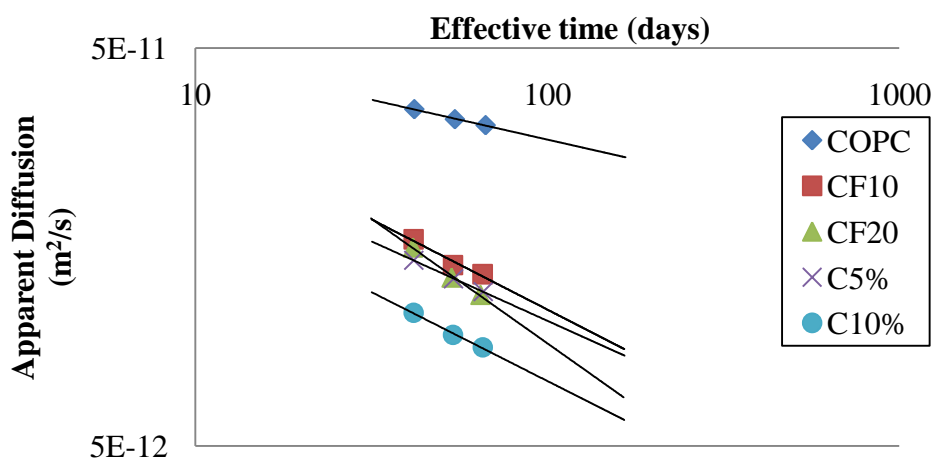


Figure 4.11 Reduction of diffusion coefficient with time-effective time basis

It is apparent from the Figure 4.9 to Figure 4.11 that  $m$  value, or the reduction in diffusivity with time, increases with increasing fly ash content. The trend in the Figures was similar to that of Figure 2.5. As discussed in Chapter 2, fly ash continuously reacts to further refine the pore structure of concrete with time. This improvement in pore structure with time would be more apparent in concretes with higher fly ash content. The close  $m$  value of CF10 and C10%, which has a stark w/cm ratio difference (0.57 and 0.54 respectively) while having similar fly ash content (10% and 9.09% respectively), indicates the insensitivity of  $m$  to w/cm ratio. This was in line with existing theory that only fly ash addition would influence the value of  $m$  [4].

### **4.3 Comparison between Experimental & Predicted Result**

A comparison of the chloride profile result from Series 1 of the experiment was made with chloride profiles from Life-365 and 4SIGHT calculation in order to evaluate the prediction based on Fick's law (Life-365), and that considers ion transport and chemical reactions within the concrete (4SIGHT). Since these softwares require various input values for their calculation, many of them requiring extended test which were beyond the scope of this research for determination, a sound approximation of the input value was necessary.

#### **4.3.1 4SIGHT Approximation and Input Values**

As seen from the screenshot of 4SIGHT in Figure 4.12, various inputs are necessary for the calculation. To simplify, the Monte Carlo option were unchanged (default). Meanwhile in the Geometry option; crack spacing, crack width, and crack depth were set to zero. This was since the original 4SIGHT program was made for concrete slabs sufficiently large to experience bending on its own weight and produce cracks. Since small cylindrical concrete specimens were used, it was assumed that the force of

bending and shrinkage would not be sufficiently high to produce significant cracks. The thickness of the specimen was set at 5 cm and the reinforcement depth was set at 3 cm. Three centimeter depth was selected since this would also be the maximum depth of the slice used for the determination of chloride profile in Series 1.

Section	Parameter	Units	External Surface	Internal Surface	Distribution
Concrete Properties	Formation Factor		0.000	0	Delta
	Porosity		0.05	0	Delta
	Permeability	cm/s	1.0E-9	0	Delta
	w/c		0.45	0	Delta
Cement Properties	K <sub>2</sub> O	Mass %	0.2		
	Na <sub>2</sub> O	Mass %	0.4		
Geometry	Concrete Thickness	m	1.0	0	Delta
	Reinforcement Depth	m	0.3	0	Delta
	Crack Spacing	m	0.0	0	Delta
	Crack Width	m	0.000100	0	Delta
	Crack Depth	[0-1]	0.2	0	Delta
	Hydraulic Pressure	m (Head)	0	0	
Boundary Conditions	OH <sup>-</sup>	mol/L	0.0	0.0	0.0
	K <sup>+</sup>	mol/L	0.0	0.0	0.0
	Na <sup>+</sup>	mol/L	0.0	0.0	0.0
	Cl <sup>-</sup>	mol/L	0.0	0.0	0.0
	SO <sub>4</sub> <sup>2-</sup>	mol/L	0.0	0.0	0.0
	Mg <sup>2+</sup>	mol/L	0.0	0.0	0.0
Monte Carlo	Random Seed		12345		
	Iterations		1		
Termination	Time Limit	hrs	100		
Response	Use Email		nobody@localhost		

Figure 4.12 Screenshot of 4SIGHT input options

For the Concrete Properties option, approximation and calculation as outlined in Chapter 2.7.2 were done. The water to cement ratio used for the calculation were taken as the effective water to cement ratio. Effective water to cement ratio considers that some fly ash component are assigned as equivalent to cement and influences the w/cm ratio. Those fly ash content not considered to influence the effective w/c ratio by being equivalent to cement were considered to be equivalent to silica fume and contributed to the Formation Factor by influencing the CSF.

For the determination of the Formation Factor, density of concrete needed to calculate  $V_{agg}$ , the degree of hydration at 28 days ( $\alpha$ ), and the effective w/c were directly obtained from NIST's Virtual RCPT website [53]. The total rate of fly ash addition was then subtracted by fly ash contributing in the effective w/c in order to determine CSF. Data on the concrete mix, aggregate properties, and chemical composition of cement and fly ash used as input in the website were taken from Table 3.1, Table 3.2, and Table 3.5 respectively.

Porosity value was approximated using the relations of Eq. 2.9. The porosity of concrete was assumed to be its maximum possible value, or equal to the porosity of cement paste. The w/c ratio used was the effective w/c obtained from NIST's Virtual RCPT website [53]. This was done since the relationship on Eq. 2.9 was based on the degree of hydration which in turn is dependent on effective w/c. The same consideration was also done in determining permeability from Eq. 2.11.

The External Surface chloride ion values in the Boundary Conditions option were calculated by assuming that the 3% NaCl (by weight) would dissolve completely in water. NaCl molar weight of 58.443 and Chloride's atomic weight of 35.452 were used to calculate the  $Cl^-$  concentration in mol/L. This calculation yields an external surface chloride ion value of 0.513 mol/L. Internal Surface ion values would be dependent on the concrete mix used. To calculate the concentration of ion inside the concrete, NIST's Pore Solution Calculator website [52] was used. Concrete mix, aggregate properties, and chemical composition of cement and fly ash used as input in the website were taken from Table 3.1, Table 3.2, and Table 3.5 respectively. The Hydraulic Pressure in the Boundary Conditions option were set to zero since the pressure depth from the ponding solution on the specimen is negligible. The summary

of all the input value used in 4SIGHT calculation are seen in Table 4.4.

Table 4.4 Input Parameters for 4SIGHT Calculation

Input Parameters	Concrete Mix				
	COPC	CF10	CF20	C5%	C10%
Formation Factor	85.637	120.519	177.79	170.736	307.209
porosity	0.256	0.268	0.282	0.252	0.249
permeability (x 10 <sup>-19</sup> m <sup>2</sup> )	7.00	8.41	10.20	5.56	4.52
effective w/c	0.569	0.585	0.602	0.549	0.531
Na <sub>2</sub> O%	0.150	0.192	0.234	0.170	0.188
K <sub>2</sub> O%	0.600	0.694	0.788	0.645	0.685
Internal K+ (mol/L)	0.230	0.270	0.310	0.260	0.290
Internal Na+ (mol/L)	0.090	0.110	0.140	0.110	0.120
Internal OH- (mol/L)	0.320	0.380	0.450	0.370	0.420
External Cl- (mol/L)	0.513	0.513	0.513	0.513	0.513
Pressure Head (m)	0	0	0	0	0

### 4.3.2 Life-365 Approximation and Input Values

Input values for Life-365 are relatively straight forward. Concrete properties, such as  $D_{28}$  and  $m$ , were determined directly from inputting the fly ash replacement and water to cement ratio of the concrete mix into the computer system. Life-365 would determine the concrete properties by using its default relationship equation. The only input values that require approximation and calculation were that for chloride build up time and  $C_{max}$ . The theoretical value of  $C_{max}$  calculated using Eq. 2.8 was used as the input in accordance to the Life-365 User Manual [4]. Porosity value necessary for the calculation were taken using Eq. 2.9 just as in the 4SIGHT calculation. Salt solution

was taken as the same density of the pore solution water with value from Mettler Toledo's website [54]. Concrete density was also taken from NIST's Virtual RCPT website [53]. The time for build up to  $C_{max}$  was taken as 6 month (a) and 1 year (b); this was done since Series 2 experiment indicated that by these exposure periods, the surface chloride concentration,  $C_s$ , has reached its maximum value,  $C_{max}$ , and stabilized. Temperature during exposure was set to a constant of 25 °C, indicating the average temperature in the laboratory. The summary of the input values used in Life-365 calculation are summarized in Table 4.5.

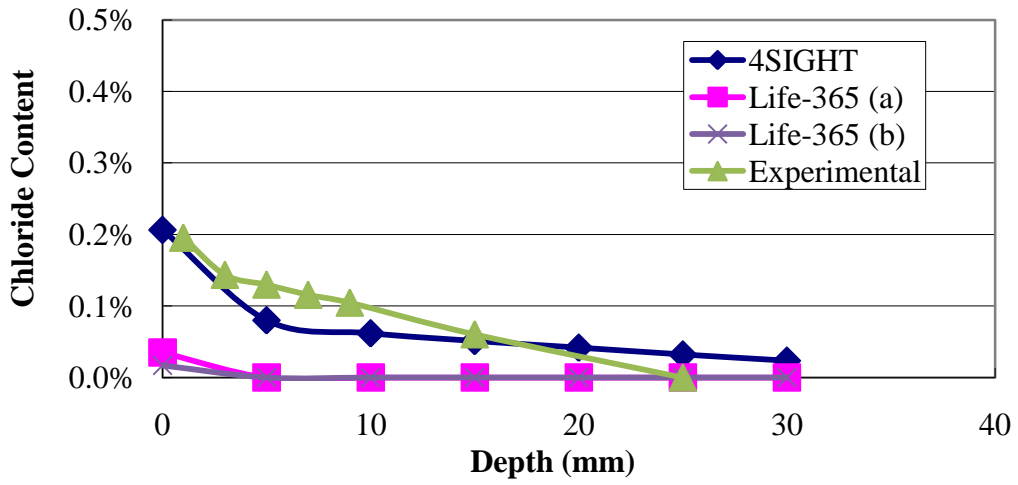
Table 4.5 Input Parameters for Life-365 Calculation

Input Parameters	Concrete Mix				
	COPC	CF10	CF20	C5%	C10%
$C_{max}$ (% wt. concrete)	0.21	0.22	0.23	0.20	0.20
Time to $C_{max}$ (year) (a)	0.5	0.5	0.5	0.5	0.5
Time to $C_{max}$ (year) (b)	1	1	1	1	1
$T$ (°C)	25	25	25	25	25
w/cm	0.57	0.57	0.57	0.54	0.52
Fly ash%	0.00	10.00	20.00	4.76	9.09

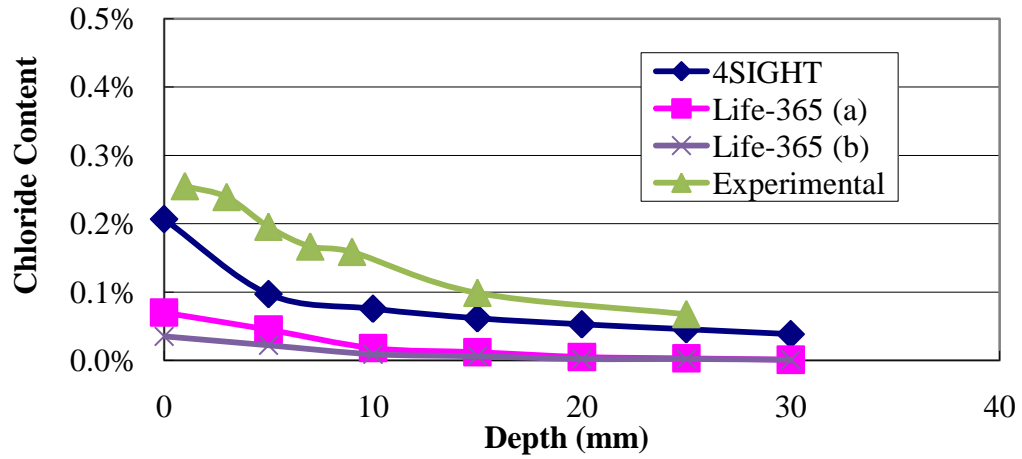
### 4.3.3 Chloride Profile Comparison

In comparing the chloride profiles predicted by Life-365, 4SIGHT and actual experimental result from Series 1, it was noticed that for all concrete mix and all exposure time, the value of curve from Life-365 were noticeable very low when compared to 4SIGHT and experiment data. Meanwhile, although the predicted curve

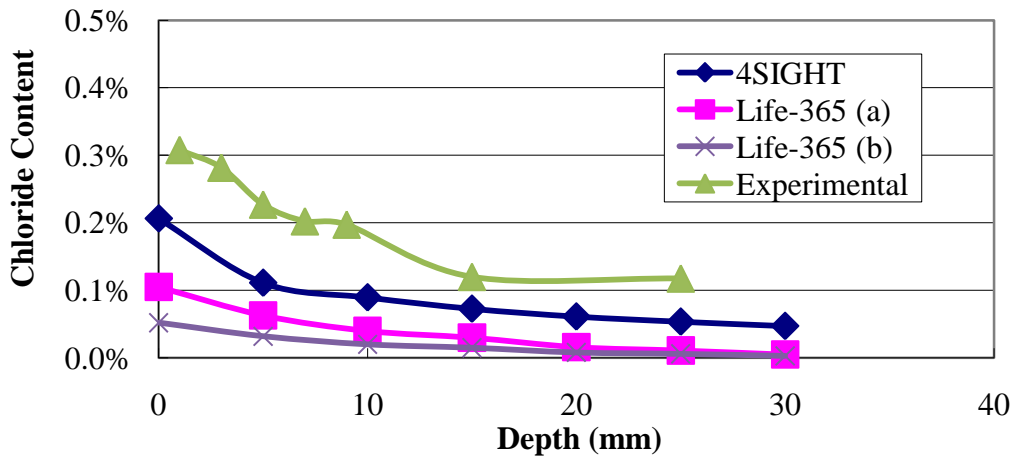
of 4SIGHT and actual experiment result seems to coincide in the 30 day exposure result, they become further apart at later exposure time. The values of Series 1 curve continue to rise while 4SIGHT data curve only tend to flatten while maintaining its surface chloride concentration. It was also noticed that with age, the Life-365 curve continues to rise and approaches the value of the 4SIGHT curve. The curve comparison for each concrete mix can be seen in Figure 4.13 until Figure 4.17. The effect of fly ash and w/cm ratio could not be easily identified from simply observing the shape of the curve produces both through prediction and through actual experimental result.



(a) 30 days

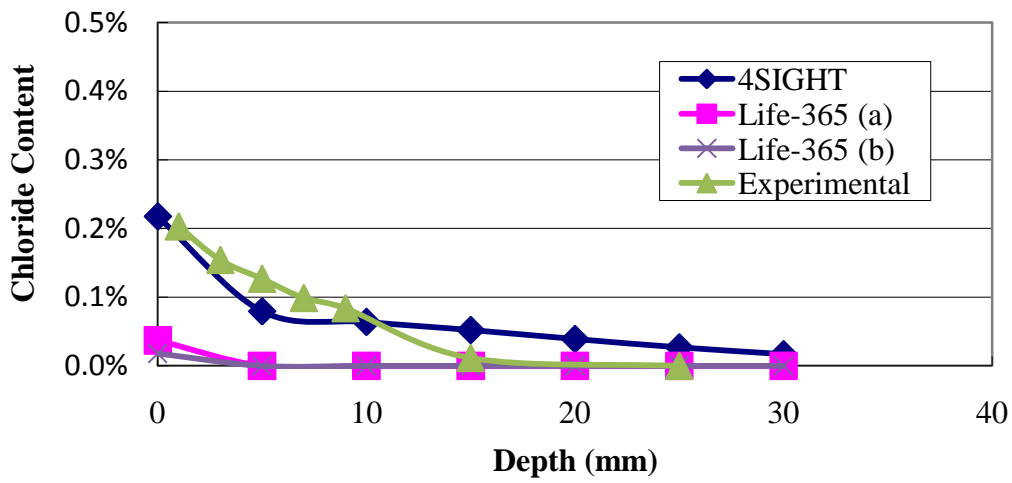


(b) 60 days

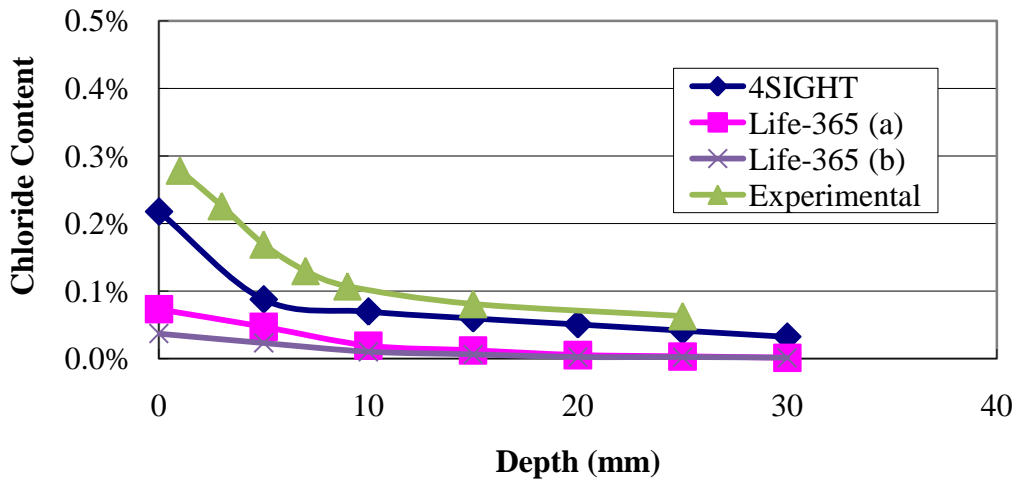


(c) 90 days

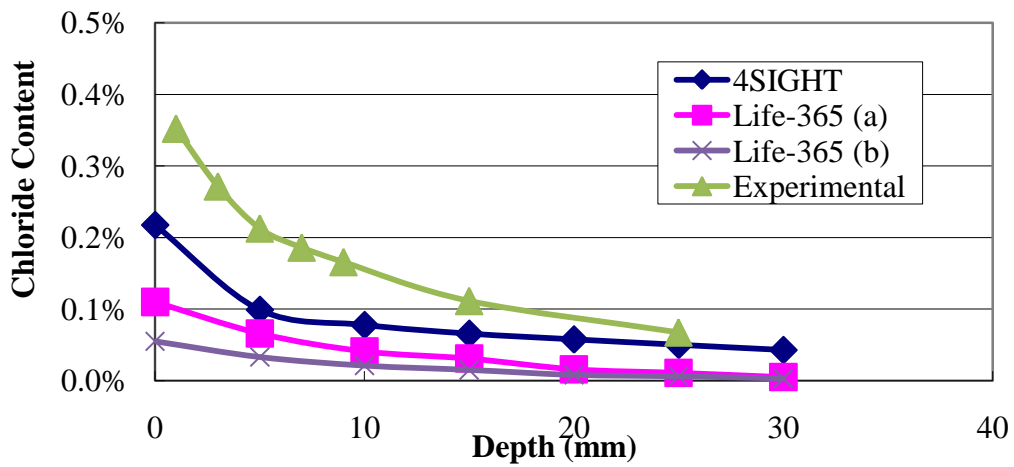
Figure 4.13 COPC Profile Comparisons



(a) 30 days

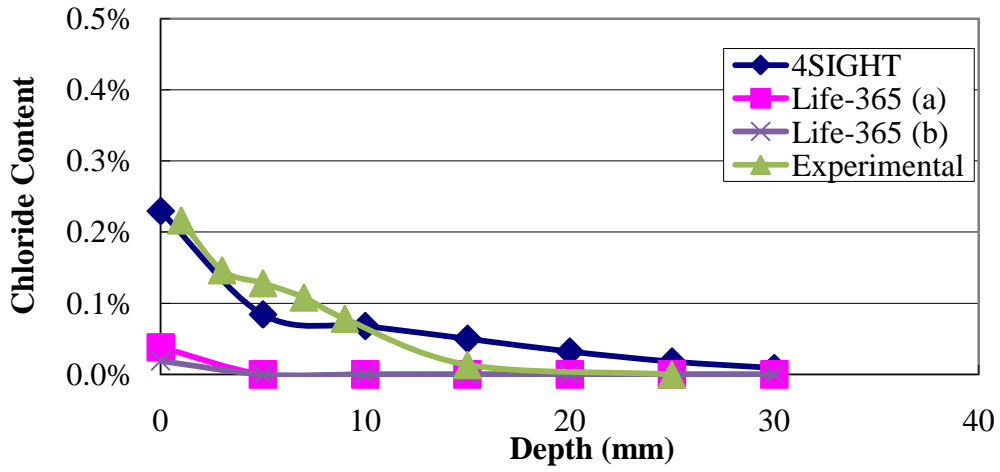


(b) 60 days

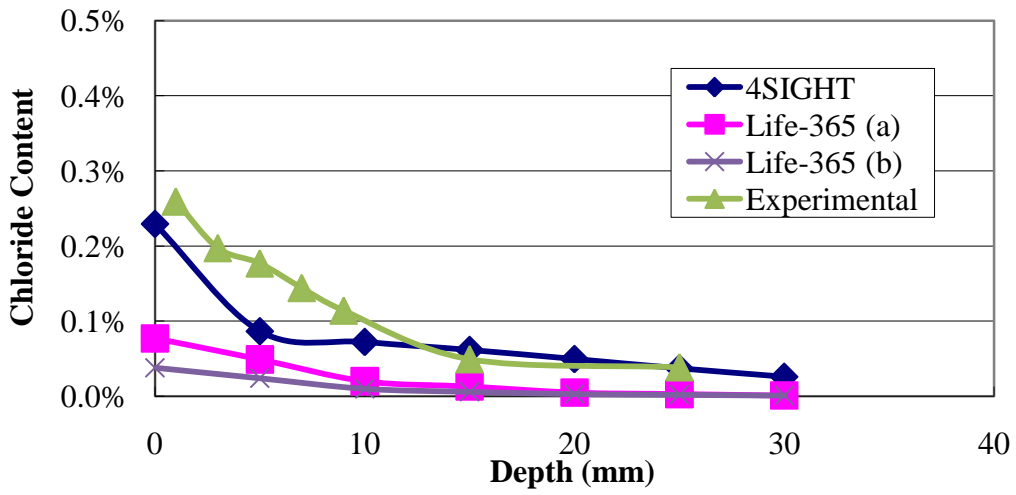


(c) 90 days

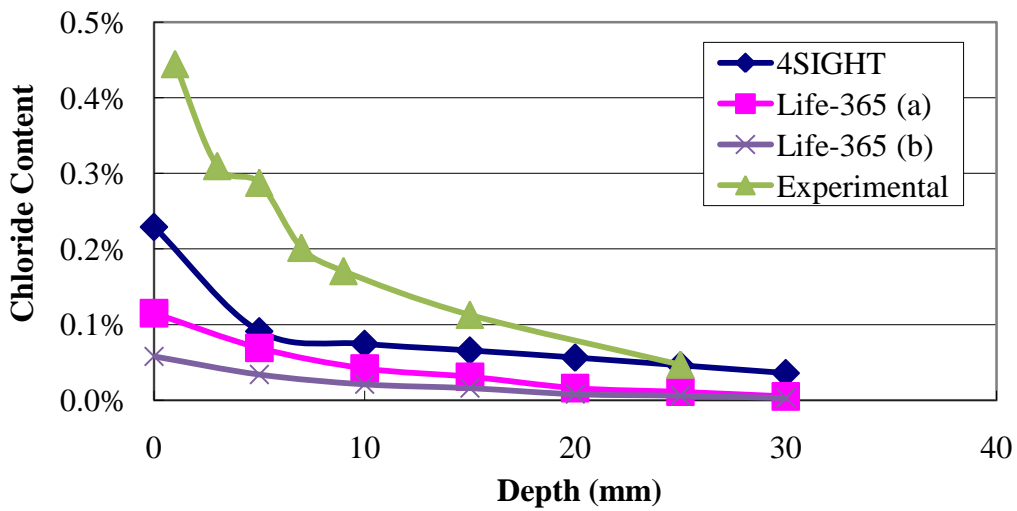
Figure 4.14 CF10 Profile Comparisons



(a) 30 days

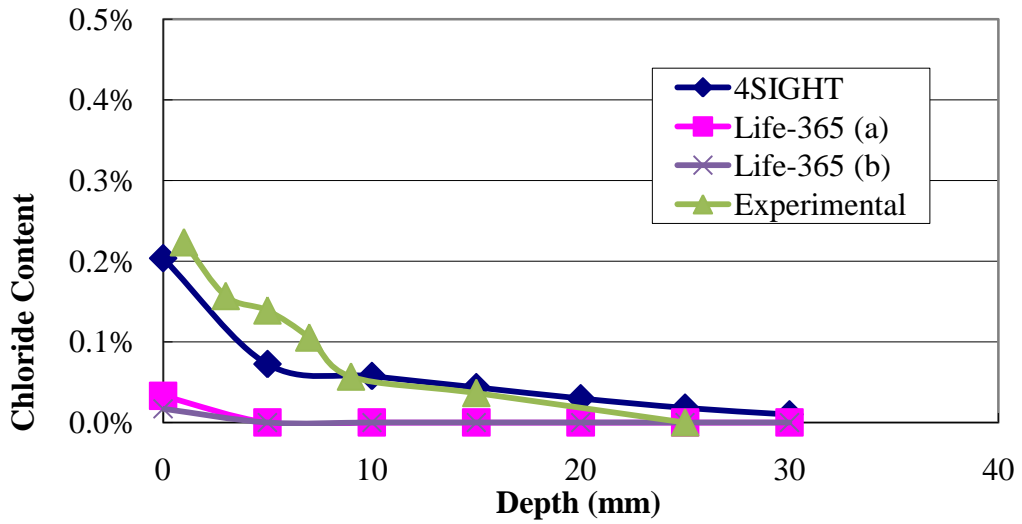


(b) 60 days

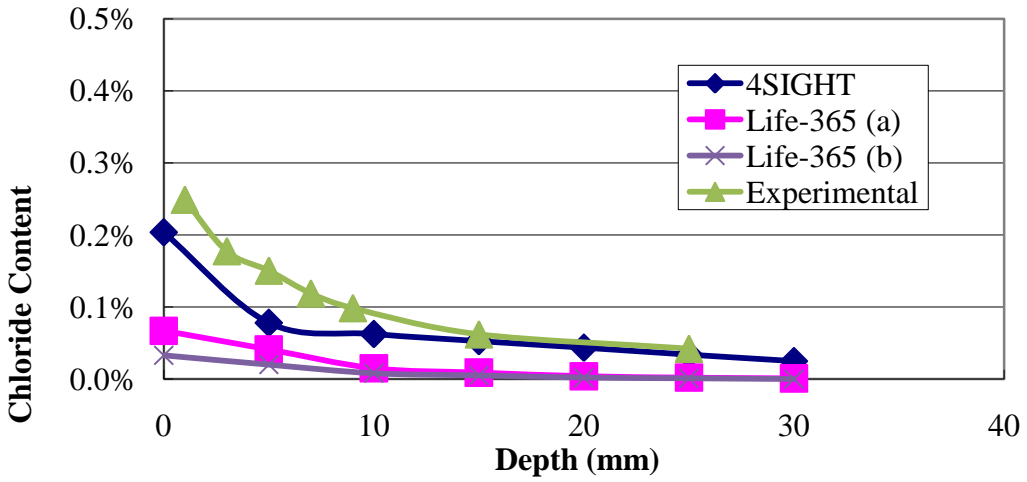


(c) 90 days

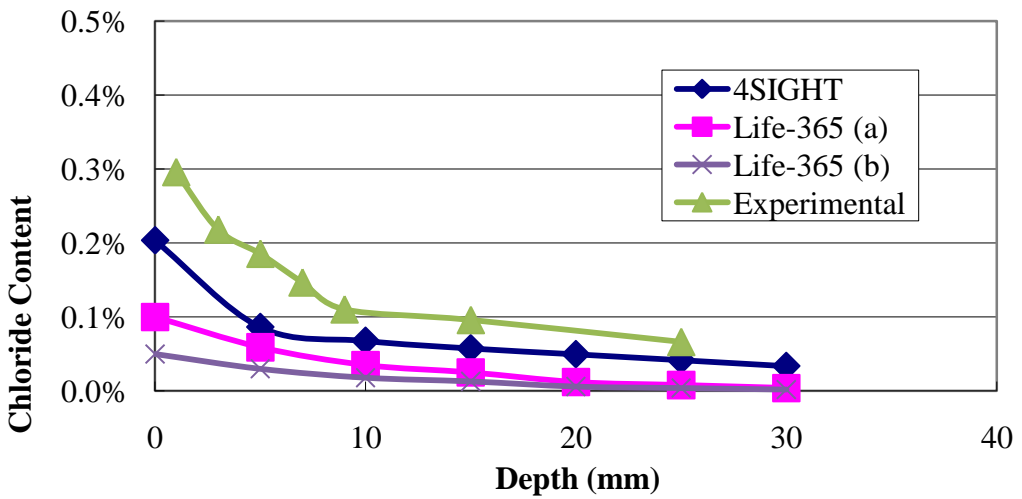
Figure 4.15 CF20 Profile Comparisons



(a) 30 days

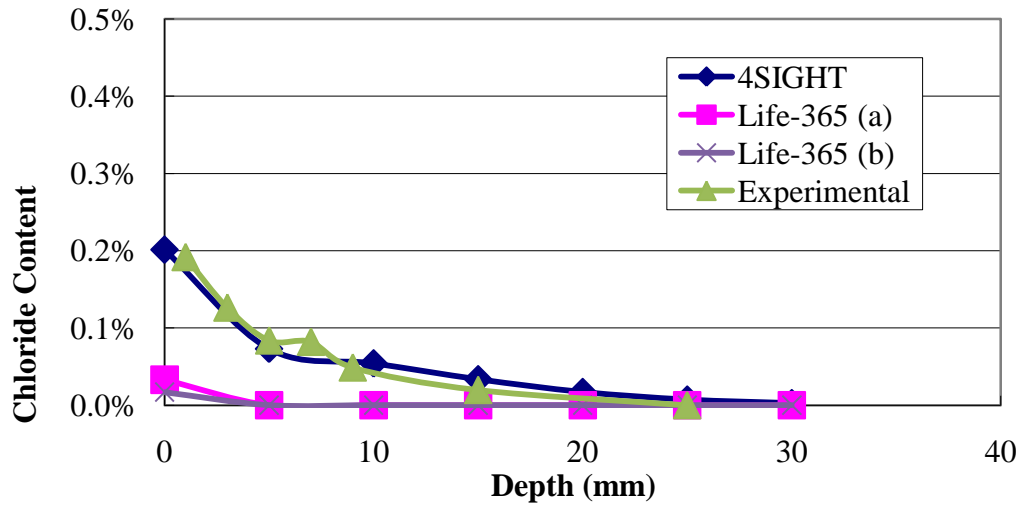


(b) 60 days

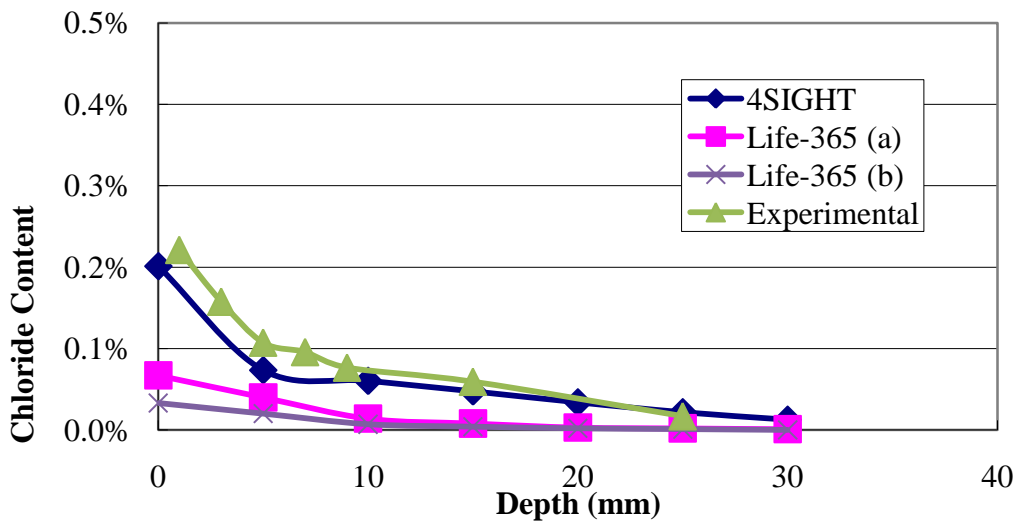


(c) 90 days

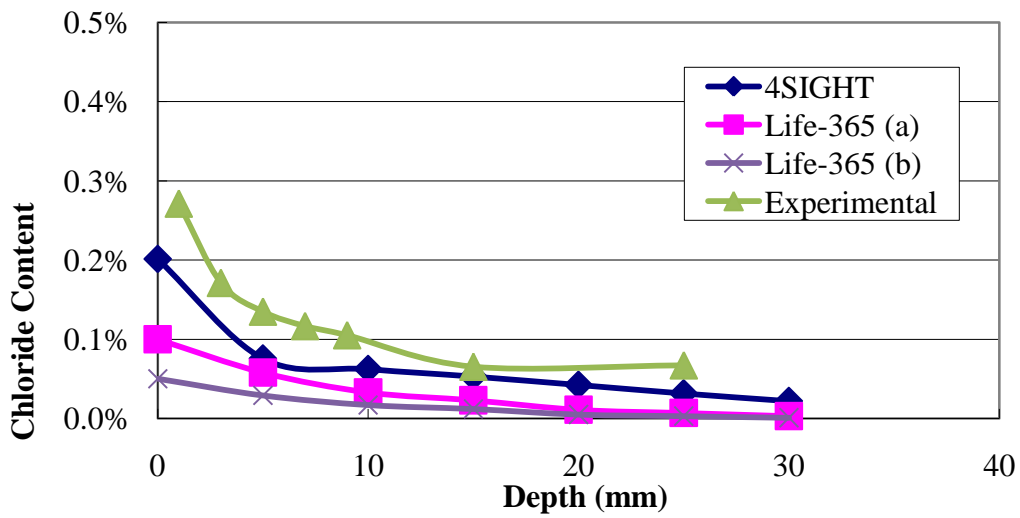
Figure 4.16 C5% Profile Comparison



(a) 30 days



(b) 60 days



(c) 90 days

Figure 4.17 C10% Profile Comparison

The comparison between predicted and experimental profile indicates the importance of the  $C_{\max}$  and build up time in the prediction of chloride profile. Doubling the chloride build up rate also doubles the chloride concentration within the concrete as seen by the difference in chloride build up time of 6 months and 1 year in Life-365. Yet, looking from low value of Life-365 prediction, it was definite that the chloride build up rate and maximum chloride surface concentration were higher than initially assumed. The high curve value of the experiment result with that of Life-365 and 4SIGHT prediction indicates the problem in assuming that  $C_{\max}$  can be determined only by theoretical calculation of the salt solution inside the pores of the concrete. The higher than calculated surface concentration was an indicator of the occurrence of salt crystallization in the concrete pores of the concrete [4]. The occurrence of these salt crystals on the surface of the concrete specimen is seen in Figure 4.18 below. The relatively stagnant condition of the solution during ponding may facilitate this crystallization process. An empirical relation that considers this salt crystallization during exposure is necessary for accurate profile prediction.



Figure 4.18 Salt crystal formations on concrete surface.

The need to accurately estimate chloride build up time is also shown by the very low curve predicted by Life-365. As seen in the 30 day exposure profile result, during ponding, the theoretical  $C_{\max}$  was achieved nearly instantaneous just within 30 days of exposure. This high build up rate needs to be quantified for accurate profile predictions, especially for prediction models based on Fick's law.

The 30 day curve result indicates the validity of a mechanistic based prediction such as that of 4SIGHT. Since younger aged specimens were not available for comparison, this stark similarity between 4SIGHT and real data for 30 days may be an early indicator of the reasonable assumptions made by 4SIGHT concerning ion transport and chemical reaction as the underlying mechanism of chloride diffusion. To confirm the accuracy of 4SIGHT, future experiments may need to be done on earlier exposure age (below 30 days) to see if the predicted and actual chloride profile is also similar. In addition chloride exposure by flowing the liquid solution may be needed for later ages (above 30 days) to eliminate the effect of salt crystallization which occurs after 30 days in this experiment program. 4SIGHT does not put into consideration salt crystallization which occurs after 30 days of ponding, which dramatically increases the surface chloride concentration at later ages. This explains why the predicted surface chloride concentration of 4SIGHT remains relatively unchanged.

#### **4.3.4 Comparison of Experimental $m$ and $D_{28}$ Values with 4SIGHT and Life-365**

The value of  $m$  and  $D_{28}$  calculated using the default relations of Life-365 were compared to the experimental values to evaluate the validity of Life-365 when used to calculate concretes with only fly ash addition. This was necessary since the original relations by Life-365 took into account slag and silica fume additions in addition to fly ash. This may reduce the accuracy of the relationship especially when calculating

for concretes with only fly ash addition. In addition, comparison with 4SIGHT result was necessary to evaluate physical meaning of the empirical coefficient  $m$ . Value of Life-365's  $D_{28}$  and  $m$  are determined using the empirical relationship in Eq. 2.6 and Eq. 2.7 which takes into consideration w/cm and fly ash content as input. Meanwhile the  $D_{28}$  and  $m$  values of 4SIGHT calculated similarly to the experiments result by using the predicted chloride profile from the program as input.

Table 4.6  $m$  and  $D_{28}$  Values Comparison

		Concrete Mix				
		COPC	CF10	CF20	C5%	C10%
Series 1 Experimental Result	Properties					
	$D_{28, \text{total}}$ ( $\times 10^{-11}$ m <sup>2</sup> /s)	3.88	1.91	2.2	1.71	1.16
	$D_{28, \text{avg}}$ ( $\times 10^{-11}$ m <sup>2</sup> /s)	3.88	1.93	1.97	1.59	1.4
	$D_{28, \text{eff}}$ ( $\times 10^{-11}$ m <sup>2</sup> /s)	3.79	1.96	2.01	1.71	1.29
	$m_{\text{total}}$	0.131	0.289	0.388	0.255	0.284
	$m_{\text{avg}}$	0.177	0.387	0.522	0.343	0.382
	$m_{\text{eff}}$	0.200	0.454	0.626	0.399	0.447
4SIGHT Prediction Result	$D_{28, \text{total}}$ ( $\times 10^{-11}$ m <sup>2</sup> /s)	3.61	3.09	2.42	2.08	1.58
	$D_{28, \text{avg}}$ ( $\times 10^{-11}$ m <sup>2</sup> /s)	3.67	3.02	2.30	1.83	1.28
	$D_{28, \text{eff}}$ ( $\times 10^{-11}$ m <sup>2</sup> /s)	3.67	2.96	2.32	2.02	1.51
	$m_{\text{total}}$	0.199	0.245	0.218	0.110	0.192
	$m_{\text{avg}}$	0.269	0.328	0.295	0.149	0.256
	$m_{\text{eff}}$	0.301	0.381	0.340	0.168	0.291
	Life-365 Result	$D_{28, \text{total}}$ ( $\times 10^{-11}$ m <sup>2</sup> /s)	2.03	2.03	2.03	1.72
$m_{\text{total}}$		0.200	0.280	0.360	0.238	0.273

Table 4.6 indicates the similarity between the general influence of fly ash towards  $D_{28}$  and  $m$  obtained through experiment with that calculated by both 4SIGHT and Life-365. All three methods highlight that chloride diffusivity would decrease by

decreasing w/cm ratio and through increasing the fly ash content of the concrete. In general, all three methods agree that the diffusion coefficient value of concrete reduces with time. As discussed in Chapter 2, the value of  $m_{\text{eff}}$  was the largest, followed by  $m_{\text{avg}}$ , with  $m_{\text{total}}$  being the smallest.

The  $D_{28}$  values calculated using experimental data were generally only slightly lower than values obtained by default Life-365 relationship despite the fact that the concretes were stored for 285 or 650 days prior to exposure. This may be caused by the relatively dry storage condition. The lack of available water during storage hampers the hydration process of the concrete to further refine its pores. The re-exposure of the specimen to water during ponding allows for the hydration process to continue.

The similarity between experimental data with that of Life-365 default value can be explained by saturation of Series 1 specimen by immersion in water prior to exposure. As explained in Chapter 2, this was similar to the NordTest (used for the determination of  $D_{28}$  value in Life-365) set up when immersion in lime water was done. The similarity between the modified AASHTO T259 used in this experiment with that of NordTest NTBuild 443 may be the underlying reason behind the similarity of the obtained  $D_{28}$  and  $m$  when total time were considered.

The similarity of 4SIGHT's trend regarding the influence of fly ash toward fly ash influence in diffusivity and reduction of diffusion coefficient with time with that of the experiment and Life-365 data raises an interesting point. As has been discussed, the mechanism for chloride transport in Life-365 is based on diffusion; the same consideration was also taken for the experiment. On the other hand 4SIGHT chloride

ingress mechanism was based on ion transport and chemical reaction of ions in the pores. The similarity in the general trend that diffusion coefficient value reduces with time, as indicated by  $m$  for all three methods, showed the correct assumption taken by 4SIGHT with regards to the chloride ingress mechanism in concrete. Thus, it can be concluded that, in accordance to 4SIGHT's assumption, fly ash within the concrete would not influence much on the initial porosity of concrete. Fly ash would only influence the formation factor which influences the conductivity of the pore solution. This conductivity in turn would influence the diffusion of ion in the concrete pore solution. The  $m$  value thus describes the reduction in chloride ion diffusivity through ion interaction, precipitation/dissolution which would influence (reduce) the diffusivity of chloride ions in concrete pores.

## **4.4 Determination of Empirical Relationships**

### **4.4.1 Empirical Relationship Equation**

When various concrete properties are unknown, empirical relationships become very important to approximate the input values needed for calculation of predicted chloride profiles. Due to the ability of Life-365 to be modified, this program was selected as the calculation platform which would utilize relationship equations obtained empirically from the experiment. Relationship to approximate the value of  $m_{avg}$ ,  $m_{total}$ ,  $m_{eff}$ ,  $D_{28,avg}$ ,  $D_{28,total}$ ,  $D_{28,effective}$ ,  $C_{max}$ , and chloride build up time (average, total, effective) based on w/cm ratio and fly ash content were determined using LAB Fit curve fitting software. The  $R^2$  value obtained indicates the relative soundness of the relationship equation in determining the values. Table 4.7 summarizes the empirical relations best suited to describe the experiment data including their  $R^2$  value.

Table 4.7 Empirical Relation Equations

Properties	Equation	Unit	$R^2$
$D_{28,total}$	$D_{28} = 0.241E-09 \times w/cm^4$	m <sup>2</sup> /s	0.322
$D_{28,avg}$	$D_{28} = 0.230E-09 \times w/cm^4$	m <sup>2</sup> /s	0.358
$D_{28,eff}$	$D_{28} = 0.230E-09 \times w/cm^4$	m <sup>2</sup> /s	0.409
$m_{total}$	$m = FA\% / (-0.506E+02 + 0.295E+03 \times w/cm^2)$	-	0.914
$m_{avg}$	$m = FA\% / (-0.377E+02 + 0.220E+03 \times w/cm^2)$	-	0.915
$m_{eff}$	$m = FA\% / (-0.299E+02 + 0.179E+03 \times w/cm^2)$	-	0.922
$C_{s,total}$ build up rate	$C_s \text{ rate} = 0.326E-04 \times FA\% + 0.845E-02 \times w/cm^2$	Cl%/day	0.927
$C_{s,avg}$ build up rate	$C_s \text{ rate} = 0.508E-04 \times FA\% + 0.131E-01 \times w/cm^2$	Cl%/day	0.931
$C_{s,eff}$ build up rate	$C_s \text{ rate} = 0.609E-04 \times FA\% + 0.140E-01 \times w/cm^2$	Cl%/day	0.938
$C_{max}$	$C_s = (w/cm) / (0.840 - 0.575E-04 \times FA\%^2)$	Cl%	0.499

Due to the similarity of  $D_{28}$  and  $m$  values between experiment data with that of initial Life-365 calculations, the importance of an accurate approximation of  $C_{max}$  and build up time was recognized. Evaluation of  $R^2$  values have shown that  $m$  value relationship equation and chloride build up time relationship equation (as a function of  $w/cm$  and fly ash content) yielded a high  $R^2$  value. This was an indicator for the soundness of the equations. Meanwhile a relatively low  $R^2$  was obtained for  $D_{28}$  and  $C_{max}$  relationship equations. This indicates that precaution must be taken when using the

equation. When compared to the  $R^2$  value of the  $D_{28}$  relationship equation used by Life-365 in Figure 2.4, which was derived from published data from six different authors, it shows that more data may be necessary for a more sound relationship to be made. As a note,  $D_{28}$  relationship was based only on w/cm ratio, an effort to use both w/cm and fly ash content to determine  $D_{28}$  yielded a relationship with a  $R^2$  value of zero. This confirms the theory that diffusivity at early age is only dependant on w/cm ratio.

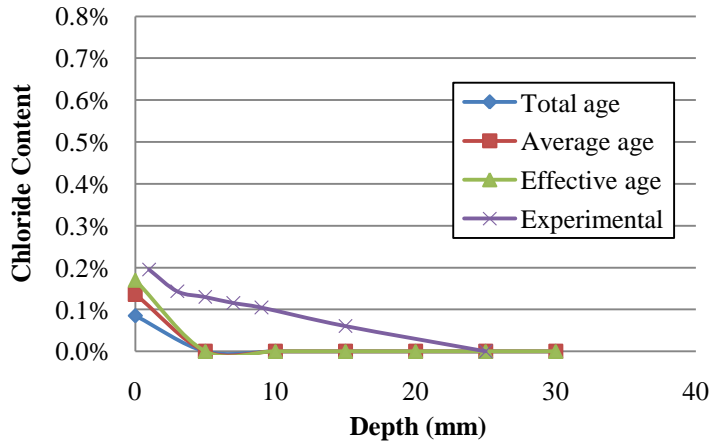
#### **4.4.2 Relationship Equation Validation**

To confirm the soundness of the equation and evaluate its usefulness in predicting chloride profiles for concrete with fly ash addition, comparison with Series 1 profile were done by re-calculating input data for Life-365 using the experiments empirical relationship equation found in Table 4.7. The modified input value for Life-365 is summarized in Table 4.8.

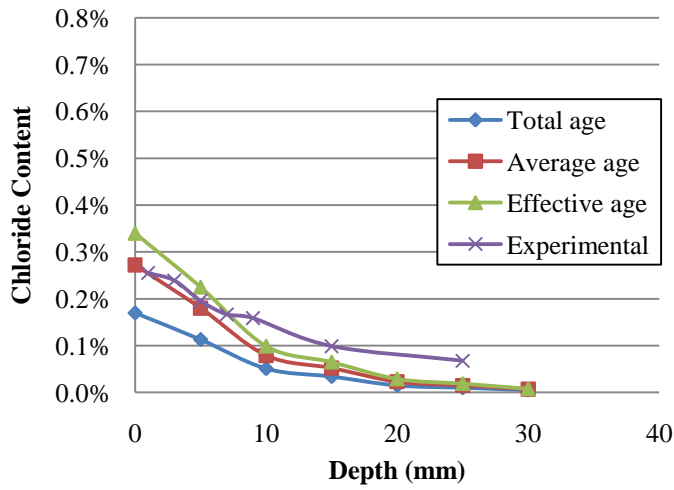
Table 4.8 Input Values for Modified Life-365 Calculations

Input	COPC		
	total age	avg age	eff age
$D_{28}$ ( $\times 10^{-11}$ m <sup>2</sup> /s)	2.54	2.43	2.43
$m$	0.00	0.00	0.00
$C_{\max}$ (% wt. concrete)	0.6786	0.6786	0.6786
time to $C_{\max}$ (year)	0.6772	0.4368	0.4087
	CF10		
	total age	avg age	eff age
$D_{28}$ ( $\times 10^{-11}$ m <sup>2</sup> /s)	2.54	2.43	2.43
$m$	0.22	0.30	0.35
$C_{\max}$ (% wt. concrete)	0.6832	0.6832	0.6832
time to $C_{\max}$ (year)	0.6095	0.3929	0.3629
	CF20		
	total age	avg age	eff age
$D_{28}$ ( $\times 10^{-11}$ m <sup>2</sup> /s)	2.54	2.43	2.43
$m$	0.44	0.59	0.71
$C_{\max}$ (% wt. concrete)	0.6977	0.6977	0.6977
time to $C_{\max}$ (year)	0.5626	0.3626	0.3315
	C5%		
	total age	avg age	eff age
$D_{28}$ ( $\times 10^{-11}$ m <sup>2</sup> /s)	2.05	1.96	1.96
$m$	0.13	0.18	0.21
$C_{\max}$ (% wt. concrete)	0.6439	0.6439	0.6439
time to $C_{\max}$ (year)	0.6735	0.4343	0.4034
	C10%		
	total age	avg age	eff age
$D_{28}$ ( $\times 10^{-11}$ m <sup>2</sup> /s)	1.76	1.68	1.68
$m$	0.31	0.42	0.49
$C_{\max}$ (% wt. concrete)	0.6226	0.6226	0.6226
time to $C_{\max}$ (year)	0.6608	0.4260	0.3931

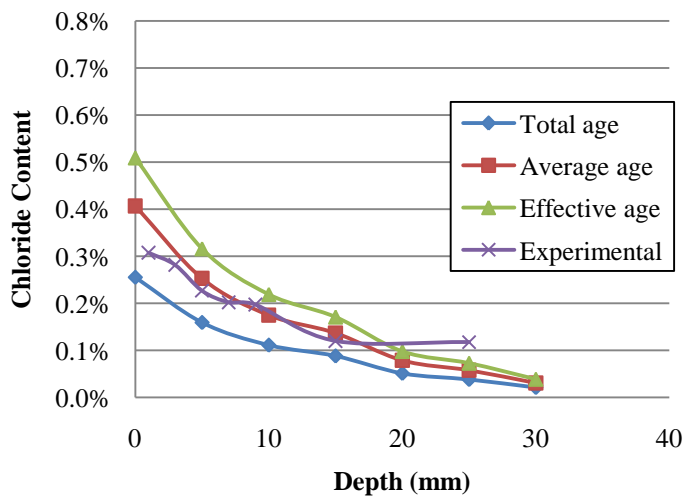
In Figure 4.19 to Figure 4.23, the improvement in profile prediction using this research's empirical relationship was evident. Although no specific time basis were the closest to the real experimental curve, but it was discovered that the actual chloride profile were generally within the band generated from the chloride profile prediction from total, average and effective time basis prediction. The figure also indicates that at later ages once  $C_{\max}$  is reached, this band will narrow, hence providing a more accurate prediction of the chloride profile. This indicates the relative usefulness of the obtained empirical result in predicting the chloride profile of concrete with fly ash addition. Meanwhile the fact that when no fly ash addition was used the empirical equation resulted in a zero value for  $m$  indicates the relative weakness for the equation relation in predicting the  $m$  value for COPC. This was since previous experimental results dictates that although no fly ash addition were used, cement also continues to hydrate with time and reduces the diffusivity of cement concrete, hence a zero  $m$  value which means that no reduction of diffusivity with time occurs is unfounded.



(a) 30 days

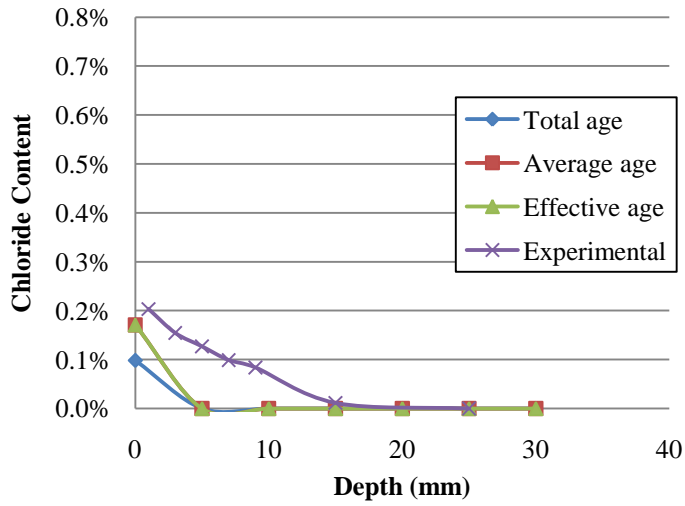


(b) 60 days

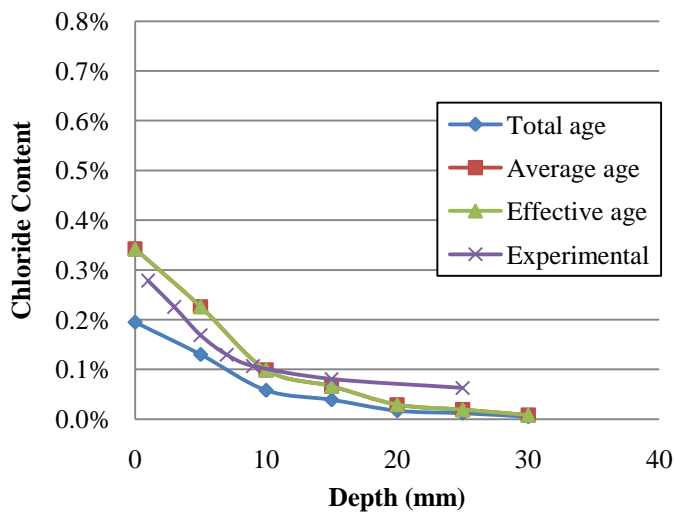


(c) 90 days

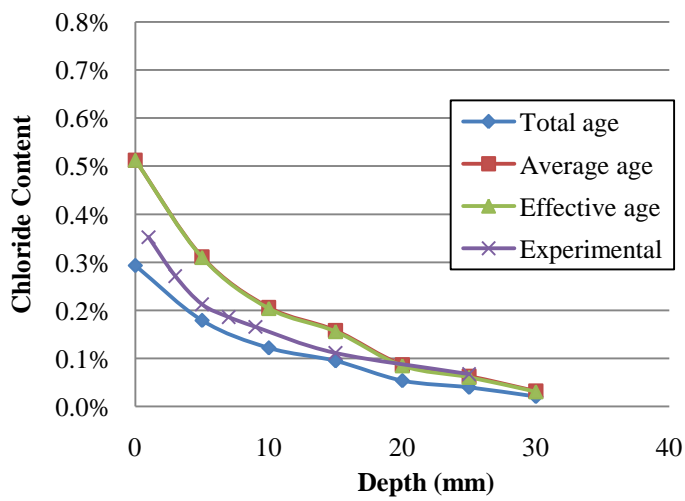
Figure 4.19 COPC with modified Life-365 calculation



(a) 30 days

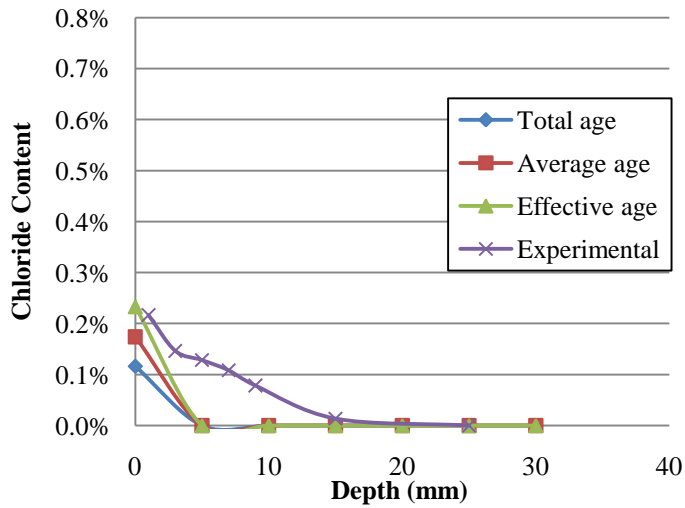


(b) 30 days

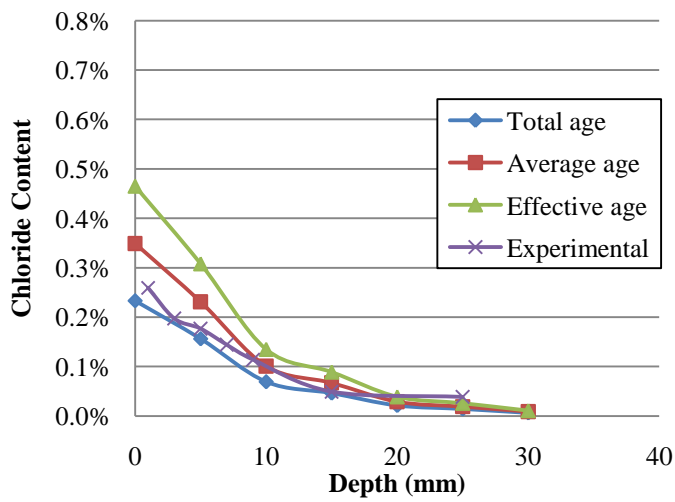


(c) 90 days

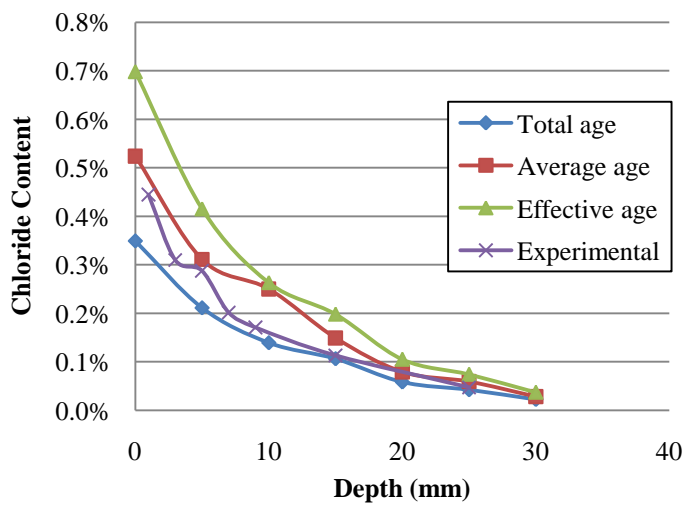
Figure 4.20 CF10 with modified Life-365 calculation



(a) 30 days

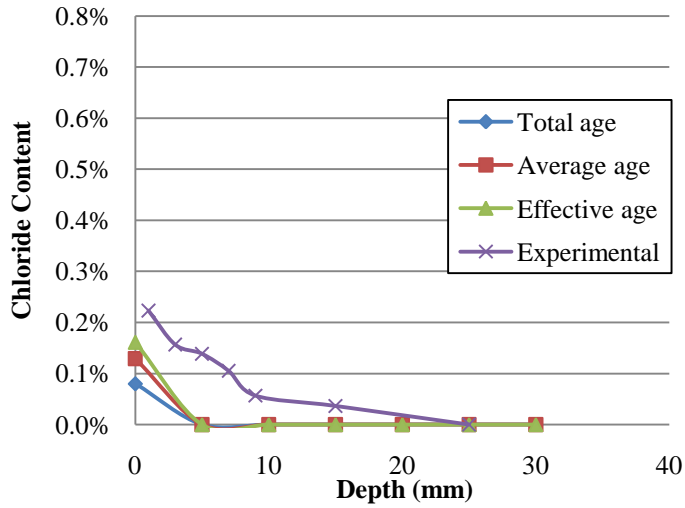


(b) 60 days

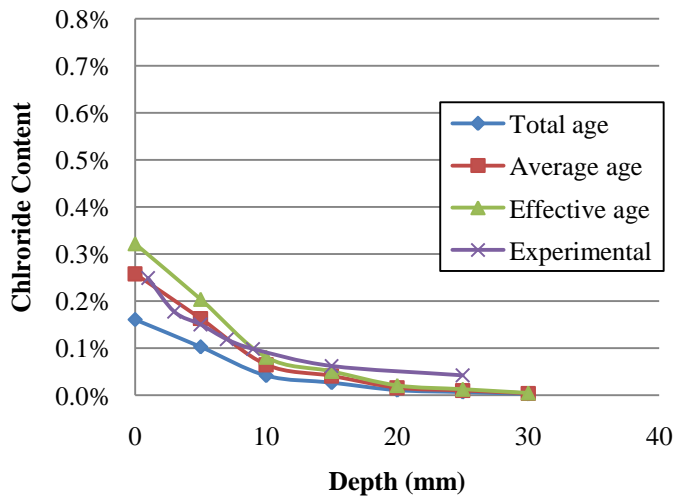


(90 days)

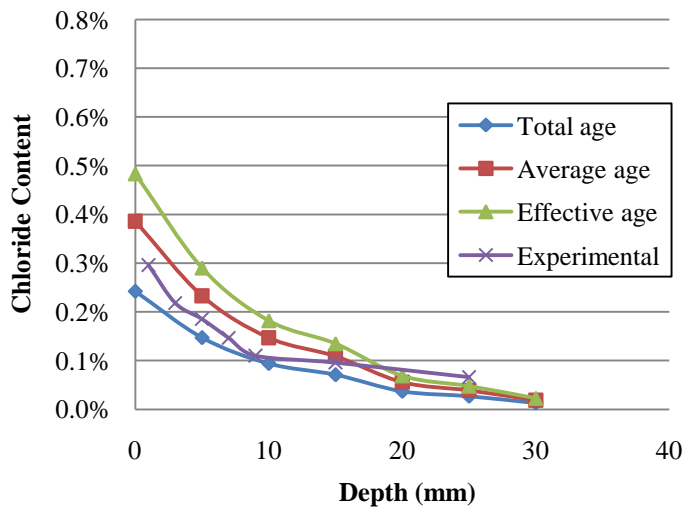
Figure 4.21 CF20 with modified Life-365 calculation



(a) 30 days

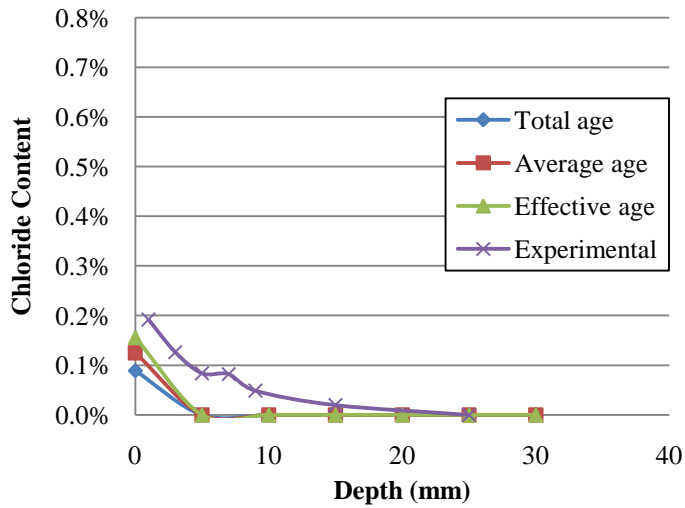


(b) 60 days

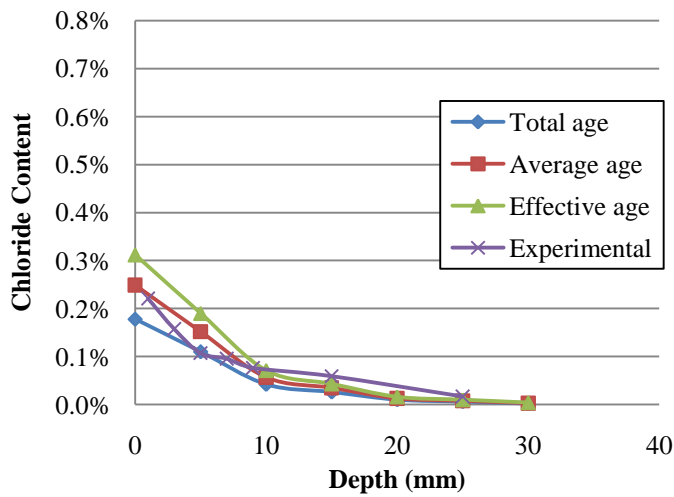


(c) 90 days

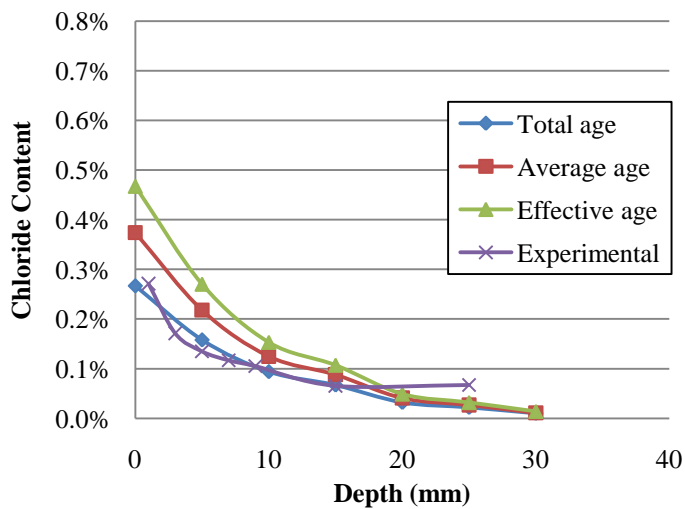
Figure 4.22 C5% with modified Life-365 calculation



(a) 30 days



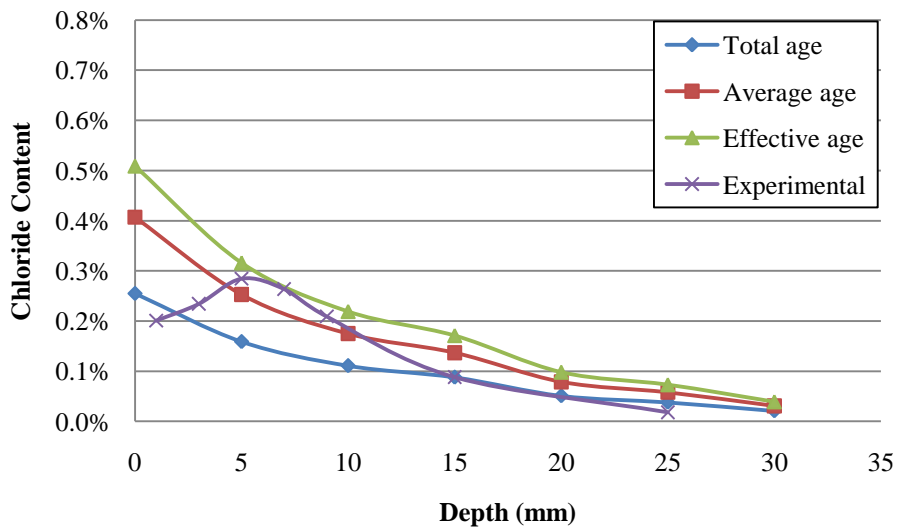
(b) 60 days



(c) 90 days

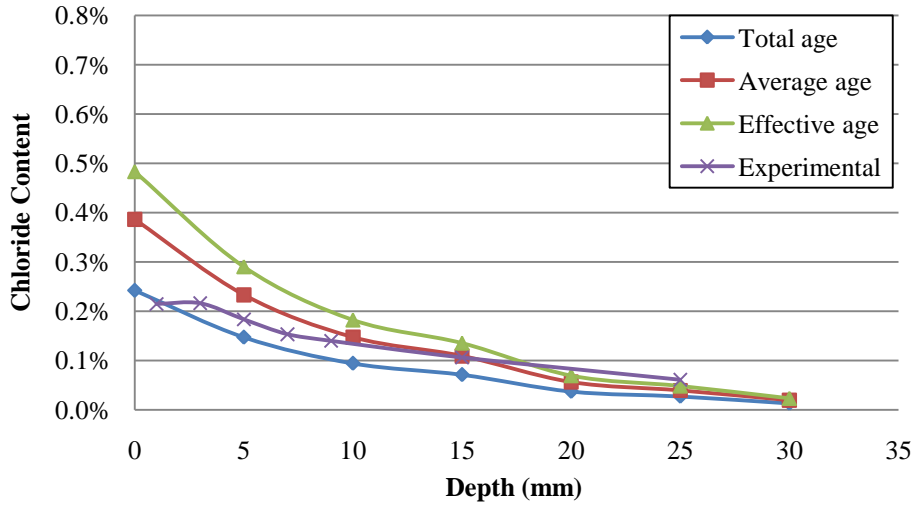
Figure 4.23 C10% with modified Life-365 calculation

For validation, COPC 90 days, CF20 180 days, C5% 90 days and C10 365 chloride profile curve obtained from Series 2 were compared with predictions using the empirical relationship obtained. The result is seen in Figure 4.24. The validation indicates the relationship equation of this experiment to be useful in predicting concrete chlorides for concretes with fly ash addition which experiences constant exposure similar to that experienced during ponding. Such exposure may be faced by concrete structures used as low level radioactive waste disposal underground vaults or marine structures submerged in water/seawater.

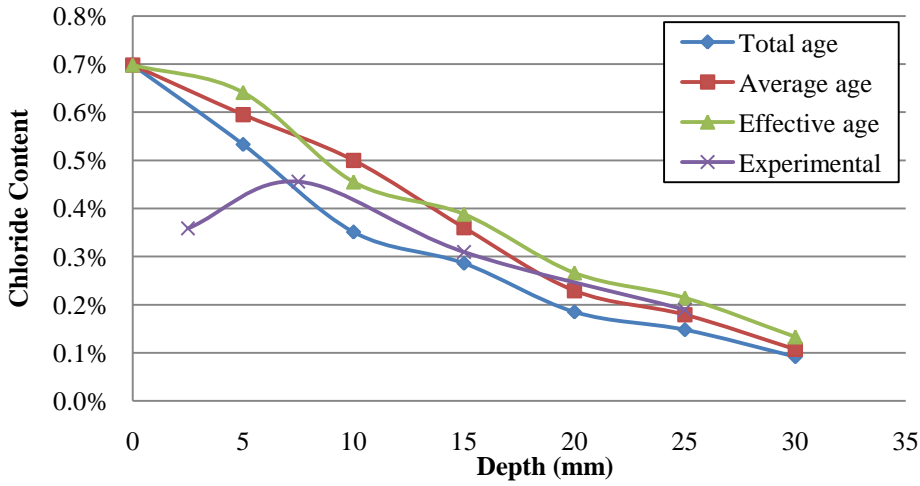


(a) COPC 90 days

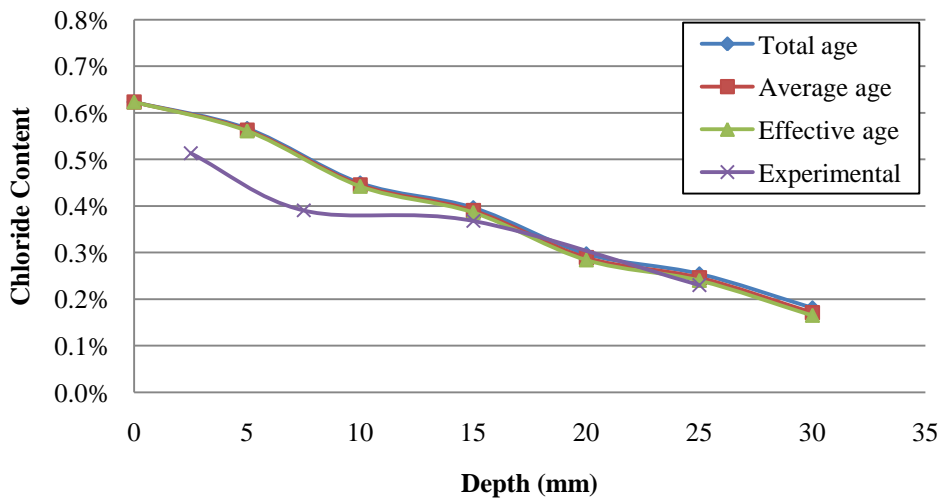
Fig. 4.24 to be continued



(b) C5% 90 days



(c) CF20 180 days



(d) C10% 365 days

Figure 4.24 Validation of empirical relation equations

## CHAPTER FIVE CONCLUSIONS & SUGGESTIONS FOR FURTHER RESEARCH

### 5.1 Conclusions

In the course of this research, salt ponding test on fly ash concrete specimens stored for 285 or 650 days prior to exposure, and on concrete immediately exposed to chloride after 28 days of moist curing were done. After exposure, concrete specimens were profiled, powdered, and titrated to determine their chloride content. Chloride diffusion coefficient ( $D_{app}$ ) and coefficient of diffusion reduction ( $m$ ) were calculated from the profile obtained and compared with predicted values from Life-365 and 4SIGHT service life prediction models. Over the course of this research, the following conclusions are derived:

1. Low w/cm ratio and higher fly ash content would result in concrete with low chloride diffusivity, the reduction in chloride diffusion coefficient were also higher for chloride with higher fly ash addition as indicated by their  $m$  values.
2. Salt crystallization occurred during ponding, causing an increase in the maximum surface chloride concentration,  $C_{max}$ , beyond its theoretical value after 30 days of exposure. The  $C_{max}$  value decreases with increasing w/cm ratio and increases with increasing fly ash content.
3. Similar  $D_{28}$  values derived from concrete specimens stored for over 285 days and those calculated using Life-365 and 4SIGHT indicate that hydration were hampered during storage and continued after the exposure of the specimen to salt ponding. This was further confirmed by the fact that the diffusivity from 90 days exposure of concrete specimens stored for over 285 days was similar or only slightly lower with those immediately exposed to chloride after 28 days of moist curing.

4. Similar  $D_{28}$  and  $m$  values obtained from experimental concrete mixes and Life-365 shows that the modified AASHTO T259 (immersion in water prior to exposure) used in this experiment produces similar result as the NordTest method used for the determination of the default values of Life-365. It also shows the importance of a sound approximation in determining chloride build up time and  $C_{\max}$  to produce accurate chloride profile prediction.
5. Similar trend on the influence of fly ash content on diffusivity and the reduction of diffusivity with time between experimental data and 4SIGHT were an indicator that the influence of fly ash toward ion transport mechanism assumed by 4SIGHT proved to be authentic.
6. Empirical relation equations to approximate  $D_{28}$  and  $C_{\max}$  yielded a low  $R^2$  value which means that precaution are necessary when using them, on the other hand the high  $R^2$  value of chloride build up time and  $m$  empirical relation equations indicates the soundness of the relationship for use in chloride profile prediction
7. Modification of the default relationship equation in Life-365 with those obtained experimentally manage to accurately place actual chloride profile between the band created by average, total, and effective time chloride profile prediction. This shows the usefulness of the experimental relationship in predicting chloride profiles for concrete with fly ash addition which was exposed to constant exposure condition (e.g. ponding, submerged, underground).

## 5.2 Suggestions

1. More data is necessary to improve the empirical relationship equation for  $D_{28}$  and  $C_{\max}$ .
2. Chloride profile for exposure below 30 days in addition to chloride profile above 30 days for non-stagnant exposure (to prevent crystallization) is needed to evaluate the accuracy of 4SIGHT assumptions.
3. More validation using chloride profiles for concrete with fly ash addition from other experiments are necessary to confirm the usefulness of the empirical relationship obtained during this research.
4. Direct measurement of  $D_{28}$  by using NordTest should be done in order to build a better  $D_{28}$  empirical relationship equation.

## REFERENCES

1. Koch, Gerhardus, et.al., *Corrosion Costs and Preventive Strategies in the United States*, FHWA-RD-01-156, Federal Highway Administration, 2007
2. Callanan, T., and Richardson, M., *Modelling Chloride Ingress in Concrete: A Comparative Study of Laboratory and Field Experience*, SP212-25, ACI Special Publication, p. 389-408, 2003
3. Maheswaran, T., and Sanjayan, J. G., A semi-closed-form solution for chloride diffusion in concrete with time-varying parameters, *Magazine of Concrete Research*, **56**, p. 359-366, 2004
4. *Life-365 Service Life Prediction Model and Computer Program for Predicting the Service Life and Life-Cycle Cost of Reinforced Concrete Exposed to Chlorides*, Life-365 Consortium II, 2010
5. Thomas, Michael D. A., Bamforth, Phil B., Modelling chloride diffusion in concrete: Effect of fly ash and slag, *Cement and Concrete Research*, **29**, p. 487-495, 1999
6. Bijen, Jan, Benefits of slag and fly ash, *Construction and Building Materials*, **10**(5), p. 309-314, 1996,
7. Luping, Tang, and Gulikers, Joost, On the mathematics of time-dependent apparent chloride diffusion coefficient in concrete, *Cement and Concrete Research*, **37**, p. 589-595, 2007
8. Saetta, Anna V., Scotta, Roberto V., and Vitalini, Renato V., Analysis of Chloride Diffusion into Partially Saturated Concrete, *ACI Materials Journal*, **90**(5), p. 441-451, 1993

9. Angst, Ueli, Elsener, Bernhard, Larsen, Claus K., Vennesland, Oystein, Critical chloride content in reinforced concrete – A review, *Cement and Concrete Research*, **39**, p. 1122-1138, 2009
10. Han, Sang-Hun, Influence of diffusion coefficient on chloride ion penetration of concrete structure, *Construction and Building Materials*, **21**, p. 370-378, 2007,
11. Martin Perez, B., Zibara, H., Hooton, R. D., and Thomas, M. D. A., A Study of the effect of chloride binding on service life predictions, *Cement and Concrete Research*, **30**, p. 1215-1223, 2000
12. Boddy, Andrea, Bentz, Evan, Thomas, M. D. A., and Hooton, R. D., An overview and sensitivity study of a multimechanistic chloride transport model, *Cement and Concrete Research*, **29**, p. 827-837, 1999
13. Martys, Nicos S., *Survey of Concrete Transport Properties and their Measurement*, NISTIR 5592, U.S. Department of Commerce, 1995
14. Wong, S. F., Wee, T. H., Swaddiwudhipong, S., and Lee, S. L., Study of water movement in concrete, *Magazine of Concrete Research*, **53**(3), p. 205-220, 2001
15. Aldred, J. M., and Rangan, B. V., *The Influence of Wick Action on Chloride Transport in Concrete*, SP212-50, ACI Special Publication, p. 807-822, 2003
16. Puyate, Y. T., and Lawrence, C. J., Steady state solutions for chloride distribution due to wick action in concrete, *Chemical Engineering Science*, **55**, p. 3329-3334, 2000
17. Song, Sheng-Rong, et.al, Hydrochemical Changes in Spring Waters in Taiwan: Implications for Evaluating Sites for Earthquake Precursory Monitoring, *TAO*, **16**(4), p. 745-762, 2005

18. Stanish, K. D., Hooton, R. D., and Thomas, M. D. A., *Testing the Chloride Penetration Resistance of Concrete: A Literature Review*, Federal Highway Administration, 2000
19. Khitab, A., Lorente, S., and Ollivier, J. P., Predictive model for chloride penetration through concrete, *Magazine of Concrete Research*, **57**, No. 9, p. 511-520, 2005
20. Chatterji, S., On the Applicability of Fick's Second Law to Chloride Ion Migration Through Portland Cement Concrete, *Cement and Concrete Research*, **25**(2), p. 299-303, 1995
21. Lu, Xinying, Application of the Nernst-Einstein Equation to Concrete, *Cement and Concrete Research*, **27**(2), p. 293-302, 1997
22. Sugiyama, T., Ritthichauy, W., Tsuji, Y., Experimental investigation and numerical modeling of chloride penetration and calcium dissolution in saturated concrete, *Cement and Concrete Research*, **38**, p. 49-67, 2008
23. Stanish, Kyle, and Thomas, Michael, The use of bulk diffusion tests to establish time-dependent concrete chloride diffusion coefficients, *Cement and Concrete Research*, **33**, p. 55-62, 2003
24. Nokken, Michelle, Boddy, Andrea, Hooton, R. D., and Thomas, M. D. A., Time dependent diffusion in concrete – three laboratory studies, *Cement and Concrete Research*, **36**, p. 200-207, 2006
25. Yeih, W. D., Huang, R., and Chang, J. J., A Study of Chloride Diffusion Properties of Concrete at Early Age, *Journal of Marine Science and Technology*, **2**(1), p. 61-67, 1994
26. Buenfeld, N. R., and Okundi, E., Effect of cement content on transport in concrete, *Magazine of Concrete Research*, **50**(4), p. 339-351, 1998

27. Hobbs, D. W., Aggregate influence on chloride ion diffusion into concrete, *Cement and Concrete Research*, **29**, p. 1995-1998, 1999
28. Bentz., Dale P., A virtual rapid chloride permeability test, *Cement and Concrete Composites*, **29**, p. 723-731, 2007
29. Song, Ha-Won, Lee, Chang-Hong, Ann, Ki Yong, Factors influencing chloride transport in concrete structures exposed to marine environments, *Cement and Concrete Composites*, **30**, p. 113-121, 2008
30. Thomas, M. D. A., Shehata, M. H., Shashiprakash, S. G., Hopkins, D. S., and Cail, K., Use of ternary cementitious systems containing silica fume and fly ash in concrete, *Cement and Concrete Research*, **29**, p. 1207-1214, 1999
31. Boddy, Andrea, Hooton, R. D., and Gruber, K. A., Long-term testing of the chloride-penetration resistance of concrete containing high-reactivity metakaolin, *Cement and Concrete Research*, **31**, p. 759-765, 2001
32. Gruber, K. A., Ramlochan, Terry, Boddy, Andrea, Hooton, R. D., and Thomas, M. D. A., Increasing concrete durability with high-reactivity metakaolin, *Cement & Concrete Composites*, **23**, p. 479-484, 2001
33. Bentz, D. P., A review of early-age properties of cement-based materials, *Cement and Concrete Research*, **38**, p. 196-204, 2008
34. Snyder, Kenneth A., and Clifton, James R., *4SIGHT Manual: A Computer Program for Modelling Degradation of Underground Low Level Waste Concrete Vaults*, NISTIR 5612, Department of Commerce, 1995
35. Tang, L., and Sorensen, H. E., Precision of the Nordic test methods for measuring the chloride diffusion/migration coefficients of concrete, *Materials and Structures*, **34**, p. 479-485, 2001
36. Zhang, Tiewei, and Gjorv, Odd E., Diffusion Behaviour of Chloride Ions in Concrete, *Cement and Concrete Research*, **26(6)**, p. 907-917, 1996

37. Snyder, K. A., The relationship between the formation factor and the diffusion coefficient of porous materials saturated with concentrated electrolytes: theoretical and experimental considerations, *Concrete Science and Engineering*, **3**(12), p. 216-224, 2001
38. Snyder, K. A., *Validation and Modification of the 4SIGHT Computer Program*, NISTIR 6747, Department of Commerce, 2001
39. Thomas, Michael, Chloride Thresholds in Marine Concrete, *Cement and Concrete Research*, **26**(4), p. 513-519, 1996
40. Malvar, L.J., *Alkali-Silica Reaction Mitigation State-of-the-Art*, TR-2195-SHR, Naval Facilities Engineering Service Center, 2001
41. *Standard Method of Test for Sampling and Testing for Chloride Ion in Concrete and Concrete Raw Materials*, T 260-1, AASHTO, 2001
42. McGrath, Patrick F., and Hooton, R. Doug, Re-evaluation of the AASHTO T259 90-day salt ponding test, *Cement and Concrete Research*, **29**, p. 1239-1248, 1999,
43. Bentz, Dale P., Feng, Xiuping, and Hooton, R. Douglas, Time-Dependent Diffusivities: Possible Misinterpretation due to Spatial Dependence, *Proc. International RILEM Workshop, Testing and Modelling the Chloride Ingress into Concrete*, Paris, France, p. 225-233, 2000
44. Costa, A., and Appleton, J., Chloride penetration into concrete in marine environment – Part I : Main parameters affecting chloride penetration, *Materials and Structures*, **32**, p. 242-259, 1999
45. Costa, A., and Appleton, J., Chloride penetration into concrete in marine environment – Part II: Prediction of long term chloride penetration, *Materials and Structures*, **32**, p. 354-359, 1999

46. Life-365 Version 2.0.1, September 2009, The Life-365 Consortium, 1 March 2010 < <http://www.life-365.org/download.html>>
47. 4SIGHT, In *Computer Integrated Knowledge System for High Performance Concrete*, Retrieved from <http://concrete.nist.gov/4sight>
48. *Standard Test Methods for Chemical Analysis of Hydraulic Cement*, C114-09a, ASTM International, 2010
49. *Standard Test Method for Acid-Soluble Chloride in Mortar and Concrete*, C 1152/ C 1152M-04, ASTM International, 2004
50. DataFit 9.0, Oakdale Engineering, 1 March 2010  
<<http://www.curvefitting.com/download.htm>>
51. LAB Fit Curve Fitting Software, Universidade Federal de Campina Grande, 1 March 2010 <<http://zeus.df.ufcg.edu.br/labfit/download.htm>>
52. Estimation of Pore Solution Conductivity, In *Computer Integrated Knowledge System for High Performance Concrete*, Retrieved from <http://ciks.cbt.nist.gov/poresolncalc.html>
53. Virtual Rapid Chloride Permeability Test, In *Computer Integrated Knowledge System for High Performance Concrete*, Retrieved from <http://ciks.cbt.nist.gov/VirtualRCPT.html>
54. Sodium Chloride Density Concentration Table, In *Mettler Toledo*, Retrieved from  
[http://us.mt.com/us/en/home/supportive\\_content/application\\_editorials.Sodium\\_Chloride\\_de\\_e.twoColEd.html](http://us.mt.com/us/en/home/supportive_content/application_editorials.Sodium_Chloride_de_e.twoColEd.html)

# APPENDIX

## 1. Series 1 Data

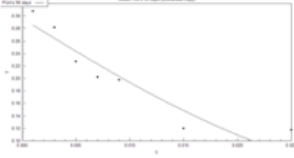
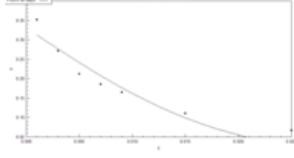
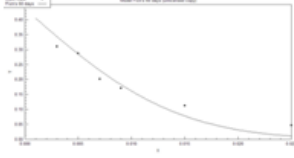
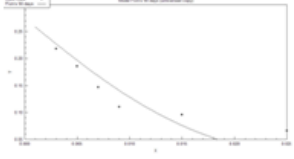
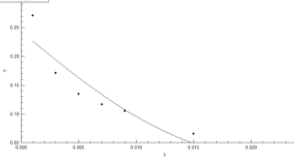
### 1.1 30 Days Exposure

COPC	30 Days	Regression Variable Results		
1	0.19542	Variable	Value	Standard Error
3	0.143529	Cs	0.19291	1.03E-02 % concrete
5	0.129867	Dapp	3.51E-11	7.34E-12 m <sup>2</sup> /s
7	0.115601			
9	0.10466			
15	0.060361			
25	0			
BG	0.006941			
Coefficient of Multiple Determination (R <sup>2</sup> ) = 0.9669954618				
CF10	30 Days	Regression Variable Results		
1	0.20325	Variable	Value	Standard Error
3	0.15437	Cs	0.21791	8.25E-03 % concrete
5	0.127	Dapp	1.65E-11	2.05E-12 m <sup>2</sup> /s
7	0.09897			
9	0.08399			
15	0.01159			
25	0			
BG	0.007436			
Coefficient of Multiple Determination (R <sup>2</sup> ) = 0.9889428096				
CF20	30 Days	Regression Variable Results		
1	0.21643	Variable	Value	Standard Error
3	0.1465	Cs	0.22481	1.19E-02 % concrete
5	0.12836	Dapp	1.58E-11	2.71E-12 m <sup>2</sup> /s
7	0.10824			
9	0.07845			
15	0.01361			
25	0			
BG	0.007006			
Coefficient of Multiple Determination (R <sup>2</sup> ) = 0.9787160358				
C5%	30 Days	Regression Variable Results		
1	0.22321	Variable	Value	Standard Error
3	0.15663	Cs	0.23539	1.31E-02 % concrete
5	0.13875	Dapp	1.46E-11	2.59E-12 m <sup>2</sup> /s
7	0.105161			
9	0.05679			
15	0.0365			
25	0			
BG	0.006995			
Coefficient of Multiple Determination (R <sup>2</sup> ) = 0.9759247071				
C10%	30 Days	Regression Variable Results		
1	0.19178	Variable	Value	Standard Error
3	0.12637	Cs	0.20039	1.39E-02 % concrete
5	0.08383	Dapp	1.08E-11	2.23E-12 m <sup>2</sup> /s
7	0.08209			
9	0.04883			
15	0.01975			
25	0			
BG	0.007548			
Coefficient of Multiple Determination (R <sup>2</sup> ) = 0.966515567				

## 1.2 60 Days Exposure

COPC 60 Days		Regression Variable Results		
1	0.254963	Variable	Value	Standard Error
3	0.239062	Cs	0.25841	1.10E-02 % concrete
5	0.195532	Dapp	3.31E-11	6.37E-12 m2/s
7	0.166585			
9	0.158702			
15	0.098752			
25	0.06758			
BG	0.006941			
Coefficient of Multiple Determination (R <sup>2</sup> ) = 0.9599600597				
CF10 60 Days		Regression Variable Results		
1	0.278329	Variable	Value	Standard Error
3	0.225687	Cs	0.27271	2.73E-02 % concrete
5	0.168865	Dapp	1.42E-11	5.33E-12 m2/s
7	0.129562			
9	0.106854			
15	0.080564			
25	0.062667			
BG	0.007436			
Coefficient of Multiple Determination (R <sup>2</sup> ) = 0.8672835317				
CF20 60 Days		Regression Variable Results		
1	0.259284	Variable	Value	Standard Error
3	0.197249	Cs	0.26396	1.40E-02 % concrete
5	0.176792	Dapp	1.33E-11	2.59E-12 m2/s
7	0.144117			
9	0.113992			
15	0.049192			
25	0.038456			
BG	0.007006			
Coefficient of Multiple Determination (R <sup>2</sup> ) = 0.9668132101				
C5% 60 Days		Regression Variable Results		
1	0.248975	Variable	Value	Standard Error
3	0.177564	Cs	0.23991	1.99E-02 % concrete
5	0.150564	Dapp	1.32E-11	4.01E-12 m2/s
7	0.118973			
9	0.098571			
15	0.062186			
25	0.042251			
BG	0.006995			
Coefficient of Multiple Determination (R <sup>2</sup> ) = 0.9158413887				
C10% 60 Days		Regression Variable Results		
1	0.221127	Variable	Value	Standard Error
3	0.157568	Cs	0.21554	2.09E-02 % concrete
5	0.107267	Dapp	9.51E-12	3.13E-12 m2/s
7	0.095684			
9	0.076555			
15	0.059215			
25	0.016879			
BG	0.007548			
Coefficient of Multiple Determination (R <sup>2</sup> ) = 0.9097120226				

### 1.3 90 Days Exposure

COPC	90 Days	Regression Variable Results		
1	0.307738	Variable	Value	Standard Error
3	0.281533	Cs	0.29594	1.93E-02 % concrete
5	0.226925	Dapp	3.20E-11	1.05E-11 m <sup>2</sup> /s
7	0.202225			
9	0.197321			
15	0.119974			
25	0.11758			
BG	0.006941			
Coefficient of Multiple Determination (R <sup>2</sup> ) = 0.8760671242				
CF10	90 Days	Regression Variable Results		
1	0.352114	Variable	Value	Standard Error
3	0.271358	Cs	0.33039	2.47E-02 % concrete
5	0.212647	Dapp	1.35E-11	4.09E-12 m <sup>2</sup> /s
7	0.185925			
9	0.165687			
15	0.111309			
25	0.067337			
BG	0.007436			
Coefficient of Multiple Determination (R <sup>2</sup> ) = 0.9141399558				
CF20	90 Days	Regression Variable Results		
1	0.444473	Variable	Value	Standard Error
3	0.309634	Cs	0.43522	3.20E-02 % concrete
5	0.28758	Dapp	1.20E-11	3.16E-12 m <sup>2</sup> /s
7	0.201481			
9	0.170747			
15	0.11291			
25	0.047073			
BG	0.007006			
Coefficient of Multiple Determination (R <sup>2</sup> ) = 0.9411834053				
C5%	90 Days	Regression Variable Results		
1	0.295913	Variable	Value	Standard Error
3	0.218243	Cs	0.27441	2.75E-02 % concrete
5	0.185476	Dapp	1.22E-11	4.84E-12 m <sup>2</sup> /s
7	0.146672			
9	0.110288			
15	0.095962			
25	0.06627			
BG	0.006995			
Coefficient of Multiple Determination (R <sup>2</sup> ) = 0.8523703857				
C10%	90 Days	Regression Variable Results		
1	0.271221	Variable	Value	Standard Error
3	0.171204	Cs	0.24291	3.39E-02 % concrete
5	0.134955	Dapp	8.84E-12	4.53E-12 m <sup>2</sup> /s
7	0.116746			
9	0.105224			
15	0.065497			
25	0.067251			
BG	0.007548			
Coefficient of Multiple Determination (R <sup>2</sup> ) = 0.7580988905				

## 2. Series 2 Data

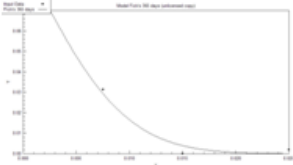
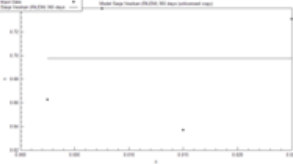
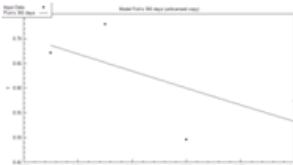
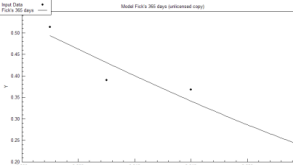
### 2.1 90 Days Exposure

COPC	90 Days	Regression Variable Results		
1	0.20099	Variable	Value	Standard Error
3	0.2344	Cs	0.28599	4.06E-02 % concrete
5	0.28466	Dapp	2.34E-11	1.52E-11 m2/s
7	0.26398			
9	0.2092			
15	0.0882			
25	0.01811			
BG	0.006941			
Coefficient of Multiple Determination (R <sup>2</sup> ) = 0.7212322008				
CF10	90 Days	Regression Variable Results		
1	0.38918	Variable	Value	Standard Error
3	0.40971	Cs	0.38866	2.14E-02 % concrete
5	0.33125	Dapp	1.11E-10	5.02E-11 m2/s
7	0.29138			
9	0.30422			
15	0.31365			
25	0.21			
BG	0.007436			
Coefficient of Multiple Determination (R <sup>2</sup> ) = 0.7734960468				
CF20	90 Days	Regression Variable Results		
1	0.324331	Variable	Value	Standard Error
3	0.361222	Cs	0.33807	2.90E-02 % concrete
5	0.360523	Dapp	1.44E-09	3.71E-09 m2/s
7	0.344903			
9	0.288554			
15	0.23151			
25	0.338706			
BG	0.007006			
Coefficient of Multiple Determination (R <sup>2</sup> ) = 0.0989869851				
C5%	90 Days	Regression Variable Results		
1	0.214358	Variable	Value	Standard Error
3	0.215766	Cs	0.22486	7.86E-03 % concrete
5	0.183193	Dapp	2.79E-11	4.69E-12 m2/s
7	0.153099			
9	0.139616			
15	0.105952			
25	0.060909			
BG	0.006995			
Coefficient of Multiple Determination (R <sup>2</sup> ) = 0.9678793273				
C10%	90 Days	Regression Variable Results		
1	0.222595	Variable	Value	Standard Error
3	0.247666	Cs	0.22553	1.61E-02 % concrete
5	0.237286	Dapp	4.79E-10	5.78E-10 m2/s
7	0.182415			
9	0.170581			
15	0.198069			
25	0.185555			
BG	0.007548			
Coefficient of Multiple Determination (R <sup>2</sup> ) = 0.324307794				

## 2.2 180 Days Exposure

COPC	180 Days	Regression Variable Results		
2.5	0.45882	Variable	Value	Standard Error
7.5	0.5078	Cs	0.56051	1.11E-01 % concrete
15	0.71792	Dapp	3.89E-23	2.27E-14 m2/s
25	0.50609			
BG	0.006941	Coefficient of Multiple Determination (R <sup>2</sup> ) = 0.0		
CF10	180 Days	Regression Variable Results		
2.5	0.52568	Variable	Value	Standard Error
7.5	0.50347	Cs	0.52539	0.02301 % concrete
15	0.44053	Dapp	4.30E-10	3.38E-10 m2/s
25	0.45164			
BG	0.007436	Coefficient of Multiple Determination (R <sup>2</sup> ) = 0.7369861824		
CF20	180 Days	Regression Variable Results		
2.5	0.358633	Variable	Value	Standard Error
7.5	0.455985	Cs	0.44735	7.29E-02 % concrete
15	0.309441	Dapp	4.14E-11	3.64E-11 m2/s
25	0.189522			
BG	0.007006	Coefficient of Multiple Determination (R <sup>2</sup> ) = 0.6811557337		
C5%	180 Days	Regression Variable Results		
2.5	0.674997	Variable	Value	Standard Error
7.5	0.797438	Cs	0.76725	0.10159 % concrete
15	0.512873	Dapp	8.08E-11	7.98E-11 m2/s
25	0.488268			
BG	0.006995	Coefficient of Multiple Determination (R <sup>2</sup> ) = 0.6175751784		
C10%	180 Days	Regression Variable Results		
2.5	0.769289	Variable	Value	Standard Error
7.5	0.677892	Cs	0.79597	6.92E-02 % concrete
15	0.740429	Dapp	1.38E-10	1.18E-10 m2/s
25	0.518831			
BG	0.007548	Coefficient of Multiple Determination (R <sup>2</sup> ) = 0.6918278119		

### 2.3 365 Days Exposure

COPC 365 Days		Regression Variable Results		
2.5	0.069855	Variable	Value	Standard Error
7.5	0.031272	Cs	9.61E-02	6.32E-03 % concrete
15	0	Dapp	8.50E-13	1.52E-13 m2/s
25	0.001964			
BG	0.006941			
Coefficient of Multiple Determination (R^2) = 0.9929238556				
CF10 365 Days		Regression Variable Results		
2.5	0.52996	Variable	Value	Standard Error
7.5	0.47864	Cs		% concrete
15	0.69115	Dapp		m2/s
25	0.52322	FICK'S FAILED		
BG	0.007436			
CF20 365 Days		Regression Variable Results		
2.5	0.662485	Variable	Value	Standard Error
7.5	0.739667	Cs	0.69773	3.60E-02 % concrete
15	0.636886	Dapp	2.53E-26	6.65E-17 m2/s
25	0.73071			
BG	0.007006			
Coefficient of Multiple Determination (R^2) = 0.0				
C5% 365 Days		Regression Variable Results		
2.5	0.671427	Variable	Value	Standard Error
7.5	0.729089	Cs	0.70388	8.74E-02 % concrete
15	0.496125	Dapp	1.03E-10	1.56E-10 m2/s
25	0.573827			
BG	0.006995			
Coefficient of Multiple Determination (R^2) = 0.4152684093				
C10% 365 Days		Regression Variable Results		
2.5	0.513298	Variable	Value	Standard Error
7.5	0.390398	Cs	0.52504	3.58E-02 % concrete
15	0.367914	Dapp	1.74E-11	5.94E-12 m2/s
25	0.230238			
BG	0.007548			
Coefficient of Multiple Determination (R^2) = 0.9313404189				